

LIBRARY
Michigan State
University

This is to certify that the
dissertation entitled

Study of *Pseudomonas syringae* effector protein HopM1 and
its host target AtMIN7 implicated in vesicle trafficking in
Arabidopsis thaliana

presented by

Young Nam Lee

has been accepted towards fulfillment
of the requirements for the

Ph.D. degree in Plant Biology


Major Professor's Signature

12/03/09

Date

MSU is an Affirmative Action/Equal Opportunity Employer

PLACE IN RETURN BOX to remove this checkout from your record.
TO AVOID FINES return on or before date due.
MAY BE RECALLED with earlier due date if requested.

DATE DUE	DATE DUE	DATE DUE

**STUDY OF *PSEUDOMONAS SYRINGAE* EFFECTOR PROTEIN HOPM1 AND
ITS HOST TARGET ATMIN7 IMPLICATED IN VESICLE TRAFFICKING IN
*ARABIDOPSIS THALIANA***

By

Young Nam Lee

A DISSERTATION

**Submitted to
Michigan State University
in partial fulfillment of the requirements
for the degree of**

DOCTOR OF PHILOSOPHY

Plant Biology

2009

ABSTRACT

STUDY OF *PSEUDOMONAS SYRINGAE* EFFECTOR PROTEIN HOPM1 AND ITS HOST TARGET ATMIN7 IMPLICATED IN VESICLE TRAFFICKING IN *ARABIDOPSIS THALIANA*

By

Young Nam Lee

In the pathogenic interaction between *Arabidopsis thaliana* and *Pseudomonas syringae* pv. *tomato* DC3000 (*Pst* DC3000), it has been suggested that one function of type III secretion system (TTSS) effector proteins of *Pst* DC3000 is to interfere with the defense-associated cellular trafficking pathway(s) in *Arabidopsis*. This study focuses on characterization of HopM1, a TTSS effector of *Pst* DC3000, and its host target AtMIN7, a putative adenosine-diphosphate ribosylation factor-guanine nucleotide-exchanging factor (ARF-GEF) implicated in intracellular vesicle trafficking in *Arabidopsis*.

The localization of full-length and truncated HopM1 was studied using confocal microscopy. In tobacco cells, full-length HopM1 fusion proteins were found in small, punctate structures, which were co-localized with a trans-Golgi network (TGN) marker VHA-a1 and an early endosome marker ARA6. The fusion protein of the N-terminus of HopM1 (HopM1₁₋₃₀₀) was found in punctate structures co-localizing with VHA-a1. Approximately 5 hours after their expression, full-length HopM1 fusion proteins were found in punctate structures, whereas truncated HopM1 fusion proteins (HopM1₁₋₃₀₀ and HopM1₃₀₁₋₇₁₂) were dispersed in the cells. Full-length HopM1 fusions induced death of tobacco leaf tissue by 48 hours after their induction. Some of the HopM1 fusion proteins transformed into *Arabidopsis* (Col-0 and *atmin7* backgrounds) showed similar localization patterns as in tobacco. It is suggested that HopM1 is localized in the

endosomes in the host cell and that HopM1₁₋₃₀₀ contains an organelle-targeting signal.

Whether other *Arabidopsis* ARF-GEFs besides AtMIN7 are involved in host defense is not known. The roles of three ARF-GEFs (*AtBIG2*, *AtBIG3* and *AtBIG4*) in defense were studied by examination of bacterial multiplication in corresponding T-DNA insertional mutants. None of the examined mutants showed a clear defect in defense against *Pst* DC3000, the Δ CEL mutant (lacking HopM1), or the *hrcC*⁻ mutant (defective in the TTSS). The HopM1₁₋₃₀₀ was previously shown to interact with the C-terminus of AtMIN7. The C-termini of four ARF-GEFs (AtBIG1, AtBIG3, GNL1 and GNL2) were examined by yeast two-hybrid assay to determine whether they also interacted with HopM1₁₋₃₀₀. The C-terminus of GNL2 did not interact with HopM1₁₋₃₀₀. The interactions between HopM1₁₋₃₀₀ and the C-termini of AtBIG1, AtBIG3 and GNL1 were not determined because of the failure to express these proteins in yeast.

To determine whether AtMIN7 regulates the secretion of defense-related proteins, three *Arabidopsis* proteins (PR1, a putative lipid-transfer protein encoded by At2g10940, and FLA9, a putative arabinogalactan protein encoded by At1g03870) were fused with GFP, and expressed in *Arabidopsis* (Col-0 and *atmin7* background) followed by confocal microscopic examination. PR1-GFP was localized in the intercellular space both in Col-0 and *atmin7* backgrounds. At2g10940-GFP was localized in the intercellular space in Col-0 background, but in *atmin7* background, unidentified intracellular structures appeared. FLA9-GFP fusion was not expressed in *Arabidopsis*. These results suggest that the localization of At2g10940-GFP may be dependent on the AtMIN7-mediated vesicle trafficking pathway(s) whereas the localization of PR1-GFP is not.

Copyright by
YOUNG NAM LEE
2009

ACKNOWLEDGEMENTS

I show my sincere gratitude to my advisor Dr. Sheng Yang He, whose support led me profound improvement of myself as a scientist. I thank my committee members, Dr. Jonathan Walton, Dr. Rebecca Grumet and Dr. Ray Hammerschmidt, for their valuable guidance and support during my Ph.D.

I want to thank my previous and current colleagues of He laboratory for their kind support and help. Especially the support from Dr. Kinya Nomura, Dr. Christy Mecey, and Wei-Ning Huang was indispensable for my study. The help from Dr. Elena Bray Speth in confocal microscopy was also valuable for me. I thank Dr. Roger Thilmony and Dr. Maeli Melotto for their kind support. I also would like to mention the warm support consistently shown to me from Lori Imboden, and the support from Francisco Uribe, Dr. Weiqing Zeng, Dr. Jian Yao, John Withers, Matt Oney, and Xiufang Xin. The previous and current undergraduate assistants provided great help to me.

I received warm and kind help from Dr. Federica Brandizzi for my confocal microscopic experiments. I was also kindly helped from Dr. Melinda Frame.

The help I received from the Plant Research Laboratory was one of the greatest supports in my life, and I am proud that I was in it.

I feel that I am lucky to share my Ph.D. time with precious friends, Janet Paper, Jessica Koczan, Hoosun Chung, Jeongwoon Kim, Julie Bordowitz, Xinchun Zhang, Eliana Gonzales-Vigil, Bill Underwood, Hiroshi Maeda, and Clarisa Bejar. I would like to show my gratitude to my families in Korea and the Netherlands. Also, I deeply thank to my husband Dr. Harrie vanErp, and our daughter Annemarie Soyeon.

TABLE OF CONTENTS

LIST OF TABLES.....	ix
----------------------------	-----------

LIST OF FIGURES	x
------------------------------	----------

CHAPTER 1	1
------------------------	----------

<i>General aspects of plant-pathogen interactions</i>	<i>2</i>
<i>The Arabidopsis thaliana-Pst DC3000 model</i>	<i>2</i>
<i>Pseudomonas syringae pv. tomato DC3000 as a bacterial phytopathogen.....</i>	<i>3</i>
<i>Arabidopsis thaliana as a model plant in plant-pathogen interactions</i>	<i>6</i>
<i>A four-part model for the interaction between Arabidopsis and Pst DC3000</i>	<i>6</i>
<i>1st step: the activation of PAMP-triggered immunity (PTI)</i>	<i>7</i>
<i>2nd step: the suppression of PTI by TTSS effector proteins</i>	<i>9</i>
<i>3rd step: the recognition of TTSS effectors by plants and activation of effector-triggered immunity (ETI)</i>	<i>10</i>
<i>4th part: evasion or suppression of ETI by pathogens through TTSS effectors ...</i>	<i>12</i>
<i>Systemic acquired resistance (SAR).....</i>	<i>13</i>
<i>Suppression of defense-associated cellular trafficking pathway in plants by TTSS effectors</i>	<i>15</i>
<i>HopM1 and AtMIN7: a TTSS effector involved in the suppression of defense-associated cellular trafficking pathway(s) and its target of Arabidopsis</i>	<i>17</i>
<i>Summary of thesis research subjects</i>	<i>18</i>
REFERENCES	20

CHAPTER 2.....	32
-----------------------	-----------

ABSTRACT.....	33
INTRODUCTION	36
MATERIALS AND METHODS.....	39
<i>Construction of HopM1 fusions</i>	<i>39</i>
<i>Introduction of HopM1 fusion ORFs into Agrobacterium</i>	<i>42</i>
<i>Transient assays of the HopM1 fusion ORFs in tobacco plants</i>	<i>45</i>
<i>Transformation of HopM1 fusions into Arabidopsis plants</i>	<i>45</i>
<i>Plant growth condition.....</i>	<i>46</i>
<i>Application of Dexamethasone (DEX).....</i>	<i>46</i>
<i>Confocal microscopy</i>	<i>47</i>
<i>Dual localization with cellular markers</i>	<i>47</i>
<i>Brefeldin A (BFA) treatment</i>	<i>49</i>
<i>Protein extraction and western blot analyses</i>	<i>49</i>
<i>The color of the images in this dissertation</i>	<i>50</i>

RESULTS	51
Transiently expressed full-length HopM1 fusion proteins induce tissue death in tobacco leaves	51
Western blot analyses of HopM1 fusions in transient assay.....	53
Transiently expressed fusions of full-length HopM1 are found in small, punctate structures in tobacco leaves	53
Dual localization tests of full-length HopM1 fusions with a Golgi marker with or without Brefeldin A (BFA).....	58
Dual localization tests of YFP-HopM1 and endosome markers.....	61
Localization of truncated HopM1 fusion proteins	63
Transgenic expression of HopM1 fusions in <i>Arabidopsis</i>	66
DISCUSSION	75
REFERENCES	82
ACKNOWLEDMENTS	33
 CHAPTER 3	 86
ABSTRACT.....	87
INTRODUCTION	89
MATERIALS AND METHODS.....	93
Identification of homozygous T-DNA insertion mutants for <i>Arabidopsis</i> ARF-GEF genes	93
Confirmation of gene knockout of T-DNA insertion mutants by reverse transcription and polymerase chain reaction (RT-PCR)	96
Construction of ARF-GEF gene clones for yeast two-hybrid assays	98
Yeast two-hybrid assay	104
Growth curve assay for determining multiplication of Pst DC3000 and its mutants in <i>Arabidopsis</i>	106
Crossing atmin7 knockout mutant (salk_012013) and knockout mutant of AtBIG2 (salk_033446)	107
RESULTS	108
Identification of homozygous T-DNA insertion mutants for <i>Arabidopsis</i> ARF-GEF genes	108
Confirmation of gene knockout in the homozygous T-DNA insertion mutants by RT-PCR	108
Determination of the multiplication of the Δ CEL mutant in the selected T-DNA insertion mutants.....	110
Determination of the multiplication of the Δ CEL mutant in the double knockout mutant of <i>AtMIN7</i> and <i>BIG2</i>	110
Yeast two- hybrid assay of selected <i>Arabidopsis</i> ARF-GEF genes with HopM1 ..	113
DISCUSSION.....	108
REFERENCES	122
ACKNOWLEDMENTS	87
 CHAPTER 4	 124
ABSTRACT.....	125

INTRODUCTION	126
MATERIALS AND METHODS.....	130
Construction of GFP fusions and their subcloning into plant expression vector....	130
Transformation of recombinant plasmids into <i>Agrobacterium</i>	133
Production of transgenic <i>Arabidopsis</i> lines expressing GFP fusions	133
Confocal microscopy	133
Plasmolysis of leaf samples	134
Protein extraction and western blot analyses	134
RESULTS	136
Production of transgenic <i>Arabidopsis</i> expressing GFP fusion proteins	136
The subcellular localization of PR1-GFP in <i>Arabidopsis</i>	139
The subcellular localization of At2g10940-GFP in <i>Arabidopsis</i>	142
DISCUSSION	145
REFERENCES	150
 CHAPTER 5	 153
REFERENCES	160
 APPENDICES	 162

LIST OF TABLES

Table 2-1. Summary of the fusion proteins created for the localization study of HopM1	40
Table 2-2. PCR primers for cloning the ORFs of <i>sGFP</i> and <i>EYFP</i>	40
Table 2-3. PCR primers for obtaining full-length or truncated <i>hopM1</i> ORFs for fusion constructions	43
Table 2-4. Summary of transgenic <i>Arabidopsis</i> expressing HopM1 fusions	73
Table 3-1. The <i>Arabidopsis</i> ARF-GEF genes, their selected T-DNA insertion mutants, and the putative insertion site of T-DNA of each mutant.....	94
Table 3-2. Primer sets designed for screening homozygous T-DNA insertion mutants for <i>ARF-GEF</i> genes	95
Table 3-3. Primers for RT-PCR for T-DNA insertion mutants of selected <i>ARF-GEF</i> genes	97
Table 3-4. Primer sequences for obtaining clones of selected <i>ARF-GEF</i> genes for yeast two-hybrid assay with the N-terminus of HopM1	99
Table 4-1. Primers used for PCR to construct GFP fusions of selected <i>Arabidopsis</i> genes	132
Table 4-2. Summary of transgenic <i>Arabidopsis</i> expressing PR1-GFP fusion protein ...	137
Table 4-3. Summary of transgenic <i>Arabidopsis</i> expressing At2g10940-GFP fusion protein	137

LIST OF FIGURES

Figure 2-1. Diagrams of HopM1 fusions used for localization studies	41
Figure 2-2. Appearance of <i>N.benthamiana</i> leaves which were infiltrated <i>Agrobacterium</i> carrying various plasmids	52
Figure 2-3. Immunoblot analyses of HopM1 fusions in transient assays in <i>N.tabacum</i> ..	54
Figure 2-4. HopM1-GFP and YFP-HopM1 transiently expressed in <i>N.tabacum</i>	57
Figure 2-5. Dual localization results of full-length HopM1 fusion proteins and ST-RFP	59
Figure 2-6. Dual localization result of HopM1-GFP and ST-RFP with BFA treatment ..	62
Figure 2-7. Dual localization results of YFP-HopM1 and VHA-a1-RFP	64
Figure 2-8. Dual localization results of YFP-HopM1 and ARA6-CFP.....	65
Figure 2-9. Localization of truncated HopM1 fusion proteins	68
Figure 2-10. Dual localization results of YFP-HopM1-N and VHA-a1-RFP	70
Figure 2-11. HopM1 fusion proteins in <i>Arabidopsis</i>	74
Figure 3-1. A phylogenetic tree of <i>Arabidopsis</i> ARF-GEF genes.....	90
Figure 3-2. Predicted amino acid sequences of the ARF-GEFs for yeast two-hybrid assays	100
Figure 3-3. Diagrams of four <i>ARF-GEF</i> genes analyzed by yeast two-hybrid assay	105
Figure 3-4. Genomic PCR results of homozygous T-DNA insertional mutants for three <i>ARF-GEF</i> genes (<i>BIG2</i> , <i>BIG3</i> and <i>BIG4</i>)	109

Figure 3-5. RT-PCR results of selected T-DNA insertional mutants of <i>AtBIG2</i> , <i>AtBIG3</i> and <i>AtBIG4</i>	111
Figure 3-6. Multiplication of <i>Pst</i> DC3000, the Δ CEL mutant and the <i>hrcC</i> ⁻ mutant in Col-0, <i>atmin7</i> and <i>ARF-GEF</i> T-DNA insertion lines	112
Figure 3-7. Genomic PCR results confirming the double knockout of <i>AtMIN7</i> and <i>AtBIG2</i>	114
Figure 3-8. Multiplication of <i>Pst</i> DC3000, the Δ CEL mutant and the <i>hrcC</i> ⁻ mutant in Col-0, <i>atmin7</i> , <i>atbig2</i> , and the double knockout of <i>AtMIN7</i> and <i>AtBIG2</i>	115
Figure 3-9. Yeast two-hybrid assay result of the C-termini of selected ARF-GEFs with HopM1 ₁₋₃₀₀	117
Figure 4-1. Diagrams of the PR1-GFP, At2g10940-GFP and FLA9-GFP fusions for the subcellular localization study.....	131
Figure 4-2. Immunoblot analysis of PR1-GFP and At2g10940-GFP in <i>Arabidopsis</i>	138
Figure 4-3. Localization and expression of PR1-GFP in <i>Arabidopsis</i> (in Col-0 background)	140
Figure 4-4. Localization of PR1-GFP in <i>Arabidopsis</i> (in <i>atmin7</i> mutant background). ..	141
Figure 4-5. Localization of At2g10940-GFP in <i>Arabidopsis</i> (in Col-0 background)	143
Figure 4-6. The localization of At2g10940-GFP in <i>Arabidopsis</i> (in the <i>atmin7</i> background)	144

CHAPTER 1

Literature Review

General aspects of plant-pathogen interactions

During evolution, plants have been exposed to a variety of micro-organisms and developed various types of interactions with them. Among these interactions, the interactions between plants and pathogenic microorganisms have been extensively studied in plant science, in order to advance our understanding of these processes and how they have been evolved. Moreover, the study of plant-pathogen interactions is important for agriculture, considering that the crop loss caused by plant disease is one of the major limiting factors in food production (reviewed by Savary et al., 2006).

The aspects of the interactions between plants and pathogens are diverse depending on types of plants and pathogens. However, an emerging theme of these interactions is that plants and their pathogens are in a continuous cycle of attack, defense, and counterattack. In this ongoing “battle”, the pathogens have continuously affected the physiological state of the plants for obtaining nutrition for their survival and proliferation. In many cases, these effects compromise or severely interfere with the normal physiology, growth and proliferation of plants. Plants have evolved defense mechanisms in order to cope with these pathogen attacks, as summarized in different reviews (Katagiri et al., 2002; Chisholm et al., 2006; Speth et al., 2007; Boller and He, 2009). This evolutionary arms race enabled both pathogens and plants to develop multiple strategies for attack and defense. As a result, this arms race has significantly affected the evolution of plants and pathogens at the genetic and molecular level (Ma et al., 2006; Stavrinides et al., 2008).

The *Arabidopsis thaliana*-Pst DC3000 model

In many cases the interactions between plants and pathogens are specific. Some of these interactions have been studied as model systems, in which a specific plant species and a specific pathogen are connected as an interaction pair. In this thesis, I focus on one plant-pathogen interaction model, in which *Arabidopsis thaliana* is the host plant and *Pseudomonas syringae* pv. *tomato* DC3000 (*Pst* DC3000) is the pathogen. This model was introduced in 1990s with several other *Arabidopsis thaliana*-*Pseudomonas syringae* interaction models, and has been widely used in plant-pathogen interaction studies since then (Davis et al., 1991; Dong et al., 1991; Whalen et al., 1991; Katagiri et al., 2002). Both *Arabidopsis* and *Pst* DC3000 have advantages for studying the molecular basis of plant-pathogen interactions, because both of them have well-developed resources of molecular genetic and genomic manipulations, including their full genome sequences (for *Arabidopsis* genome, refer to Rhee et al. (2003) and www.arabidopsis.org; for *Pst* DC3000 genome, refer to Buell et al. (2003) and <http://pseudomonas-syringae.org>).

Pseudomonas syringae pv. *tomato* DC3000 as a bacterial phytopathogen

P.syringae is a gram-negative bacterium. It is included in the *Pseudomonas* genus, which has approximately 50 pathogenic species with different host specificities (Deng et al., 1998; Anzai et al., 2000). As a plant pathogen *P.syringae* has more than 50 pathovars (Gardan et al., 1999) which differ largely in host range among different plants (Gardan et al., 1999). Different races and strains are assigned to these pathovars, based on their ability to infect different plant cultivars (Alfano and Collmer, 1997; <http://pseudomonas-syringae.org>). Pathovars of *P.syringae* infect various crops such as tomato, soybean, rice, tobacco and wheat (Gardan et al., 1999).

Pst DC3000 is a strain included in the pathovar *P.syringae* pv. *tomato*, which is the cause of speck disease in tomato (Cuppels, 1986). Speck disease on tomato is one of the representative examples of disease caused by *P.syringae*, with characteristic symptoms such as necrotic lesions on the tomato leaves and dark spots on the fruit (Cuppels et al., 1990; <http://pseudomonas-syringae.org>). *Pst* DC3000 is assigned to race 0, on the basis of its avirulence on tomato cultivars carrying Pto resistance (Ronald et al., 1992). *Pst* DC3000 is also a pathogen of *A. thaliana* (Whalen et al., 1991; Katagiri et al. 2002).

Pst DC3000 is considered as a hemibiotrophic pathogen: it typically enters plant leaves through openings such as stomata or through wounds and aggressively multiplies (to the level of 10^8 cells/cm² of leaf) in the intercellular space (also known as apoplast), followed by formation of necrotic lesions (Whalen et al., 1991; Hirano and Upper, 2000; Katagiri et al., 2002; Nomura et al., 2005; Melotto et al., 2008). Upon infection by *Pst* DC3000, *A. thaliana* displays disease with visible symptoms, such as leaf yellowing (chlorosis) and the water-soaking phenomenon, followed by eventual tissue necrosis (Whalen et al., 1991; Katagiri et al., 2002).

The pathogenicity and virulence of *Pst* DC3000 depend on at least two pathogenicity factors, the type III secretion system (TTSS) with its effector proteins and the phytotoxin coronatine (Katagiri et al., 2002). *Pst* DC3000 injects 30-40 bacterial proteins collectively called “TTSS effectors” into the plant cells through its TTSS (Alfano and Collmer, 2004). The TTSS of *Pst* DC3000 is encoded by a cluster of hypersensitive response and pathogenicity (*hrp*) genes; *hrp*⁻ mutants of *Pst* DC3000 are impaired in regulation or secretion of type III effectors, and lose the ability to multiply

and cause disease in compatible hosts (Yuan and He, 1996; Roine et al., 1997). The TTSS (and its effector proteins) and *hrp* genes are not specific to *Pseudomonas*, but found in other plant pathogens such as *Xanthomonas*, *Ralstonia*, and *Erwinia spp.* (Alfano and Collmer, 1997; Alfano and Collmer, 2004) and in several animal pathogens like *Yersinia*, *Salmonella*, and *Shigella spp.* (He et al., 2004).

The TTSS and its effectors are essential for the pathogenicity and virulence of *Pst* DC3000 and other pathogens (Yuan and He, 1996; Deng et al., 1998; Collmer et al., 2002). Accumulated research results indicate that TTSS effectors contribute to pathogenicity and virulence by manipulating the physiological states of host plants (Nobuta and Meyers, 2005; Cunnac et al., 2009). These manipulations will be further discussed in later parts of this chapter.

On the other hand, coronatine is a phytotoxin made by several pathovars of *P.syringae* including *Pst* DC3000 (Bender et al., 1999). It is composed of two moieties, coronafacic acid and coronamic acid. The structure of coronatine shares a high similarity to that of jasmonoyl isoleucine (JA-Ile), and it has been thought that coronatine is a functional mimic of JA-Ile in plant-pathogen interactions (Katagiri et al., 2002; Melotto et al., 2008). The role of coronatine in pathogenicity and virulence of *Pst* DC3000 has been studied in *Arabidopsis* and tomato, and it is generally accepted that coronatine contributes to symptom development, activation of jasmonate (JA)-related responses and suppression of the expression of defense-related genes in plants (Mittal and Davis, 1995; Zhao et al., 2003; Thilmony et al., 2006). The JA-mediated defense pathways and the salicylic acid (SA)-mediated defense pathways are often antagonistic (Kunkel and Brooks, 2002; Heil and Bostock, 2002), and the suppression of SA-mediated defenses in plants by

coronatine was shown in multiple studies (Zhao et al., 2003; Uppalapati et al., 2007). More recently a role of coronatine in the regulation of stomatal opening was shown (Melotto et al., 2006; Melotto et al., 2008).

Arabidopsis thaliana as a model plant in plant-pathogen interactions

Arabidopsis thaliana has advantages in laboratory research due to its small plant size, short generation time (around 8 weeks), high seed production, natural self-pollination, small genome size and well-established genomic resource (Meyerowitz, 1987; Ausubel et al., 1995; Nobuta and Meyers, 2005). *Arabidopsis* has been used as a model plant for studying the interactions with several pathogenic *P.syringae* strains including *Pst* DC3000 and showed clear resistance or susceptibility to different strains of *P.syringae*, depending on the genotypes of those strains (Davis et al., 1991; Dong et al., 1991; Whalen et al., 1991; Ausubel et al., 1995). As mentioned above, *Arabidopsis* exhibits susceptibility to *Pst* DC3000, showing symptom development including water-soaking, chlorosis, and tissue necrosis, followed by death of whole plant (Katagiri et al., 2002).

A four-part model for the interaction between *Arabidopsis* and *Pst* DC3000

The *Arabidopsis*-*Pst* DC3000 interaction can be explained by a recently suggested “four-part model” (Bent and Mackey, 2007). This model shows the roles of TTSS effector proteins of *Pst* DC3000 in inducing plant resistance and susceptibility (Chisholm et al., 2006; Jones and Dangl, 2006; Bent and Mackey, 2007) and includes two major

concepts of two major plant defenses, PAMP-triggered immunity (PTI) and effector-triggered immunity (ETI). This model also reflects the hypothetical evolutionary steps of the interaction between *Arabidopsis* and *Pst* DC3000.

1st step: the activation of PAMP-triggered immunity (PTI)

In the first part of four-part model, generic, conserved components of micro-organismic pathogens called pathogen-associated molecular patterns (PAMPs), or more recently called microbe-associated molecular patterns (MAMPs: Ausubel, 2005), are perceived by plants. This recognition of PAMPs/MAMPs by plants activates a basal layer of defense responses, which are believed to be sufficient for preventing infections by a wide range of microbes (Alfano and Collmer, 2004; Nomura et al., 2005; Bent and Mackey, 2007). In recent reviews this layer of defense responses are referred to as PAMP-triggered immunity (PTI) (Chisholm et al., 2006; Jones and Dangl, 2006; Bent and Mackey, 2007). In earlier studies PTI was not an independent concept, but it was incorporated in “nonhost” resistance, which allows a given plant species to confer broad-spectrum resistance against most microorganisms (Heath, 2000; Nürnberger and Brunner, 2002; Mysore and Ryu, 2004). In this context PAMPs/MAMPs were studied as “general elicitors” activating defense responses in the species level (Boller, 1995; Nürnberger et al., 2004). However, the PTI is now accepted as the first line of plant defense against different microorganisms.

Well-known PTI-associated defense responses include formation of papillae (localized apposition of callose and other materials) in the plant cell wall, induction of defense genes, accumulation of reactive oxygen species (ROS) and plant secondary

metabolites (Alfano and Collmer, 2004; Nomura et al., 2005). Modification of the plant cell wall is likely an important part of plant immunity (Hauck et al., 2003; DebRoy et al., 2004; Keshavarzi et al., 2004).

Various PAMPs/MAMPs have been reported from different pathogens. They include bacterial flagellin, bacterial lipopolysaccharide (LPS), fungal cell wall components like chitin, heptagluco-sides of oomycetes, and fungal ergosterol (Nürnberg et al., 2004; Bent and Mackey, 2007). Among these PAMPs/MAMPs, bacterial flagellin (especially the 22-amino-acid conserved epitope in the N-terminus of flagellin (flg22)) has been well studied (Felix et al., 1999; Gomez-Gomez et al., 1999). The flg22 peptide is sufficient to induce PTI (Gomez-Gomez et al., 1999). Recognition of flg22 contributes to enhanced resistance against non-pathogenic bacteria (Hann and Rathjen, 2007). Flg22 is recognized by and binds to *Arabidopsis* FLS2, which is a transmembrane receptor protein with extracellular leucine-rich repeats (LRR) and intracellular protein kinase (Gomez-Gomez et al., 1999; Gomez-Gomez and Boller, 2000; Zipfel et al., 2004; Chinchilla et al., 2006). The recognition of flg22 by FLS2 enhances plant resistance against *Pst* DC3000, presumably through activation of downstream signal transduction pathways, including expression of defense-related genes (Asai et al., 2002; Navarro et al., 2004; Zipfel et al., 2004; Livaja et al., 2008).

Besides flagellin (or its flg22), the elongation factor Tu (EF-Tu) of bacteria was also reported as a PAMP/MAMP (Kunze et al., 2004). EF-Tu induces defense responses in plants including *Arabidopsis*, such as ethylene biosynthesis and oxidative burst (Kunze et al., 2004). Later, another *Arabidopsis* transmembrane LRR-receptor-like kinase, EFR, was reported as the binding receptor of EF-Tu (Zipfel et al., 2006). EFR and FLS2

induce a common set of defense-related responses, including oxidative burst and MAP kinase activation, after recognizing EF-Tu and flg22, respectively (Zipfel et al., 2006). LPS, another example of bacterial PAMPs/MAMPs, extracted from *Xanthomonas campestris* pv. *vesicatoria* induced papilla formation and delay of symptom development in pepper (Keshavarzi et al., 2004).

Although not common, there are a few cases that PAMPs/MAMPs induce localized cell death in nonhost plants. For example, the flagellin monomer or flg22 from *Pst* DC3000 induces cell death in *Nicotiana benthamiana*, which is a nonhost plant to *Pst* DC3000 (Taguchi et al., 2003; Hann and Rathjen, 2007). This cell death is dependent on an orthologue of *Arabidopsis* FLS2 in *N.benthamiana*, *NbFls2* (Hann and Rathjen, 2007). Also, certain LPS activates the generation of ROS and activations of defense genes associated with local cell death (Desaki et al., 2006).

2nd step: the suppression of PTI by TTSS effector proteins

In the 2nd step of the “four-part model”, successful pathogens including *Pst* DC3000 release pathogenic proteins, which target host plants and suppress PTI. TTSS effectors of *Pst* DC3000 is among the most extensively studied examples of PTI suppression by bacterial proteins.

As shown in previous reports, wild type bacterial pathogens with intact TTSS (Keshavarzi et al., 2004) or even specific TTSS effectors such as AvrPto (Hauck et al., 2003; He et al., 2006; Hann and Rathjen, 2007) suppress PTI. AvrPto was later shown to also suppress flg22-induced MAP kinase signal transduction pathways and early gene expressions for defense (He et al., 2006). Remarkably, it was recently shown that AvrPto

physically interacts with FLS2 or EFR to block innate immunity of *Arabidopsis* (Xiang et al., 2008). In addition to AvrPto, other TTSS effectors of *Pst* DC3000 like AvrPtoB (de Torres et al., 2006; Hann and Rathjen, 2007), HopM1 (DebRoy et al., 2004), HopU1 (Fu et al., 2007), AvrRpt2 and AvrRpm1 (Kim et al., 2005), or HopAO1 (also known as HopPtoD2 [Underwood et al., 2007; Guo et al., 2009]) suppress PTI.

The local cell death in nonhost plants is also a target of some TTSS effectors. AvrPto and AvrPtoB expressed in *Nicotiana benthamiana* suppresses the localized PAMP-induced cell death (Kang et al., 2004; Hann and Rathjen, 2007). There are cases in which the induction of certain plant genes during PTI is suppressed by TTSS effectors (de Torres et al., 2006; He et al., 2006; Underwood et al., 2007).

The suppression of PTI by the TTSS effectors often contributes to the enhanced multiplication of non-pathogens or mutants of virulent pathogens, as shown in the cases of AvrPto or AvrPtoB (Hauck et al., 2003; He et al., 2006; de Torres et al., 2006; Hann and Rathjen, 2007).

3rd step: the recognition of TTSS effectors by plants and activation of effector-triggered immunity (ETI)

The third part of the four-part model is essentially the classic gene-for-gene interaction model (Flor, 1971), in which TTSS effectors are recognized by plant resistance (R) proteins, followed by the eliciting of defense responses called the hypersensitive response (HR). It is a relatively recent trend that the gene-for-gene interaction is incorporated in the bigger plant-pathogen interaction model emphasizing its evolution as a counterattack to the suppression of plant defenses by TTSS effectors, and

it is called effector-triggered immunity (ETI) (Chisholm et al., 2006; Jones and Dangl, 2006; Bent and Mackey, 2007).

Gene-for-gene resistance was studied in the context of specific plant genotypes (for instance, cultivars) and specific pathogen genotypes (strain or race). According to this model, a plant-pathogen interaction can be compatible (leading to plant disease) or incompatible (leading to plant resistance). The incompatible interaction occurs when the plant expresses a specific plant resistance gene (*R*) and the (avirulent) pathogen expresses a specific avirulence (*avr*) gene (Dangl and Jones, 2001). During the incompatible interaction, downstream signal transduction pathways lead to defense responses, such as the expression of pathogenesis-related (PR) genes (Uknes et al., 1992), the rapid and localized cell death in the infected region (HR) (Heath, 2000), and the activation of systemic acquired resistance (SAR).

Many *avr* and *R* gene pairs have been discovered in various plant-pathogen interactions (Martin et al., 2003; Alfano and Collmer, 2004). In the four-part model, bacterial Avr proteins (TTSS effectors) suppress basal defense, and the R proteins detect this defense-suppressing virulence factors by detecting the effect of a TTSS effector on the designated host protein. The host protein which is affected by the TTSS effector is indispensable to the plant defense (Chisholm et al., 2006; Bent and Mackey, 2007). Initially it was thought that Avr proteins and R proteins were directly interacting and that this interaction activates downstream defense pathways. This is based on several examples of direct interactions between Avr proteins and R proteins, such as the interaction between Pi-ta of rice and AVR-Pita of rice blast fungus (*Magnaporthe grisea*) (Jia et al., 2000) and that between R proteins of flax and AvrL567 variants of rust

(*Melampsora lini*) (Dodds et al., 2006). However, this was not the case for the majority of Avr-R interactions, and an alternative explanation called “guard hypothesis” was introduced (Dangl and Jones, 2001). In this hypothesis, Avr proteins interact with and manipulate plant target proteins which are independent of, but often physically associated with, R proteins. This indirect recognition of Avr protein by R protein through the third plant target protein induces downstream defense pathways. The interaction between AvrPto of *P.syringae* and tomato proteins Pto and Prf is explained by the guard hypothesis: AvrPto physically interact with Pto (Scofield et al., 1996; Tang et al., 1996), which may be a virulence target in tomato, and this interaction is recognized by Prf followed by HR (Salmeron et al., 1996; van der Biezen and Jones, 1998; Dangl and Jones, 2001; Zipfel and Rathjen, 2008). Other TTSS effectors of *P.syringae*, AvrRpm1, AvrB or AvrRpt2 phosphorylates or eliminates RIN4, which is a regulator of basal defense of *Arabidopsis*, and these modifications of RIN4 activate RPM1- or RPS2-mediated defense responses (Mackey et al., 2002; Axtell and Staskawicz, 2003; Mackey et al., 2003).

Recently another model referred to as “decoy model” was introduced for explaining the relationship between Avr protein (TTSS effector), its corresponding R protein and the plant target protein of Avr protein. Compared to the guard hypothesis, in the decoy model the plant protein targeted by Avr protein (TTSS effector) does not have functions in virulence, and this target protein works as a decoy to detect pathogen effector protein (Zipfel and Rathjen, 2008; van der Hoorn and Kamoun, 2008).

4th part: evasion or suppression of ETI by pathogens through TTSS effectors

In the final part of the four-part model, ETI activated by the recognition of TTSS effectors by plant R proteins are evaded or suppressed (Bent and Mackey, 2007). The suppression of ETI is summarized in several reviews (Abramovitch and Martin, 2004; Nomura et al., 2005; Grant et al., 2006).

The HR induced by gene-for-gene resistance can be suppressed by TTSS effectors. Ritter and Dangl (1996) reported that AvrRpt2 suppresses HR and disease resistance activated by the AvrRpm1-RPM1 interaction in *Arabidopsis*. This suppression of HR by AvrRpt2 is mediated by the action of AvrRpt2 as a cysteine protease, cleaving *Arabidopsis* RIN4 which is required for HR activated by the AvrRpm1-RPM1 interaction (Axtell et al., 2003; Mackey et al., 2003). In addition, in the interaction between *P.syringae* pv. *phaseolicola* and soybean, it was shown that the TTSS effectors of *P.syringae* pv. *phaseolicola* can suppress HR induced by gene-for-gene resistance on the cultivar level (Jackson et al., 1999; Tsiamis et al., 2000). On the other hand, Abramovitch et al. (2003) showed that HR induced by AvrPto-Pto was suppressed by AvrPtoB; however, this result is based on the transient expression of AvrPto, Pto and AvrPtoB in the nonhost plant *N. benthamiana*, not in the host plant tomato or *Arabidopsis*.

Systemic acquired resistance (SAR)

Systemic acquired resistance (SAR) is a long-lasting, broad-spectrum resistance which is systemically induced in plant by pathogen infection (Durrant and Dong, 2004) and not included in the four-step model. SAR is usually activated during the incompatible interaction between a pathogen with an *avr* gene and a plant with an *R* gene (with HR). However, non-HR-inducing bacteria also can activate SAR through their

PAMPs/MAMPs, showing the systemic resistance against bacterial infection, accumulation of SA and defense-associated gene transcripts (such as flg22 or LPS: Mishina and Zeier, 2007). During SAR, local and systemic accumulation of salicylic acid (SA) occurs, followed by expression of defense-related genes such as pathogenesis-related (PR) genes and activation of signal transduction cascades (Durrant and Dong, 2004; Vlot et al., 2008).

Salicylic acid (SA) is an essential signal for SAR (Gaffney et al., 1993), and exogenous application of SA (Ryals et al., 1995) or SA analogues such as benzothiadiazole (BTH) or 2,6-dichloroisonicotinic acid (INA) can activate SAR as well (Uknes et al., 1992; Lawton et al., 1996). However, SA itself is not a mobile signal for activating SAR in systemic tissue (Vernooji et al., 1994). Several metabolites such as methyl salicylate (MeSA), jasmonic acid (JA) or azelaic acid were suggested as potential mobile signals in SAR (Park et al., 2007; Truman et al., 2007; Jung et al., 2009).

Research results show that SA induces redox reactions to reduce the protein NPR1 (non-expressor of pathogenesis-related 1, also known as non-immunity 1 (NIM1)), which is activated and moves to the nucleus of the plant cell in order to activate transcription of defense-related genes. This activation is regulated by several proteins in plants. Also, there are NPR1-independent signaling pathways affecting SAR activation and regulation (Durrant and Dong, 2004; Grant and Lamb, 2006; Loake and Grant, 2007). SA-mediated defense signaling pathway is also affected by cross-talk with other signaling pathways, including JA/ethylene, abscisic acid (ABA), and nitric oxide (NO)-mediated signaling pathways (Loake and Grant, 2007).

Suppression of defense-associated cellular trafficking pathway in plants by TTSS effectors

Recent literature suggests that plant vesicle trafficking machineries are associated with PTI, ETI and SAR, and are a target of TTSS effector-mediated suppression. The importance of vesicle trafficking system in plant defense was initially suggested from studies of cell wall-associated PTI, the formation of papillae. As briefly mentioned above, the papilla is a microscopic apposition which is formed in the intercellular space of the plant (apoplast) (Smart et al., 1985); it consists of heterogeneous materials such as callose (β -1,3-glucan), phenolics and proteins (reviewed by Schmelzer, 2002). Papilla formation were reported in the interactions between fungal pathogens (such as *Blumeria graminis* or *Erysiphe graminis*) and plants (Zeyen and Bushnell, 1979; Smart et al., 1985; Koga et al., 1990; Mendgen et al., 1995; Collins et al., 2003; Gjetting et al., 2004), as well as those between bacterial pathogens such as *P. syringae* or *Xanthomonas campestris* (Bestwick et al., 1995; Brown et al., 1995) and plants. Papillae also can be induced by treatment of PAMPs/MAMPs such as flg22 (Gomez-Gomez et al., 1999; Zipfel et al., 2004; de Torres et al., 2006).

It has been suggested that the cellular vesicle trafficking pathway is important for papilla deposition. Although callose is synthesized in the plasma membrane (Turner et al., 1998; Jacobs et al., 2003; Nishimura et al., 2003), earlier research results suggested that polarized vesicle trafficking may be involved in the formation of papillae (Bestwick et al., 1995; Mendgen et al., 1995). Later, more evidence showing that components of vesicle trafficking pathways of plants play roles in papilla formation was obtained. In particular, mutation of the *Arabidopsis PEN1* gene which encodes a plasma membrane syntaxin

(SYP121), which is a member of soluble *N*-ethylmaleimide-sensitive factor adaptor protein receptors (SNAREs) involved in vesicle docking to a target membrane (Bassham et al., 2008), resulted in delayed papilla formation in response to a fungal pathogen *Blumeria graminis* f.sp. *hordei* (*Bgh*) (Collins et al., 2003). Also, both PEN1 and its closest homologue SYP122 accumulated at the papilla formation site upon *Bgh* infection, indicating that vesicle trafficking plays an important role in papilla formation (Collins et al., 2003; Assaad et al., 2004).

Another syntaxin from *Nicotiana benthamiana*, *NbSYP132* (an orthologue of SYP132 in *Arabidopsis*), is required for gene-for-gene resistance activated by the AvrPto-Pto interaction and for extracellular accumulation of the PR1 protein. *NbSYP132* contributes to basal defense against the *hrpA*⁻ mutant of *Pst* DC3000 and SA-associated defense (Kalde et al., 2007). Also, an ER-chaperone BiP2 was required for SA-associated defense responses and PR1 accumulation in *Arabidopsis* (Wang et al., 2005). In addition, the importance of cellular trafficking in plant defense is suggested in several studies of gene expression profiling: microarray data of Wang et al. (2005) showed that protein secretion pathway-associated genes were included in the primary targets of *Arabidopsis NPR1*, which is a key regulator of SAR.

Hauck et al. (2003) showed that around 40% of the *Arabidopsis* genes which are suppressed by a TTSS-dependent manner encoded putative secretion-related proteins. Similar results were obtained later in a whole-genome microarray study (Thilmony et al., 2006). Supporting evidence for the hypothesis that TTSS effectors suppress defense-associated cellular trafficking pathway(s) comes from the following studies: one of the putative host cellular targets of AvrPto is *Arabidopsis* RabE1d, which is involved in

vesicle targeting (Speth et al., 2009). A TTSS effector of *Xanthomonas campestris* pv. *vesicatoria* (XopJ) suppresses cell wall-associated PTI by interfering with plant protein secretion (Bartetzko et al., 2009). Finally, research on the *Pst* DC3000 effector HopM1 provide more detailed information, as summarized below, about the action of a TTSS effector on the defense-associated trafficking mechanisms in host plants (Badel et al., 2003; DebRoy et al., 2004; Badel et al., 2006; Nomura et al., 2006).

HopM1 and AtMIN7: a TTSS effector involved in the suppression of defense-associated cellular trafficking pathway(s) and its target in Arabidopsis

HopM1 is one of the TTSS effectors whose contribution to the virulence of *Pst* DC3000 was experimentally confirmed (Badel et al., 2003; DebRoy et al., 2004). The virulence-associated functions of HopM1 were mainly studied in cell wall-associated PTI: transgenic expression of HopM1 in *Arabidopsis* plants caused suppression of papilla formation, restored multiplication of the *Pst* DC3000 Δ CEL mutant, in which *hopM1* and several adjacent TTSS effector genes are deleted (Alfano et al., 2000), and eventually caused tissue death (Nomura et al., 2006). Nomura et al. (2006) found that HopM1 interacts and destroys several *Arabidopsis* proteins (AtMINs), including AtMIN7. AtMIN7 is a member of the *Arabidopsis* adenosine-diphosphate ribosylation factor-guanine nucleotide-exchanging factor (ARF-GEF) family, whose members have roles in vesicle formation for intracellular trafficking (Memon, 2004; Gillingham and Munro, 2007; Anders and Jürgens, 2008; Bassham et al., 2008). T-DNA insertional mutants of *AtMIN7* show enhanced multiplication of the Δ CEL mutant of *Pst* DC3000 (Nomura et al., 2006). Also, callose deposition in papillae of *atmin7* by the Δ CEL mutant is reduced

compared with that in wild-type *Arabidopsis* plants (Nomura et al., 2006). Therefore, AtMIN7 functions in the defense-associated vesicle trafficking pathway(s), and HopM1 interferes with the action of AtMIN7 by degrading it.

Summary of thesis research subjects

One of the major questions in the study of plant-pathogen interactions is how a virulent pathogen suppresses the plant defense mechanisms. Various mechanisms of suppression of plant defenses by pathogens have begun to be determined. In the interaction between *Pst* DC3000 and *Arabidopsis thaliana*, it has been suggested that one function of TTSS effector proteins of *Pst* DC3000 is to interfere with the defense-associated cellular trafficking pathway(s) in *Arabidopsis*. The strongest evidence for this comes from the discovery of the action of HopM1 on AtMIN7 in *Arabidopsis* (Nomura et al., 2006). The activity of HopM1 on a regulator of vesicle trafficking is intriguing and raises a number of questions for further study. My thesis research focuses on answering some of these questions.

In chapter 2, I describe the results of my study to determine the subcellular localization of HopM1 in plant cells. In a membrane fractionation experiment, HopM1 was not present in the plasma membrane, but was detected in an unidentified endomembrane compartment of *Arabidopsis* cells (Nomura et al., 2006). To more precisely determine the localization of HopM1 in plant cells, I constructed fusions of HopM1 with fluorescence proteins, and examined the localization of these fusion proteins by confocal microscopy.

As mentioned above, there are seven other ARF GEF genes in *Arabidopsis*, besides AtMIN7 (Cox et al., 2004; Anders and Jürgens, 2008). In chapter 3, I describe my study to determine whether any of these other *ARF-GEF* genes has a role in defense. Nomura et al (2006) studied this possibility with a few *ARF-GEF* genes, but not all *ARF-GEF* genes were studied. Therefore, I focused on the unstudied *ARF-GEF* genes using two approaches: one was yeast two-hybrid assay between ARF-GEFs and HopM1 in order to determine whether HopM1 interact with those ARF-GEFs in addition to AtMIN7. The other was the investigation of multiplication of the Δ CEL mutant in T-DNA insertional mutants of these ARF-GEF genes to determine if mutants of other *ARF-GEF* genes, like *atmin7*, also showed enhanced multiplication of the Δ CEL mutant.

In chapter 4, I describe a study of several defense-associated *Arabidopsis* extracellular proteins. By tagging them with fluorescence proteins and confocal microscopic examination, I monitored the localization of those fluorescence protein fusions in wild type and *atmin7* background to determine whether the secretion of these selected *Arabidopsis* extracellular proteins is affected in the *atmin7* background.

REFERENCES

- Abramovitch, R.B., Kim, Y.J., Chen, S., Dickman, M.B., and Martin, G.B. (2003) *Pseudomonas* type III effector AvrPtoB induces plant disease susceptibility by inhibition of host programmed cell death. *EMBO J* **22**: 60-69.
- Abramovitch, R.B. and Martin, G.B. (2004) Strategies used by bacterial pathogens to suppress plant defenses. *Curr Opin Plant Biol* **7**: 356-364.
- Alfano, J.R. and Collmer, A. (1997) The type III (Hrp) secretion pathway of plant pathogenic bacteria: trafficking harpins, Avr proteins, and Death. *J Bacteriol* **179**: 5655-5662.
- Alfano, J.R., Charkowski, A.O., Deng, W.L., Badel, J.L., Petnicki-Ocwieja, T., van Dijk, K., and Collmer, A. (2000) The *Pseudomonas syringae* Hrp pathogenicity island has a tripartite mosaic structure composed of a cluster of type III secretion genes bounded by exchangeable effector and conserved effector loci that contribute to parasitic fitness and pathogenicity in plants. *Proc Natl Acad Sci U S A* **97**: 4856-4861.
- Alfano, J.R. and Collmer, A. (2004) Type III secretion system effector proteins: double agents in bacterial disease and plant defense. *Annu Rev Phytopathol* **42**: 385-414.
- Anders, N. and Jürgens, G. (2008) Large ARF guanine nucleotide exchange factors in membrane trafficking. *Cell Mol Life Sci* **65**: 3433-3445.
- Anzai, Y., Kim, H., Park, J.Y., Wakabayashi, H., and Oyaizu, H. (2000) Phylogenetic affiliation of the *Pseudomonads* based on 16S rRNA sequence. *Int J Syst Evol Microbiol* **50**: 1563-1589.
- Asai, T., Tena, G., Plotnikova, J., Willmann, M.R., Chiu, W.-L., Gomez-Gomez, L., Boller, T., Ausubel, F.M., and Sheen, J. (2002) MAP kinase signalling cascade in *Arabidopsis* innate immunity. *Nature* **415**: 977-983.
- Assaad, F.F., Qiu, J.L., Youngs, H., Ehrhardt, D., Zimmerli, L., Kalde, M., Wanner, G., Peck, S.C., Edwards, H., Ramonell, K., Somerville, C.R., and Thordal-Christensen, H. (2004) The PEN1 syntaxin defines a novel cellular compartment upon fungal attack and is required for the timely assembly of papillae. *Mol Biol Cell* **15**: 5118-5129.
- Ausubel, F.M., Katagiri, F., Mindrinos, M., and Glazebrook, J. (1995) Use of *Arabidopsis thaliana* defense-related mutants to dissect the plant response to pathogens. *Proc Natl Acad Sci USA* **92**: 4189-4196.

- Ausubel, F.M. (2005) Are innate immune signaling pathways in plants and animals conserved? *Nat Immunol* **6**: 973-979.
- Axtell, M.J., Chisholm, S.T., Dahlbeck, D., and Staskawicz, B.J. (2003) Genetic and molecular evidence that the *Pseudomonas syringae* type III effector protein AvrRpt2 is a cysteine protease. *Mol Microbiol* **49**:1537-1546.
- Axtell, M.J. and Staskawicz, B.J. (2003) Initiation of RPS2-specified disease resistance in *Arabidopsis* is coupled to the AvrRpt2-directed elimination of RIN4. *Cell* **112**: 369-377.
- Badel, J.L., Nomura, K., Bandyopadhyay, S., Shimizu, R., Collmer, A., and He, S.Y. (2003) *Pseudomonas syringae* pv. *tomato* DC3000 HopPtoM (CEL ORF3) is important for lesion formation but not growth in tomato and is secreted and translocated by the Hrp type III secretion system in a chaperone-dependent manner. *Mol Microbiol* **49**: 1239-1251.
- Badel, J.L., Shimizu, R., Oh, H.S., and Collmer, A. (2006) A *Pseudomonas syringae* pv. *tomato* avrE1/hopM1 mutant is severely reduced in growth and lesion formation in tomato. *Mol Plant-Microbe Interact* **19**:99-111.
- Bartetzko, V., Sonnewald, S., Vogel, F., Hartner, K., Stadler, R., Hammes, U.Z., and Börnke, F. (2009) The *Xanthomonas campestris* pv. *vesicatoria* Type III effector protein XopJ inhibits protein secretion: evidence for interference with cell wall-associated defense responses. *Mol Plant-Microbe Interact* **22**: 655-664.
- Bassham, D.C., Brandizzi, F., Otegui, M.S., and Sanderfoot, A.A. (2008) The secretory system of Arabidopsis: September 30, 2008. The *Arabidopsis* Book. Rockville, MD: American Society of Plant Biologists.
<http://www.aspb.org/publications/arabidopsis/>
- Bender, C.L., Alarcón-Chaidez, F, and Gross, D.C. (1999) *Pseudomonas syringae* phytotoxins: mode of action, regulation, and biosynthesis by peptide and polyketide synthetases. *Microbiol Mol Biol Rev* **63**: 266-292.
- Bent, A.F. and Mackey, D. (2007) Elicitors, effectors, and R genes: the new paradigm and a lifetime supply of questions. *Annu Rev Phytopathol* **45**: 399-436.
- Bestwick, C.S., Bennett, M.H., and Mansfield, J.W. (1995) Hrp mutant of *Pseudomonas syringae* pv. *phaseolicola* induces cell wall alterations but not membrane damage leading to the hypersensitive reaction in lettuce. *Plant Physiol* **108**: 503-516.
- Bestwick, C.S., Brown, I.R., Bennett, M.H., and Mansfield, J.W. (1997) Localization of hydrogen peroxide accumulation during the hypersensitive reaction of lettuce cells to *Pseudomonas syringae* pv. *phaseolicola*. *Plant Cell* **9**: 209-221.

- Boller, T. (1995) Chemoperception of microbial signals in plant cells. *Annu Rev Plant Physiol Plant Mol Biol* **46**: 189-214.
- Boller, T. and He, S.Y. (2009) Innate immunity in plants: an arms race between pattern recognition receptors in plants and effectors in microbial pathogens. *Science* **324**:742-744.
- Bretz, J.R., Mock, N.M., Charity, J.C., Zeyad, S., Baker, C.J., and Hutcheson, S.W. (2003) A translocated protein tyrosine phosphatase of *Pseudomonas syringae* pv. *tomato* DC3000 modulates plant defence response to infection. *Mol Microbiol* **49**: 389-400.
- Brown, I., Mansfield, J., and Bonas, U. (1995) Hrp genes in *Xanthomonas campestris* pv. *vesicatoria* determine ability to suppress papilla deposition in pepper mesophyll cells. *Mol Plant-Microbe Interact* **8**: 825-836.
- Buell, C.R., Joardar, V., Lindeberg, M., Selengut, J., Paulsen, I.T., Gwinn, M.L., Dodson, R.J., Deboy, R.T., Durkin, A.S., Kolonay, J.F., Madupu, R., Daugherty, S., Brinkac, L., Beanan, M.J., Haft, D.H., Nelson, W.C., Davidsen, T., Zafar, N., Zhou, L., Liu, J., Yuan, Q., Khouri, H., Fedorova, N., Tran, B., Russell, D., Berry, K., Utterback, T., Van Aken, S.E., Feldblyum, T.V., D'Ascenzo, M., Deng, W.-L., Ramos, A.R., Alfano, J.R., Cartinhour, S., Chatterjee, A.K., Delaney, T.P., Lazarowitz, S.G., Martin, G.B., Schneider, D.J., Tang, X., Bender, C.L., White, O., Fraser, C.M., and Collmer, A. (2003) The complete genome sequence of the *Arabidopsis* and tomato pathogen *Pseudomonas syringae* pv. *tomato* DC3000. *Proc Natl Acad Sci U S A* **100**: 10181-10186.
- Chinchilla, D., Bauer, Z., Regenass, M., Boller, T., and Felix, G. (2006) The *Arabidopsis* receptor kinase FLS2 binds flg22 and determines the specificity of flagellin perception. *Plant Cell* **18**: 465-476.
- Chisholm, S.T., Coaker, G., Day, B., and Staskawicz, B.J. (2006) Host-microbe interactions: shaping the evolution of the plant immune response. *Cell* **124**: 803-814.
- Collins, N.C., Thordal-Christensen, H., Lipka, V., Bau, S., Kombrink, E., Qiu, J.L., Huckelhoven, R., Stein, M., Freialdenhoven, A., Somerville, S.C., and Schulze-Lefert, P. (2003) SNARE-protein-mediated disease resistance at the plant cell wall. *Nature* **425**: 973-977.
- Collmer, A., Lindeberg, M., Petnicki-Ocwieja, T., Schneider, D.J., and Alfano, J.R. (2002) Genomic mining type III secretion system effectors in *Pseudomonas syringae* yields new picks for all TTSS prospectors. *Trends Microbiol* **10**: 462-469.
- Cox, R., Mason-Gamer, R.J., Jackson, C.L., and Segev, N. (2004) Phylogenetic analysis of Sec7-domain-containing Arf nucleotide exchangers. *Mol Biol Cell* **15**: 1487-

1505.

- Cunnac, S., Lindeberg, M., and Collmer, A. (2009) *Pseudomonas syringae* type III secretion system effectors: repertoires in search of functions. *Curr Opin Microbiol* **12**: 53-60.
- Cuppels, D.A. (1986) Generation and Characterization of Tn5 insertion mutations in *Pseudomonas syringae* pv. *tomato*. *Appl Environ Microbiol* **51**: 323-327.
- Cuppels, D.A., Moore, R.A., and Morris, V.L. (1990) Construction and use of a nonradioactive DNA hybridization probe for detection of *Pseudomonas syringae* pv. *tomato* on tomato plants. *Appl Environ Microbiol* **56**: 1743-1749.
- Dangl, J.L. and Jones, J.D. (2001) Plant pathogens and integrated defense responses to infection. *Nature* **411**: 826-833.
- Davis, K.R., Schott, E. and Ausubel, F.M. (1991) Virulence of selected phytopathogenic *Pseudomonads* in *Arabidopsis thaliana*. *Mol Plant-Microbe Interact* **4**: 477-488.
- DebRoy, S., Thilmony, R., Kwack, Y.B., Nomura, K., and He, S.Y. (2004) A family of conserved bacterial effectors inhibits salicylic acid-mediated basal immunity and promotes disease necrosis in plants. *Proc Natl Acad Sci U S A* **101**: 9927-9932.
- Deng, W.L., Preston, G., Collmer, A., Chang, C.J., and Huang, H.C. (1998) Characterization of the *hrpC* and *hrpRS* operons of *Pseudomonas syringae* pathovars *syringae*, *tomato*, and *glycinea* and analysis of the ability of *hrpF*, *hrpG*, *hrcC*, *hrpT*, and *hrpV* mutants to elicit the hypersensitive response and disease in plants. *J Bacteriol* **180**: 4523-4531.
- Desaki, Y., Miya, A., Venkatesh, B., Tsuyumu, S., Yamane, H., Kaku, H., Minami, E., and Shibuya, N. (2006) Bacterial lipopolysaccharides induce defense responses associated with programmed cell death in rice cells. *Plant Cell Physiol* **47**: 1530-1540.
- Dodds, P.N., Lawrence, G.J., Catanzariti, A-M., Teh, T., Wang, C.I., Ayliffe, M.A., Kobe, B., and Ellis, J.G. (2006) Direct protein interaction underlies gene-for-gene specificity and coevolution of the flax resistance genes and flax rust avirulence genes. *Proc Natl Acad Sci U S A* **103**: 8888-8893.
- Dong, X., Mindrinos, M., Davis, K.R., and Ausubel, F.M. (1991) Induction of *Arabidopsis* defense genes by virulent and avirulent *Pseudomonas syringae* strains and by a cloned avirulence gene. *Plant Cell* **3**: 61-72.
- Durrant, W.E. and Dong, X. (2004) Systemic acquired resistance. *Annu Rev Phytopathol* **42**: 185-209.

- Felix, G., Duran, J.D., Volko, S., and Boller, T. (1999) Plants have a sensitive perception system for the most conserved domain of bacterial flagellin. *Plant J* **18**: 265-276.
- Flor, H.H. (1971) Current status of the gene-for-gene concept. *Annu Rev Phytopathol* **9**: 275-296.
- Fu, Z.Q., Guo, M., Jeong, B.R., Tian, F., Elthon, T.E., Cerny, R.L., Staiger, D., and Alfano, J.R. (2007) A type III effector ADP-ribosylates RNA-binding proteins and quells plant immunity. *Nature* **447**: 284-288.
- Gaffney, T., Friedrich, L., Vernooij, B., Negrotto, D., Nye, G., Uknes, S., Ward, E., Kessmann, H., and Ryals, J. (1993) Requirement of salicylic acid for the induction of systemic acquired resistance. *Science* **261**: 754-756.
- Gardan, L., Shafik, H., Belouin, S., Broch, R., Grimont, F., and Grimont, P.A. (1999) DNA relatedness among the pathovars of *Pseudomonas syringae* and description of *Pseudomonas tremiae* sp. nov. and *Pseudomonas cannabina* sp. nov. (ex Sutic and Dowson 1959). *Int J Syst Bacteriol* **49**: 469-478.
- Gillingham, A.K. and Munro, S. (2007) The small G proteins of the Arf family and their regulators. *Annu Rev Cell Dev Biol* **23**: 579-611.
- Gjetting, T., Carver, T.L., Skot, L., and Lyngkjaer, M.F. (2004) Differential gene expression in individual papilla-resistant and powdery mildew-infected barley epidermal cells. *Mol Plant-Microbe Interact* **17**: 729-738.
- Gomez-Gomez, L., Felix, G., and Boller, T. (1999) A single locus determines sensitivity to bacterial flagellin in *Arabidopsis thaliana*. *Plant J* **18**: 277-284.
- Gomez-Gomez, L., and Boller, T. (2000) FLS2: An LRR receptor-like kinase involved in the perception of the bacterial elicitor flagellin in *Arabidopsis*. *Mol Cell* **5**: 1003-1011.
- Grant, S.R., Fisher, E.J., Chang, J.H., Mole, B.M., and Dangl, J.L. (2006) Subterfuge and manipulation: type III effector proteins of phytopathogenic bacteria. *Annu Rev Microbiol* **60**: 425-449.
- Grant, M. and Lamb, C. (2006) Systemic immunity. *Curr Opin Plant Biol* **9**: 414-420.
- Guo, M., Tian, F., Wamboldt, Y., and Alfano, J.R. (2009) The majority of the type III effector inventory of *Pseudomonas syringae* pv. *tomato* DC3000 can suppress plant immunity. *Mol Plant-Microbe Interact* **22**: 1069-1080.
- Hann, D.R. and Rathjen, J.P. (2007) Early events in the pathogenicity of *Pseudomonas syringae* on *Nicotiana benthamiana*. *Plant J* **49**: 607-618.

- Hauck, P., Thilmony, R., and He, S.Y. (2003) A *Pseudomonas syringae* type III effector suppresses cell wall-based extracellular defense in susceptible *Arabidopsis* plants. *Proc Natl Acad Sci U S A* **100**: 8577-8582.
- He, S.Y., Nomura, K., and Whittam, T.S. (2004) Type III protein secretion mechanism in mammalian and plant pathogens. *Biochim Biophys Acta - Mol Cell Res* **1694**: 181-206.
- He, P., Shan, L., Lin, N.C., Martin, G.B., Kemmerling, B., Nürnberger, T., and Sheen, J. (2006) Specific bacterial suppressors of MAMP signaling upstream of MAPKKK in *Arabidopsis* innate immunity. *Cell* **125**: 563-575.
- Heath, M.C. (2000) Nonhost resistance and nonspecific plant defenses. *Curr Opin Plant Biol* **3**: 315-319.
- Heil, M. and Bostock, R.M. (2002) Induced systemic resistance (ISR) against pathogens in the context of induced plant defences. *Annu Bot.* **89**: 503-512.
- Hirano, S.S. and Upper, C.D. (2000) Bacteria in the leaf ecosystem with emphasis on *Pseudomonas syringae*-a pathogen, ice nucleus, and epiphyte. *Microbiol Mol Biol Rev* **64**: 624-653.
- Jackson, R.W., Athanassopoulos, E., Tsiamis, G., Mansfield, J.W., Sesma, A., Arnold, D.L., Gibbon, M.J., Murillo, J., Taylor, J.D., and Vivian, A. (1999) Identification of a pathogenicity island, which contains genes for virulence and avirulence, on a large native plasmid in the bean pathogen *Pseudomonas syringae* pathovar *phaseolicola*. *Proc Natl Acad Sci U S A* **96**: 10875-10880.
- Jacobs, A.K., Lipka, V., Burton, R.A., Panstruga, R., Strizhov, N., Schulze-Lefert, P., and Fincher, G.B. (2003) An *Arabidopsis* callose synthase, GSL5, is required for wound and papillary callose formation. *Plant Cell* **15**: 2503-2513.
- Jia, Y., McAdams, S.A., Bryan, G.T., Hershey, H.P., and Valent, B. (2000) Direct interaction of resistance gene and avirulence gene products confers rice blast resistance. *EMBO J* **19**: 4004-4014.
- Jones, J.D.G., and Dangl, J.L. (2006) The plant immune system. *Nature* **444**: 323-329.
- Jung, H.W., Tschaplinski, T.J., Wang, L., Glazebrook, J., and Greenberg, J.T. (2009) Priming in systemic plant immunity. *Science*. 2009 **324**: 89-91.
- Kalde, M., Nühse, T.S., Findlay, K., and Peck, S.C. (2007) The syntaxin SYP132 contributes to plant resistance against bacteria and secretion of pathogenesis-related protein 1. *Proc Natl Acad Sci U S A* **104**: 11850-11855.
- Kang, L., Tang, X. and Mysore, K.S. (2004) *Pseudomonas* Type III effector AvrPto

- suppresses the programmed cell death induced by two nonhost pathogens in *Nicotiana benthamiana* and tomato. *Mol Plant-Microbe Interact* **17**: 1328–1336.
- Katagiri, F., Thilmony, R., and He, S.Y. (2002) The *Arabidopsis thaliana*-*Pseudomonas syringae* interaction. CR Somerville, EM Meyerowitz, eds., *The Arabidopsis Book*. American Society of Plant Biologists, Rockville, MD, <http://www.aspb.org/publications/arabidopsis/>.
- Keshavarzi, M., Soylu, S., Brown, I., Bonas, U., Nicole, M., Rossiter, J., and Mansfield, J. (2004) Basal defenses induced in pepper by lipopolysaccharides are suppressed by *Xanthomonas campestris* pv. *vesicatoria*. *Mol Plant-Microbe Interact* **17**: 805-815.
- Kim, M.G., da Cunha, L., McFall, A.J., Belkadir, Y., DebRoy, S., Dangl, J.L., and Mackey, D. (2005) Two *Pseudomonas syringae* type III effectors inhibit RIN4-regulated basal defense in *Arabidopsis*. *Cell* **121**: 749-759.
- Koga, H. Bushnell, W.R. and Zeyen, R.J. (1990) Specificity of cell type and timing of events associated with papilla formation and the hypersensitive reaction in leaves of *Hordeum vulgare* attacked by *Erysiphe graminis* f. sp. *hordei*. *Can J Bot* **68**: 2344-2352.
- Kunze, G., Zipfel, C., Robatzek, S., Niehaus, K., Boller, T., and Felix, G. (2004) The N terminus of bacterial elongation factor Tu elicits innate immunity in *Arabidopsis* plants. *Plant Cell* **16**: 3496-3507.
- Kunkel, B.N. and Brooks, D.M. (2002) Cross talk between signaling pathways in pathogen defense. *Curr Opin Plant Biol* **5**: 325-331.
- Lawton, K.A., Friedrich, L., Hunt, M., Weymann, K., Delaney, T., Kessmann, H., Staub, T., and Ryals, J. (1996) Benzothiadiazole induces disease resistance in *Arabidopsis* by activation of the systemic acquired resistance signal transduction pathway. *Plant J* **10**: 71-82.
- Livaja, M., Zeidler, D., von Rad, U., and Durner, J. (2008) Transcriptional responses of *Arabidopsis thaliana* to the bacteria-derived PAMPs harpin and lipopolysaccharide. *Immunobiology* **213**: 161-171.
- Loake, G. and Grant, M. (2007) Salicylic acid in plant defence-the players and protagonists. *Curr Opin Plant Biol* **10**: 466-477.
- Ma, W., Dong, F.F., Stavrinides, J., and Guttman, D.S. (2006) Type III effector diversification via both pathoadaptation and horizontal transfer in response to a coevolutionary arms race. *PLoS Genet* **2**: e209.
- Mackey, D., Holt, B.F. 3rd, Wiig, A., and Dangl, J.L. (2002) RIN4 interacts with

- Pseudomonas syringae* type III effector molecules and is required for RPM1-mediated resistance in *Arabidopsis*. *Cell* **108**: 743-754.
- Mackey, D., Belkhadir, Y., Alonso, J.M., Ecker, J.R., and Dangl, J.L. (2003) *Arabidopsis* RIN4 is a target of the type III virulence effector AvrRpt2 and modulates RPS2-mediated resistance. *Cell* **112**: 379-389.
- Martin, G. B., Bogdanove, A. J., and Sessa, G. (2003) Understanding the functions of plant disease resistance proteins. *Annu Rev Plant Biol* **54**: 23-61.
- Melotto, M., Underwood, W., Koczan, J., Nomura, K., and He, S.Y. (2006) Plant stomata function in innate immunity against bacterial invasion. *Cell* **126**: 969-980.
- Melotto, M., Underwood, W., and He, S.Y. (2008) Role of stomata in plant innate immunity and foliar bacterial disease. *Annu Rev Phytopathol* **46**: 101-122.
- Memon, A.R. (2004) The role of ADP-ribosylation factor and SAR1 in vesicular trafficking in plants. *Biochim Biophys Acta* **1664**: 9-30.
- Mendgen, K., B.achem, U., Stark-Urnau, M., and Xu, H. (1995) Secretion and endocytosis at the interface of plants and fungi. *Can J Bot* **73**: S640-S648.
- Meyerowitz, E.M. (1987) *Arabidopsis thaliana*. *Annu Rev Genet* **21**: 93-111.
- Mishina, T.E. and Zeier, J. (2007) Pathogen-associated molecular pattern recognition rather than development of tissue necrosis contributes to bacterial induction of systemic acquired resistance in *Arabidopsis*. *Plant J* **50**: 500-513.
- Mittal, S. and Davis, K.R. (1995) Role of the phytotoxin coronatine in the infection of *Arabidopsis thaliana* by *Pseudomonas syringae* pv. *tomato*. *Mol Plant-Microbe Interact* **8**: 165-171.
- Mysore, K.S. and Ryu, C.M. (2004) Nonhost resistance: how much do we know? *Trends Plant Sci* **9**: 97-104.
- Navarro, L., Zipfel, C., Rowland, O., Keller, I., Robatzek, S., Boller, T., and Jones, J.D. (2004) The transcriptional innate immune response to flg22. Interplay and overlap with Avr gene-dependent defense responses and bacterial pathogenesis. *Plant Physiol.* **135**: 1113-1128.
- Nishimura, M.T., Stein, M., Hou, B.H., Vogel, J.P., Edwards, H., and Somerville S.C. (2003) Loss of a callose synthase results in salicylic acid-dependent disease resistance. *Science* **301**: 969-972.
- Nobuta, K. and Meyers, B.C. (2005) *Pseudomonas* versus *Arabidopsis*: models for genomic research into plant disease resistance. *BioScience* **55**: 679-686.

- Nomura, K., Melotto, M., and He, S.Y. (2005) Suppression of host defense in compatible plant-*Pseudomonas syringae* interactions. *Curr Opin Plant Biol* **8**: 361-368.
- Nomura, K., Debroy, S., Lee, Y.H., Pumplin, N., Jones, J., and He, S.Y. (2006). A bacterial virulence protein suppresses host innate immunity to cause plant disease. *Science* **313**: 220-223.
- Nürnberger, T. and Brunner, F. (2002) Innate immunity in plants and animals: emerging parallels between the recognition of general elicitors and pathogen-associated molecular patterns. *Curr Opin Plant Biol* **5**: 318-324.
- Nürnberger, T., Brunner, F., Kemmerling, B., and Piater, L. (2004) Innate immunity in plants and animals: striking similarities and obvious differences. *Immunol Rev* **198**: 249-266.
- Park, S.W., Kaimoyo, E., Kumar, D., Mosher, S., and Klessig, D.F. (2007) Methyl salicylate is a critical mobile signal for plant systemic acquired resistance. *Science* **318**: 113-116.
- Rhee, S.Y., Beavis, W., Berardini, T.Z., Chen, G., Dixon, D., Doyle, A., Garcia-Hernandez, M., Huala, E., Lander, G., Montoya, M., Miller, N., Mueller, L.A., Mundodi, S., Reiser, L., Tacklind, J., Weems, D.C., Wu, Y., Xu, I., Yoo, D., Yoon, J., and Zhang, P. (2003) The *Arabidopsis* Information Resource (TAIR): a model organism database providing a centralized, curated gateway to *Arabidopsis* biology, research materials and community. *Nucleic Acids Research* **31**: 224-8.
- Ritter, C. and Dangl, J.L. (1996) Interference between two specific pathogen recognition events mediated by distinct plant disease resistance genes. *Plant Cell* **8**: 251-257.
- Roine, E., Wei, W., Yuan, J., Nurmiaho-Lassila, E.-L., Kalkkinen, N., Romantschuk, M., and He, S.Y. (1997) Hrp pilus: an Hrp-dependent bacterial surface appendage produced by *Pseudomonas syringae* pv. *tomato* DC3000. *Proc Natl Acad Sci U S A* **94**: 3459-3464.
- Ronald, P. C., J. M. Salmeron, F. M. Carland, and B. J. Staskawicz. (1992) The cloned avirulence gene *avrPto* induces disease resistance in tomato cultivars containing the *Pto* resistance gene. *J Bacteriol* **174**: 1604-1611.
- Ryals, J., Lawton, K.A., Delaney, T.P., Friedrich, L., Kessmann, H., Neuenschwander, U., Uknes, S., Vernooij, B., and Weymann, K. (1995) Signal transduction in systemic acquired resistance. *Proc Natl Acad Sci U S A* **92**: 4202-4205.
- Salmeron, J.M., Oldroyd, G.E., Rommens, C.M., Scofield, S.R., Kim, H.S., Lavelle, D.T., Dahlbeck, D., and Staskawicz, B.J. (1996) Tomato Prf is a member of the leucine-rich repeat class of plant disease resistance genes and lies embedded within the *Pto* kinase gene cluster. *Cell* **86**: 123-133.

- Savary, S., Teng, P.S., Willocquet, L., and Nutter, F.W. Jr. (2006) Quantification and modeling of crop losses: a review of purposes. *Annu Rev Phytopathol* **44**: 89-112.
- Schmelzer, E. (2002) Cell polarization, a crucial process in fungal defense. *Trends Plant Sci.* **7**: 411-415.
- Scofield, S.R., Tobias, C.M., Rathjen, J.P., Chang, J.H., Lavelle, D.T., Michelmore, R.W., and Staskawicz, B.J. (1996) Molecular basis of gene-for-gene specificity in bacterial speck disease of tomato. *Science* **274**: 2063-2065.
- Smart, M.G., Aist, J.R., and Israel, H.W. (1985) Structure and function of wall appositions. 1. General histochemistry of papillae in barley coleoptiles attacked by *Erysiphe graminis* f. sp. *hordei*. *Can J Bot* **64**: 793-801.
- Speth, E.B., Lee, Y.N., and He, S.Y. (2007) Pathogen virulence factors as molecular probes of basic plant cellular functions. *Curr Opin Plant Biol* **10**: 580-586.
- Speth, E.B., Imboden, L., Hauck, P., and He, S.Y. (2009) Subcellular localization and functional analysis of the *Arabidopsis* GTPase RabE. *Plant Physiol* **149**: 1824-1837.
- Stavrinos, J., McCann, H.C., and Guttman, D.S. (2008) Host-pathogen interplay and the evolution of bacterial effectors. *Cell Microbiol* **10**: 285-292.
- Taguchi, F., Shimizu, R., Inagaki, Y., Toyoda, K., Shirashi, T. and Ichinose, Y. (2003) Post-translational modification of flagellin determines the specificity of HR induction. *Plant Cell Physiol.* **44**: 342-349.
- Tang, X., Frederick, R.D., Zhou, J., Halterman, D.A., Jia, Y., and Martin, G.B. (1996) Initiation of plant disease resistance by physical interaction of AvrPto and Pto kinase. *Science* **274**: 2060-2063.
- Thilmony, R., Underwood, W., and He, S.Y. (2006) Genome-wide transcriptional analysis of the *Arabidopsis thaliana* interaction with the plant pathogen *Pseudomonas syringae* pv. *tomato* DC3000 and the human pathogen *Escherichia coli* O157:H7. *Plant J* **46**: 34-53.
- de Torres, M., Mansfield, J.W., Grabov, N., Brown, I.R., Ammoun, H., Tsiamis, G., Forsyth, A., Robatzek, S., Grant, M., and Boch, J. (2006) *Pseudomonas syringae* effector AvrPtoB suppresses basal defense in *Arabidopsis*. *Plant J* **47**: 368-382.
- Tsiamis, G., Mansfield, J.W., Hockenull, R., Jackson, R.W., Sesma, A., Athanassopoulos, E., Bennett, M.A., Stevens, C., Vivian, A., Taylor, J.D., and Murillo, J. (2000) Cultivar-specific avirulence and virulence functions assigned to avrPphF in *Pseudomonas syringae* pv. *phaseolicola*, the cause of bean halo-blight disease. *EMBO J* **19**: 3204-3214.

- Truman, W., Bennett, M.H., Kubigsteltig, I., Turnbull, C., and Grant, M. (2007) *Arabidopsis* systemic immunity uses conserved defense signaling pathways and is mediated by jasmonates. *Proc Natl Acad Sci U S A* **104**: 1075-1080.
- Turner, A., Bacic, A., Harris, P.J., and Read, S.M. (1998) Membrane fractionation and enrichment of callose synthase from pollen tubes of *Nicotiana glauca*. *Planta* **205**: 380-388.
- Uknes, S., Mauch-Mani, B., Moyer, M., Potter, S., Williams, S., Dincher, S., Chandler, D., Slusarenko, A., Ward, E., and Ryals, J. (1992) Acquired resistance in *Arabidopsis*. *Plant Cell* **4**: 645-656.
- Underwood, W., Zhang, S., and He, S.Y. (2007) The *Pseudomonas syringae* type III effector tyrosine phosphatase HopAO1 suppresses innate immunity in *Arabidopsis thaliana*. *Plant J.* **52**: 658-672.
- Uppalapati, S.R., Ishiga, Y., Wangdi, T., Kunkel, B.N., Anand, A., Mysore, K.S., and Bender, C.L. (2007) The phytotoxin coronatine contributes to pathogen fitness and is required for suppression of salicylic acid accumulation in tomato inoculated with *Pseudomonas syringae* pv. *tomato* DC3000. *Mol Plant-Microbe Interact* **20**: 955-965.
- van der Biezen, E.A. and Jones, J.D. (1998) Plant disease-resistance proteins and the gene-for-gene concept. *Trends Biochem Sci* **23**: 454-456.
- van der Hoorn, R.A.L., and Kamoun, S. (2008) From guard to decoy: a new model for perception of plant pathogen effectors. *Plant Cell* **20**: 2009-2017.
- Vernooij, B., Friedrich, L., Morse, A., Reist, R., Kolditz-Jawhar, R., Ward, E., Uknes, S., Kessmann, H., and Ryals, J. (1994) Salicylic acid is not the translocated signal responsible for inducing systemic acquired resistance but is required in signal transduction. *Plant Cell* **6**: 959-965.
- Vlot, A.C., Klessig, D.F., and Park, S.W. (2008) Systemic acquired resistance: the elusive signal(s). *Curr Opin Plant Biol* **11**: 436-442.
- Wang, D., Weaver, N.D., Kesarwani, M., and Dong, X. (2005) Induction of protein secretory pathway is required for systemic acquired resistance. *Science* **308**: 1036-1040.
- Whalen, M.C., Innes, R.W., Bent, A.F., and Staskawicz, B.J. (1991) Identification of *Pseudomonas syringae* pathogens of *Arabidopsis* and a bacterial locus determining avirulence on both *Arabidopsis* and soybean. *Plant Cell* **3**: 49-59.
- Xiang, T., Zong, N., Zou, Y., Wu, Y., Zhang, J., Xing, W., Li, Y., Tang, X., Zhu, L., Chai, J., and Zhou, J.M. (2008) *Pseudomonas syringae* effector AvrPto blocks

- innate immunity by targeting receptor kinases. *Curr Biol* **18**: 74-80.
- Yuan, J., and He, S.Y. (1996) The *Pseudomonas syringae* Hrp regulation and secretion system controls the production and secretion of multiple extracellular proteins. *J Bacteriol* **178**:6399-6402.
- Zeyen, R.J., and Bushnell, W.R. (1979) Papilla response of barley epidermal cells caused by *Erysiphe graminis*: rate and method of deposition determined by microcinematography and transmission microscopy. *Can J Bot* **57**: 898-913.
- Zhao, Y., Thilmony, R., Bender, C.L., Schaller, A., He, S.Y., and Howe, G.A. (2003) Virulence systems of *Pseudomonas syringae* pv. *tomato* promote bacterial speck disease in tomato by targeting the jasmonate signaling pathway. *Plant J* **36**: 485-499.
- Zipfel, C., Robatzek, S., Navarro, L., Oakeley, E.J., Jones, J.D., Felix, G., and Boller, T. (2004) Bacterial disease resistance in *Arabidopsis* through flagellin perception. *Nature* **428**: 764-767.
- Zipfel, C., Kunze, G., Chinchilla, D., Caniard, A., Jones, J.D.G., Boller, T., and Felix, G. (2006) Perception of the bacterial PAMP EF-Tu by the receptor EFR restricts *Agrobacterium*-mediated transformation. *Cell* **125**: 749-760.
- Zipfel, C. and Rathjen, J.P. (2008) Plant immunity: AvrPto targets the frontline. *Curr Biol* **18**: R218-220.

CHAPTER 2

Subcellular Localization of HopM1 in Plant Cells

Christy Mecey contributed to Figure 2-4, Figure 2-5, Figure 2-7, Figure 2-8, Figure 2-9 and Figure 2-10.

ACKNOWLEDMENTS

I appreciate the great help of Dr. Christy Mecey who contributed to the figures of this chapter by important confocal microscopic data.

I would like to thank Dr. Federica Brandizzi for her helpful suggestions and discussion of the microscopy data presented in this chapter. She also kindly provided ST-RFP, and helped me obtain endosome markers. I thank Dr. Takeshi Ueda (Tokyo University, Tokyo, Japan) who kindly provided the information of ARA6-CFP, and Dr. Jurgen Denecke (University of Leeds, Leeds, United Kingdom) kindly provided the information for BP80-YFP, which was not used in this chapter. Dr. Karin Schmacher (University of Heidelberg, Heidelberg, Germany) showed the kindness to provide the VHA-a1-RFP. I thank Dr. Jen Sheen (Harvard Medical School, Boston, MA) for providing sGFP, and Dr. Jeff Dangl (University of North Carolina, Chapel Hill, NC) for providing pBD vector. I also would like to thank Dr. Jianping Hu (Plant Research Laboratory, MSU, MI), who kindly provided the ORFs of EYFP and ECFP, and PTS1-dsRED2. Dr. Melinda Frame (Center for Advanced Microscopy, MSU, MI) helped me perform confocal microscopy over several semesters. Xinchun Zhang in Hu laboratory helped me perform confocal microscopy for dual localization of HopM1-GFP and PTS1-dsRED2, and provided helpful discussions.

I would like to thank Krithika Shanmugasundaram who was in the High School Honors Science/Mathematics/Engineering Program of MSU (2007) and assisted the subcloning of HopM1 ORF.

ABSTRACT

HopM1, a bacterial effector protein secreted through the type III secretion system (TTSS), is important for the virulence of *Pseudomonas syringae* pv. *tomato* (*Pst*) DC3000. HopM1 interacts with and mediates degradation of several *Arabidopsis* proteins (AtMINs), including AtMIN7. AtMIN7 is a putative ARF-GEF protein, which has a role in vesicle formation and budding during intracellular trafficking. To further understand the action of HopM1 in host cells, I studied the subcellular localization of HopM1 in tobacco and *Arabidopsis*. Full-length HopM1 and its truncated versions (HopM1₁₋₃₀₀ and HopM1₃₀₁₋₇₁₂) were fused with GFP or YFP, and they were transiently expressed in tobacco followed by examination by confocal microscopy. After 8 hours of DEX-induction, full-length HopM1 fusion proteins caused tissue death in tobacco leaves, in contrast to truncated HopM1 fusion proteins which did not induce tissue death.

Approximately between 2.5 hours and 4 hours after DEX-induction, full-length HopM1 and HopM1₁₋₃₀₀, which were fused with GFP or YFP, were found in small, punctate structures in tobacco cells. These small structures were co-localized with VHA-a1-RFP, a marker for trans-Golgi network (TGN), and ARA6-CFP, a marker for early endosome. They were not co-localized with ST-RFP (a Golgi marker). After 4 to 6 hours, full-length HopM1 fusion proteins were still detected in punctate structures, but truncated HopM1 fusion proteins were found dispersed in the tobacco cells. These data indicate that HopM1 is localized in certain parts of the endosomal components, suggesting that its virulence function affects vesicle trafficking in host cells. Also, HopM1₁₋₃₀₀ is sufficient for the localization in the endosomal compartments.

HopM1 fusion constructs were transformed into *Arabidopsis* Col-0 (wild type), and some were also transformed into the *atmin7* plants. Eight hours after DEX-induction, full-length HopM1 fusion constructs were found in small, punctate structures, whereas the fusions of HopM1₁₋₃₀₀ were dispersed in *Arabidopsis* cells. This localization is consistent with the localization of HopM1 fusion proteins in later time points of microscopic observation in tobacco cells.

INTRODUCTION

Research on TTSS effector proteins of *Pst* DC3000 in *Arabidopsis* led to the hypothesis that one of their virulence functions is to interfere with the secretion of defense-associated proteins of host plants. This hypothesis was suggested based on a cDNA microarray analysis of *Arabidopsis* (Hauck et al., 2003): *Pst* DC3000 suppressed the expression of certain *Arabidopsis* genes, around 40% of which encoded putative secreted proteins. This biased suppression of gene expression occurred in a TTSS-dependent manner (Hauck et al., 2003).

Other reports also showed that intracellular trafficking and protein secretion pathways have roles in plant defense: several defense-associated proteins are components of trafficking pathways, such as PEN1 or *NbSYP132* (Collins et al., 2003; Assaad et al. 2004; Kalde et al., 2007). Also, protein secretion pathway-associated genes are among the targets of *Arabidopsis NPR1*, which is a key regulator of systemic acquired resistance (SAR; Wang et al., 2005). Direct evidence for the suppression of trafficking pathways and protein secretion by TTSS effectors was provided by Nomura and colleagues (Nomura et al., 2006), who showed that a *Pst* DC3000 effector, HopM1, mediates 26S-proteasome-dependent degradation of AtMIN7, which is a member of the adenosine-diphosphate ribosylation factor-guanine nucleotide-exchanging factor (ARF-GEF) family of proteins necessary for the initiation of vesicle trafficking (Memon, 2004; Gillingham and Munro, 2007; Anders and Jürgens, 2008; Bassham et al., 2008).

The *hopM1* ORF is located in the conserved effector locus (CEL) cluster in the genome of *Pst* DC3000 (Alfano et al., 2000; Buell et al., 2003). Other ORFs present in

the CEL encode additional TTSS effectors, including AvrE, HrpW1, and HopPtoA1 (Alfano et al., 2000). HopM1 is translocated into plant cells with the assistance of its chaperone ShcM (Alfano et al., 2000; Badel et al., 2003). The *hopM1* ORF (also known as ORF3: Alfano et al., 2000) consists of 2,139 bases, encoding a protein of 712 amino acids (predicted molecular weight: 75.23 kDa [Buell et al., 2003; <http://www.ncbi.nlm.nih.gov/>, NC_004578.1]).

HopM1 is important for *Pst* DC3000 virulence. Reduced multiplication and symptom development were observed when *Arabidopsis* was inoculated with the Δ CEL mutant of *Pst* DC3000. This virulence defect of Δ CEL mutant was restored by a plasmid carrying the *hopM1* gene and its chaperone gene *shcM* whose product is required for the translocation of HopM1 into plant cell (Badel et al., 2003; DebRoy et al., 2004). Transgenic expression of HopM1 in *Arabidopsis* plants caused two phenotypes: 1) Low-level expression restored multiplication of the Δ CEL mutant, and 2) High-level expression induced host cell death (Nomura et al., 2006). Interestingly, when the N-terminal 300 amino acids of HopM1 (HopM1₁₋₃₀₀) were expressed in *Arabidopsis*, it did not enhance the multiplication of the Δ CEL mutant, suggesting that HopM1₁₋₃₀₀ is not functional. Moreover, transgenically expressed HopM1₁₋₃₀₀ suppressed the multiplication of the Δ CEL mutant complemented with full-length *hopM1* and its chaperone *shcM* (Nomura et al., 2006). This dominant negative effect was not found with the C-terminus of HopM1 (HopM1₃₀₁₋₇₁₂) (Nomura et al., 2006).

Immunoblot analyses by Nomura et al. (2006) showed that HopM1 is found in the endomembrane fractions of transgenic *Arabidopsis* cells. However, the endomembrane system includes many different compartments, and the exact subcellular localization of

HopM1 remains elusive. In this study, I used the fluorescence tagging approach combined with confocal microscopy to investigate the subcellular localization of HopM1 in tobacco and *Arabidopsis* cells. By determining the cellular localization of HopM1 in the plant cells, I expect to obtain a more complete understanding of the virulence action of HopM1 inside the host cells. I also examined the localization of the N-terminus of HopM1 (HopM1₁₋₃₀₀), which has a dominant-negative effect, and that of the C-terminus of HopM1 (HopM1₃₀₁₋₇₁₂) to explore a possible relationship between the cellular localization and virulence function of HopM1.

MATERIALS AND METHODS

Construction of HopM1 fusions

Full-length or truncated *hopM1* ORFs were selected for fusion construction.

Computer prediction based on the amino acid sequence of HopM1 did not give a clue of subcellular targeting signals (<http://www.cbs.dtu.dk/services/TargetP>: Emanuelsson et al., 2007; <http://psort.ims.u-tokyo.ac.jp>: Nakai and Kanehisa, 1991). Therefore, to avoid possible interference with hidden subcellular targeting signals at the N- or C-terminus, both N-terminal and C-terminal GFP/YFP fusion were designed per each fusion construct (Table 2-1, Figure 2-1).

Synthetic green fluorescence protein (sGFP: Chiu et al., 1996) and enhanced yellow fluorescence protein (EYFP: Clontech, Mountain View, CA) were selected for fusion construction. The ORFs of sGFP and EYFP were amplified by PCR using *PfuTurbo*[®] DNA polymerase and relevant primers (Table 2-2). The PCR products were subcloned into the pBluescript II SK(+) (Stratagene, La Jolla, CA) using T₄ ligase (New England Biolabs, Ipswich, MA), at its *Pst*I/*Spe*I sites and *Xho*I/*Eco*RI sites, respectively. Mutation-free fusion ORFs were selected for the next cloning steps.

Full-length *hopM1* ORF was amplified by PCR with *PfuTurbo*[®] DNA polymerase (Stratagene, La Jolla, CA) using the genomic DNA of *Pst* DC3000 and primers covering the whole ORF (Table 2-3). The sequence of the PCR product was compared to the sequence of *hopM1* ORF deposited in the NCBI (<http://www.ncbi.nlm.nih.gov/>, NC_004578.1). Mutation-free *hopM1* ORF was cloned into a GATEWAY-compatible vector pENTR/D-TOPO (Invitrogen, Carlsbad, CA) and used as a template for further

Table 2-1. Summary of the fusion proteins created for the localization study of HopM1.

Construct	Description
HopM1-GFP	3' end of the full-length <i>hopM1</i> ORF was fused with 5' end of <i>GFP</i> ORF
YFP-HopM1	5' end of the full-length <i>hopM1</i> ORF was fused with 3' end of <i>YFP</i> ORF
HopM1-N-GFP	3' end of the N-terminus of <i>hopM1</i> ORF was fused with 5' end of <i>GFP</i> ORF
YFP-HopM1-N	5' end of the N-terminus of <i>hopM1</i> ORF was fused with 3' end of <i>YFP</i> ORF
HopM1-C-GFP	3' end of the C-terminus of <i>hopM1</i> ORF was fused with 5' end of <i>GFP</i> ORF
YFP-HopM1-C	5' end of the C-terminus of <i>hopM1</i> ORF was fused with 3' end of <i>YFP</i> ORF

Table 2-2. PCR primers for cloning the ORFs of *sGFP* and *EYFP*.

Primer name	Primer sequence
Forward primer for <i>sGFP</i> ORF	5'-GGG <u>CTGCAG</u> ATG [*] GTGAGCAAGGGCGAGGAG-3'(<i>Pst</i> I)
Reverse primer for <i>sGFP</i> ORF	5'- CGC <u>ACTAGTT</u> TA ^{**} CTTGTACAGCTCGTCC-3'(<i>Spe</i> I)
Forward primer for <i>EYFP</i> ORF	5'- CTT <u>CTCGAG</u> ATG [*] GTGAGCAAGGGCGAG-3'(<i>Xho</i> I)
Reverse primer for <i>EYFP</i> ORF	5'-CTA <u>GAAATTC</u> CTT ^{**} GTACAGCTCGTCCATGCCGA-3' (<i>Eco</i> RI)

Bold and underlined letters indicate the restriction enzyme sites for subcloning and fusions (*Eco*RI, *Pst*I, *Spe*I and *Xho*I).

* Start codons are with bold and red letters.

** Stop codons are with bold and blue letters.

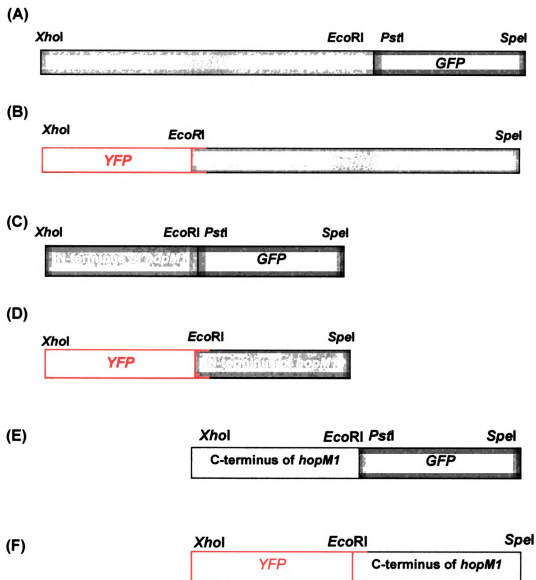


Figure 2-1. Diagrams of HopM1 fusions used for localization studies. *hopM1* indicates a full-length ORF, which encodes 712 amino acids. The N-terminus of *hopM1* indicates a truncated ORF encoding 1-300 amino acids. The C-terminus of *hopM1* indicates a truncated ORF encoding 301-712 amino acids. *XhoI*, *EcoRI*, *PstI*, and *SpeI* indicate the restriction enzyme sites added for fusion construction. (A) A diagram of the HopM1-GFP fusion. (B) A diagram of the YFP-HopM1 fusion. (C) A diagram of the HopM1-N-GFP fusion. (D) A diagram of the YFP-HopM1-N fusion. (E) A diagram of the HopM1-C-GFP fusion. (F) A diagram of the YFP-HopM1-C fusion.

PCRs to obtain full-length or truncated HopM1 ORFs. Primers for the PCRs are shown in Table 2-3. Full-length and truncated *hopM1* ORFs were obtained by PCRs with *PfuTurbo*[®] DNA polymerase (Stratagene, La Jolla, CA). The PCR products of full-length or truncated *HopM1* ORFs were subcloned into the multiple cloning sites next to the 3' end of the *EYFP* ORF in pBluescript II SK(+) (*XhoI*/*EcoRI* sites) in order to generate *YFP-hopM1*, *YFP-hopM1-N* and *YFP-hopM1-C* fusion ORFs. Alternatively, they were subcloned into the multiple cloning sites next to the 5' end of the *sGFP* ORF in pBluescript II SK(+) (*EcoRI*/*SpeI* sites) to construct *hopM1-GFP*, *hopM1-N-GFP* and *hopM1-C-GFP* fusion ORFs. All of these fusion ORFs were sequenced and mutation-free gene fusions were selected. The *hopM1-C-GFP* fusion was excluded from further experiments due to its mutations introduced during PCR.

Introduction of HopM1 fusion ORFs into *Agrobacterium*

The mutation-free fusion ORFs were subcloned into the *XhoI*/*SpeI* sites of the pBD vector (a gift From Dr. Jeff Dangl laboratory, University of North Carolina, Chapel Hill, NC). This is a binary vector containing a kanamycin-resistance gene for selecting bacterial transformants, and a BASTA (glufosinate)-resistance gene for selection of transgenic plants. The expression of the transgene in pBD vector depends on a promoter inducible by the rat glucocorticoid hormone dexamethasone (DEX, Aoyama and Chua, 1997). The recombinant pBD plasmids were transformed into *E.coli* strains (DH5 α , One Shot[®] TOP10 competent cell (Invitrogen, Carlsbad, CA), or One Shot[®] Mach[™]-T1^R (Invitrogen, Carlsbad, CA)), and kanamycin-resistant colonies were obtained on the solid Luria-Bertani (LB) medium with kanamycin (50 mg/ml). The kanamycin-resistant *E.coli*

Table 2-3. PCR primers for obtaining full-length or truncated *hopM1* ORFs for fusion constructions.

Primer name	Primer sequence
Forward primer for the <i>hopM1</i> ORF from <i>Pst</i> DC3000	5'-CACCATGATCAGTTCGCGGAT CGG-3'
Reverse primer for the <i>hopM1</i> ORF from <i>Pst</i> DC3000	5'- TTAACGCGGGTCAAGCAAGC-3'
Forward primer for YFP-HopM1	5' -CGC <u>GAATTC</u> ATG*ATCAGTTCGCGGATCGG-3'(<i>EcoRI</i>)
Reverse primer for YFP-HopM1	5'-CCG <u>ACTAGTTTA</u> **ACGCGG GTCAAGCAAGCC-3'(<i>SpeI</i>)
Forward primer for HopM1-GFP	5'-GCG <u>CTCGAG</u> ATG*ATCAGTTCGCGGATCGGC-3'(<i>XhoI</i>)
Reverse primer for HopM1-GFP	5'-GGC <u>GAATTC</u> ACGCGGGTCAAGCAAGCC-3'(<i>EcoRI</i>)
Forward primer for HopM1-N-GFP	5'-GCG <u>CTCGAG</u> ATG*ATCAG TTCGCGGATCGGC-3'(<i>XhoI</i>)
Reverse primer for HopM1-N-GFP	5'-CTG <u>GAATTC</u> TGCACCTTTCCAGCCAC-3'(<i>EcoRI</i>)
Forward primer for YFP-HopM1-N	5'-CTT <u>GAATTC</u> ATG*ATCAGTTCGCGGATCGGC-3'(<i>EcoRI</i>)
Reverse primer for YFP-HopM1-N	5'-GTC <u>ACTAGTTTA</u> **TGCACCTTTCCAGCCACCC-3'(<i>SpeI</i>)
Forward primer for HopM1-C-GFP	5'-CTA <u>CTCGAG</u> ATG*GGGCCGATTGTCGCGG-3'(<i>XhoI</i>)
Reverse primer for HopM1-C-GFP	5'- GTA <u>GAATTC</u> ACGCGGGTCAA GCAAGCC-3'(<i>EcoRI</i>)
Forward primer for YFP-HopM1-C	5'- CTA <u>GAATTC</u> ATG*GGGCGATTGTCGCGG-3' (<i>EcoRI</i>)

Table 2-3 (continued).

Reverse primer for YFP- HopM1-C 5'-CTA**ACTAGTT**TA**ACGCGGGTCAAGCAAGCC-3'(*SpeI*)

Bold and underlined letters are corresponding to selected restriction enzyme sites (*EcoRI*, *SpeI* and *XhoI*) for cloning and gene fusions.

*Start codons are with bold and red letters.

**Stop codons are with bold and blue letters.

colonies containing the fusion ORFs were used for introducing recombinant plasmids into *Agrobacterium* strain C58C1 by tri-parental mating using the *E.coli* helper strain pRK2013.

Transient assays of the HopM1 fusion ORFs in tobacco plants

Transient assays were performed in the leaves of *Nicotiana benthamiana* or *Nicotiana tabacum* plants. The protocol for *Agrobacterium* preparation for transient assay was adapted from the experimental methods of Goodin et al. (2002). Each *Agrobacterium* carrying desirable *hopM1* fusion plasmids was inoculated in LB liquid medium with antibiotics (rifampicin, tetracycline and kanamycin) and incubated at 28-30°C for 8-9 hours with shaking at 250 rpm, until the OD₆₀₀ of *Agrobacterium* reached 0.8-0.9. These cultures were centrifuged at 3,000 rpm in a Beckman GS-6R tabletop centrifuge at room temperature. The pellet of each culture was resuspended in the induction medium (10 mM MgCl₂, 10mM MES [pH 5.6], 150 µM acetosyringone [3',5'-Dimethoxy-4'-hydroxyacetophenone: Sigma-Aldrich, St. Louis, MO]) and the OD₆₀₀ was adjusted to 0.1-0.2. These re-suspended cultures were collected in sterile test tubes, covered with sterile caps, and left at room temperature for 2-3 hours prior to their injection into tobacco leaves. Each culture was hand-infiltrated with 1 ml needless syringe into leaves and inoculated plants were left for 36-48 hours prior to DEX treatment.

Transformation of HopM1 fusions into *Arabidopsis* plants

The HopM1 fusions were transformed into *Arabidopsis* plants (Col-0 or *atmin7* knockout mutant) by floral dipping (Clough and Bent, 1998). T₁ seeds were collected and

germinated in soil. Ten-day-old T₁ plants were sprayed with 0.2 % BASTA solution (glufosinate-ammonium, trade name Finale, AgroEvo Environmental Health, Montvale, NJ) containing 0.025% Silwet L-77. One leaf from each BASTA-survived T₁ plant was detached and dipped in a DEX solution (30 μ M) and observed with confocal microscopy, in order to examine the expression of the fluorescent fusion proteins.

Plant growth condition

Tobacco plants were raised in the laboratory, at the room temperature, using a light of 300 microeinstein. *Arabidopsis* plants were grown in soil in growth chambers, under a 12 hr dark/12 hr light cycle. The light was with 100 microeinstein, and the temperature was 20°C.

Application of Dexamethasone (DEX)

DEX powder (Sigma-Aldrich, St. Louis, MO) was dissolved in 100% ethanol at 30 mM, and stored at -20°C. This solution was diluted in water to 15-30 μ M just before spraying, dabbing or dipping. For spraying, 0.01 % surfactant Tween-20 (Sigma-Aldrich, St. Louis, MO) was added, as suggested by Aoyama and Chua (1997). DEX spray was performed at least 36 hours after *Agrobacterium* infiltration. DEX solution was either sprayed on the surface of tobacco leaves with Tween-20 or dabbed on the leaf surface without Tween-20. The time allowed for DEX induction was variable, between 2 hours and 48 hours, depending on experiments. *Arabidopsis* leaves were detached from the plants and dipped in 30 μ M DEX solution, at room temperature for at least 8 hours.

Confocal microscopy

Leaf samples (5 mm x 5 mm) were cut from the *Agrobacterium*-infiltrated areas of tobacco leaves and mounted in water. The confocal microscopy and imaging were performed with a LSM510 META inverted confocal laser scanning microscope (hereafter META: Carl Zeiss MicroImaging, Inc., Thornwood, NY) or FV1000D laser confocal scanning microscope (hereafter FV1000D: Olympus America Inc., Center Valley, PA). The 40x or 60x oil immersion objectives were used.

The GFP fusions were excited at 488 nm from the argon laser of META, and the emission light was filtered with a 505-530 nm band-pass filter for obtaining GFP fluorescence, and with a 615 nm long-pass filter for obtaining autofluorescence from chloroplasts. The YFP fusions were excited at 514 nm from the argon laser of META, or at 515 nm from the multi-argon laser of FV1000D. The emission light of YFP was filtered with a 520-555 nm band-pass filter of META, or with a 535-565 nm band-pass filter of FV1000D. For these experiments the autofluorescence from chloroplasts was not collected. The images obtained from the confocal microscopy with META were examined and processed with Carl Zeiss AIM Version 3.2. Some images were adjusted for brightness or contrast using Adobe Photoshop Element version 5.5 or 7.0.

Dual localization with cellular markers

The following subcellular markers fused with red fluorescence protein (RFP, monomer of dsRED: Campbell et al., 2002) or dsRED2 (Clontech, Mountain View, CA) were selected for dual localization experiments with HopM1-GFP or YFP-HopM1 in

Agrobacterium-mediated transient expression assays: rat sialyl transferase fused to RFP (ST-RFP [Saint-Jore et al., 2002; a gift from Dr. Federica Brandizzi, MSU, East Lansing, MI]), dsRED2 fused with the conserved C-terminal, peroxisome-targeting signal type 1 (PTS1) consisting of serine-lysine-leucine (PTS1-dsRED2 [Gould et al., 1989; Reumann, 2004; Fan et al., 2005]), a CFP-fusion of the endosomal compartment marker ARA6 (ARA6-CFP [Ueda et al., 2001]), and a RFP-fusion of the trans-Golgi network marker VHA-a1 (VHA-a1-GFP [Dettmer et al., 2006]). All of these markers are constitutively expressed in plants from the CaMV 35S promoter. Procedures for dual localization experiments were the same as those of transient assays for HopM1 fusions. The *Agrobacterium* culture containing each marker gene was mixed with the *Agrobacterium* culture of the desired HopM1 fusion gene in a 1:1 ratio.

Dual localization with HopM1-GFP and ST-RFP or PTS1-dsRED2 was performed with META. The condition of confocal microscopy for HopM1-GFP was the same as described in page 46. ST-RFP or PTS1-dsRED2 were excited at 543 nm Helium-Neon laser, and emission light from the RFP or dsRED2 was filtered with a 560 nm long-pass filter or with the 560-615 nm band-pass filter. Dual localization of YFP-HopM1 and ARA6-CFP was performed with META or FV1000D. The condition of confocal microscopy for YFP-HopM1 was the same as described in page 46. ARA6-CFP was excited by 458 nm laser of META or FV1000D, and the emission light was filtered by a 465-510 nm band-pass filter of META or by a 465-510 nm band-pass filter of FV1000D. Dual localization was performed in a sequential mode to avoid false signal. The examination and processing procedure for the images acquired from the confocal microscopy for dual localization are identical to those described in page 46.

Brefeldin A (BFA) treatment

The fungal toxin Brefeldin A (BFA, γ ,4-Dihydroxy-2[6-hydroxy-1-heptenyl]-4-cyclopentanecrotonic acid λ -lactone) extracted from *Penicillium brefeldianum* was purchased from Sigma-Aldrich (St. Louis, MO). A stock of 1.8 mM BFA (10mg/ml) was prepared in 100% methanol and stored at -20°C. For BFA treatment of tobacco leaf samples, 360 μ M BFA solution was prepared in water, and tobacco leaf samples which had been hand-infiltrated with *Agrobacterium* cultures carrying HopM1-GFP and ST-RFP plasmids were treated with DEX to induce the expression of HopM1 fusions, and then immersed in the BFA solution for 30-35 minutes prior to confocal microscopy.

Protein extraction and western blot analyses

Total protein samples were obtained from tobacco leaves in transient assays or from the leaves of transgenic *Arabidopsis*. Tobacco leaf samples were obtained from the leaf areas infiltrated with *Agrobacterium* expressing HopM1 fusions (i.e., these leaf areas were sprayed with 30 μ M DEX solution with 0.01% Tween-20, and left at room temperature for 8 hours to allow protein expression). *Arabidopsis* leaf samples were obtained from the detached leaves which were dipped in DEX (30 μ M) for 24 hours. Twenty mg of each leaf sample (fresh weight) was ground in 200 μ l SDS buffer [100 mM Tris-HCl pH 6.8, 200 mM DTT, 4% SDS, 20% glycerol] for protein extraction. Extracts were immediately heated at 90°C for 10 minutes and then frozen at -20°C.

Prior to loading of each protein sample on a protein gel, extracts were thawed on ice, heated at 90°C for 3 minutes, and centrifuged at 10,000 $\times g$ for 1 minute. Ten to

twenty μ L of each sample was used for SDS-PAGE (equal volumes were used in a given gel). Total proteins were separated on precast gradient gels (4-20%, ISC BioExpress) or hand-made SDS-PAGE gels (7.5, 10, or 12% gels), then transferred onto Immobilon-P membrane (Millipore, Billerica, MA) using a semi-dry transfer apparatus (SEMIPHOR, Hoefer Scientific Instruments, San Francisco, CA). Immunoblot analyses were performed using a HopM1-specific antibody (Nomura et al., 2006) or a GFP-specific antibody (Santa Cruz Biotechnology, Inc., Santa Cruz, CA). For estimating the sizes of proteins, PageRuler™ Prestained Protein Ladder Plus (#SM1811, Fermentas International Inc, Ontario, Canada) was used.

The color of the images in this dissertation

The images in this dissertation (chapter 2, chapter 3, chapter 4 and appendices) are presented in color.

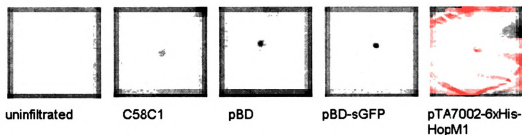
RESULTS

Transiently expressed full-length HopM1 fusion proteins induce tissue death in tobacco leaves

Agrobacterium strains containing pBD derivatives designed to express the HopM1-GFP or YFP-HopM1 fusion were hand-infiltrated into the leaves of *Nicotiana benthamiana* or *Nicotiana tabacum*. After 48 hours, the transgenes were sprayed with 30 μ M DEX. The infiltrated areas of tobacco leaves started losing turgor approximately 8 hours after DEX induction. Two days after DEX spray, the infiltrated area died. This was similar to a previous report of tissue death induced by another TTSS effector of *Pst* DC3000, AvrE, in tobacco (Badel et al., 2006). To confirm that the tissue death was caused by the HopM1 fusion proteins, the transient assay was repeated with following controls: *Agrobacterium* C58C1 alone, C58C1 carrying pBD vector, C58C1 carrying the *sGFP* ORF in pBD, and C58C1 with the *hopM1* ORF in pTA7002 (another DEX-inducible vector which carries a hygromycin resistance gene [DebRoy et al., 2004; Nomura et al., 2006]). These strains were hand-infiltrated into the leaves of *Nicotiana benthamiana* or *Nicotiana tabacum*, and sprayed with 30 μ M DEX. Two days after DEX spray, only the areas injected with *Agrobacterium* carrying pTA7002-*hopM1*, pBD-HopM1-GFP or pBD-YFP-HopM1 showed tissue death. C58C1, C58C1 carrying pBD vector and C58C1 carrying pBD-sGFP did not show tissue death, and the appearance of the infiltrated areas was indistinguishable from the uninfiltrated areas (Figure 2-2).

The fusion constructs of truncated *hopM1* were also transiently expressed in tobacco leaves. In contrast to HopM1-GFP or YFP-HopM1, none of the truncated

(A)



(B)

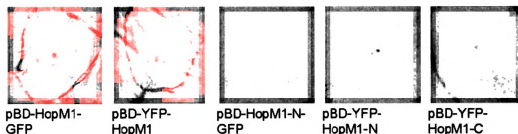


Figure 2-2. Appearance of *N.benthamiana* leaves which were infiltrated with *Agrobacterium* carrying various plasmids. (A) *N.benthamiana* leaves which were infiltrated with nothing, *Agrobacterium* C58C1, C58C1 transformed with pBD vector, C58C1 with sGFP ORF in pBD vector, C58C1 with 6xHis-HopM1 in pTA7002 (DebRoy et al., 2004; Nomura et al., 2006). (B) *N.benthamiana* leaves which were infiltrated with *Agrobacterium* carrying pBD derivatives designed to express HopM1 (full-length or truncated) fused with GFP or YFP ORFs under the DEX-inducible promoter. Black lines in the photos of pTA7002-6xHis-HopM1, pBD-HopM1-GFP and pBD-YFP-HopM1 mark the *Agrobacterium*-infiltrated area. Leaves were sprayed with 30 μ M DEX solution and left at the room temperature for 48 hours prior to photography.

HopM1 fusions induced tissue death (Figure 2-2B). Therefore, only full-length HopM1 or HopM1 fusions were able to induce tissue death in tobacco plants.

Western blot analyses of HopM1 fusions in transient assay

The expression of the fusion proteins of full-length HopM1 or truncated HopM1 in transient assays was analyzed by immunoblot. Several controls were included:

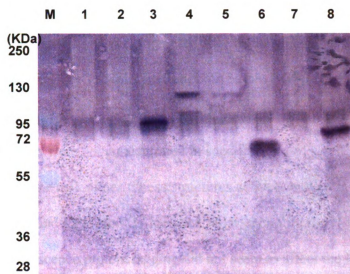
N.tabacum leaf sample without bacterial infiltration, pEGAD-eGFP for constitutive expression of eGFP and pTA7002-6XHis-HopM1 for DEX-inducible expression of HopM1. Immunoblotting was performed with an anti-HopM1 antibody or anti-GFP antibody (Figure 2-3). The results showed approximately expected sizes of each HopM1 fusion (HopM1-GFP: 102 kDa, YFP-HopM1: 102 kDa, HopM1-N-GFP: 59 kDa, YFP-HopM1-C: 72 kDa), except that the expression of YFP-HopM1-N was too low to detect. The gel lanes of HopM1-N-GFP (Figure 2-3B, lane 6) and YFP-HopM1-N (Figure 2-3B, lane 7) had faint bands of the approximate size of GFP detected by GFP antibody.

Transiently expressed fusions of full-length HopM1 are found in small, punctate structures in tobacco cells

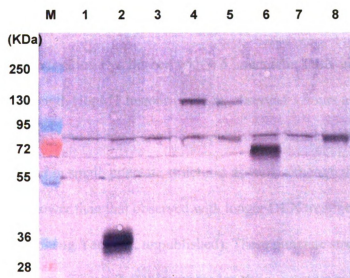
To determine the localization of full-length HopM1 in plant cells, HopM1-GFP and YFP-HopM1 were transiently expressed in tobacco plants. After 8 hours of DEX induction (on average), some leaf tissue began to lose turgor, leading to tissue death eventually. Based on this observation, DEX induction time for preparing confocal microscope samples did not exceed 6 hours. Confocal microscopy was performed between 4 and 6 hours after DEX spraying. Both epidermal cells and mesophyll cells of tobacco plants were

Figure 2-3. Immunoblot analyses of HopM1 fusions in transient assays in *N.tabacum*, using (A) the anti-HopM1 antibody, and (B) the anti-GFP antibody. M: protein size markers. Lane 1 to 8 represent *N.tabacum* leaf samples infiltrated with *Agrobacterium* containing the following plasmids: lane 1, leaf sample without bacterial infiltration; lane 2, pEGAD; lane 3, pTA7002-6xHis-HopM1; lane 4, pBD-HopM1-GFP; lane 5, pBD-YFP-HopM1; lane 6, pBD-HopM1-N-GFP; lane 7, pBD-YFP-HopM1-N; lane 8, pBD-YFP-HopM1-C. All leaf samples were collected after 8 hour of DEX induction with 30 M of DEX solution. None of the leaf samples were observed by confocal microscopy to confirm the expression of proteins prior to sample preparation.

(A)



(B)



examined, but the majority of images were from epidermal cells.

Neither HopM1-GFP (Figure 2-4A and B) nor YFP-HopM1 (Figure 2-4C) was found in the plasma membrane or large organelles such as the chloroplast, nucleus, endoplasmic reticulum (ER), or vacuole. Instead, both HopM1-GFP (Figure 2-4A and B) and YFP-HopM1 (Figure 2-4C) were found in small, punctate structures in the cell. These punctate structures were not concentrated in specific areas of a cell, but they were not evenly dispersed in the cell, either. These structures actively moved in the cells. The images of HopM1-GFP and YFP-HopM1 looked similar, therefore the N-terminal or C-terminal fusion of fluorescence protein tagging did not seem to affect the localization of HopM1 fusion proteins.

To determine the localization of HopM1 at the earliest detectable stage, the condition of DEX-induction was modified in some experiments: 30 μ M DEX solution was dabbed onto the surface of tobacco leaves without surfactant Tween-20, and the confocal microscopic observation was limited within 5 hours after DEX induction. The fluorescence from full-length HopM1 fusions could be observed 3 hours after DEX application (Christy Mecey and Sheng Yang He, unpublished). Full-length HopM1 fusion proteins were again found in small, punctate structures as well, although the density of punctate structures was lower than that observed with longer DEX treatment (Figure 2-4D: Christy Mecey and Sheng Yang He, unpublished). These punctate structures were more even in size and shape (Figure 2-4D), compared to the punctate structures observed 5 hours after DEX treatment (Figure 2-4A, B and C). According to the observations made at different time points of DEX treatment, I conclude that the fluorescence intensity and signal density of the punctate structures associated with full-length HopM1 fusion

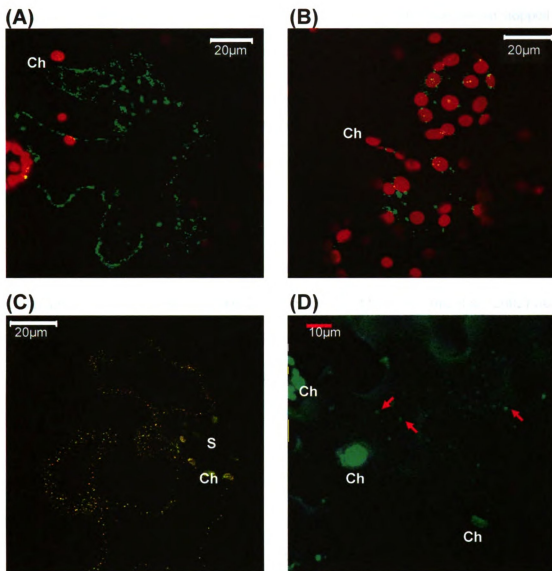


Figure 2-4. HopM1-GFP and YFP-HopM1 transiently expressed in *N. tabacum*. (A) HopM1-GFP expressed in epidermal cells. (B) HopM1-GFP expressed in mesophyll cells. (C) and (D) YFP-HopM1 expressed in epidermal cells. Panels A, B and C were from the images of the leaf samples which were sprayed with DEX solution containing 0.01% Tween-20. Panel D was from the images of the leaf sample which was dabbed with DEX solution without Tween-20. HopM1-associated punctate structures are yellow in C and green in other panels (indicated punctate with red arrows in D). All images are from single focal planes. Ch: chloroplast. S: stomata.

proteins increased over time. The movement of punctate structures was almost stopped approximately 7 hours after DEX application.

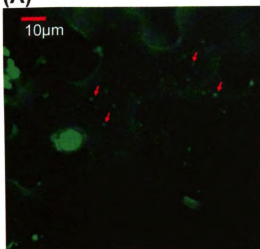
Dual localization tests of full-length HopM1 fusions with a Golgi marker with or without Brefeldin A (BFA)

The localization of full-length HopM1 fusions further was investigated by dual localization tests with different subcellular marker proteins that are associated with small organelles. First, I examined the possibility that HopM1-GFP may be localized to the Golgi apparatus. The rat sialyl transferase (Wee et al., 1998; Saint-Jore et al., 2002) fused to RFP (ST-RFP: the gift from Dr. Federica Brandizzi laboratory, Michigan State University, East Lansing, MI) was selected as a marker for this purpose. ST-RFP was transiently co-expressed with HopM1-GFP or YFP-HopM1 in tobacco leaves, and confocal microscopy analyses were performed both at early time points (within 5 hours) and later time points (after 5 hours) after the DEX-induction. In both conditions, there was no significant co-localization of full-length HopM1 fusions (Figure 2-5). At later time point, punctate structures associated with HopM1 fusion protein (HopM1-GFP) and ST-RFP showed distinct sizes, densities and distributions in the cells (Figure 2-5).

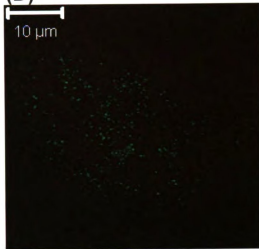
Fungal toxin Brefeldin A (BFA) was also tested to further investigate the relationship between the localization of HopM1-GFP and Golgi, based on the known effects of BFA on disruption of Golgi stacks and fusion of Golgi into ER (Brandizzi et al., 2002; Ritzenthaler et al., 2002; Saint-Jore et al., 2002). The BFA solution was applied to the leaf samples 5-6 hours after the leaves were co-infiltrated with *Agrobacterium* strains carrying pBD-HopM1-GFP and/or pVKH-ST-RFP. As expected, ST-RFP-associated

Figure 2-5. Dual localization results of full-length HopM1 fusion proteins and ST-RFP. The fluorescence from HopM1-GFP (A), ST-RFP (B) and their merged image (C) within 5 hours after DEX treatment; the fluorescence from YFP-HopM1 (D), ST-RFP (E) and their merged image (F) 5 hours after DEX treatment. Images A, B and C were from the leaf sample which was dabbed with DEX solution without Tween-20. Image D, E and F were from the leaf sample which was sprayed with DEX solution containing 0.01% Tween-20. HopM1-associated punctate structures are green (A, C, D and F) and ST-RFP are red (B, C, E and F). YFP-HopM1 in panel A and ST-RFP in panel B are indicated with red arrows and white arrows, respectively. A, B and C are from Z-stack, and D, E and F are from single focal planes of the epidermal cell layer of *N.tabacum.*, respectively

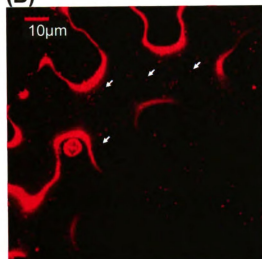
(A)



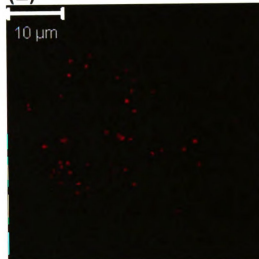
(D)



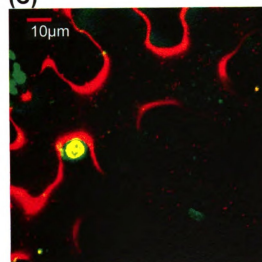
(B)



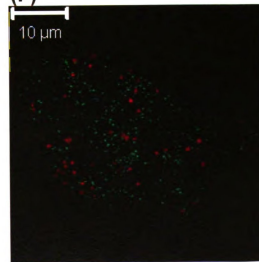
(E)



(C)



(F)



punctate structures disappeared and fluorescence was changed into a mesh-like network (Figure 2-6), reflecting the re-distribution of ST-RFP into the ER by BFA (Brandizzi et al., 2002; Saint-Jore et al., 2002). Contrary to this change, HopM1-GFP did not disappear, and there was no significant morphological change of the punctate structures associated with HopM1-GFP (Figure 2-6).

Dual localization tests of YFP-HopM1 and endosome markers

Besides Golgi, endosomal compartments were selected for determining the localization of HopM1 fusions. Endosome is a collection of small, vesicular organelles the main function of which is to transport and sort cargo materials between Golgi, vacuole and plasma membrane (Jürgens and Geldner, 2002; Bassham et al., 2008; Robinson et al., 2008). The endosomes are shown as small, punctate structures (Ueda et al., 2001; Ueda et al., 2004; daSilva et al., 2006; Dettmer et al., 2006). In eukaryotic cells several different types of endosomes exist: they are different in structure, function and biochemical composition (Bassham et al., 2008). There are three known subgroups of endosomes (Robinson et al., 2008; Otegui and Spitzer, 2008): early endosome, late endosome and recycling endosome. Early endosomes are produced from endocytosis of the plasma membrane. In plants, trans-Golgi network (TGN) is considered to be early endosomes (Dettmer et al., 2006; Lam et al., 2007). Late endosomes function in the vesicle trafficking from early endosomes to the vacuole, and include distinctive structures such as multivesicular bodies (MVB) or prevacuolar compartment (PVC) (Otegui and Spitzer, 2008; Robinson et al., 2008). Recycling endosomes are thought to function from early and late endosomes to the plasma membrane (Otegui and Spitzer, 2008; Robinson

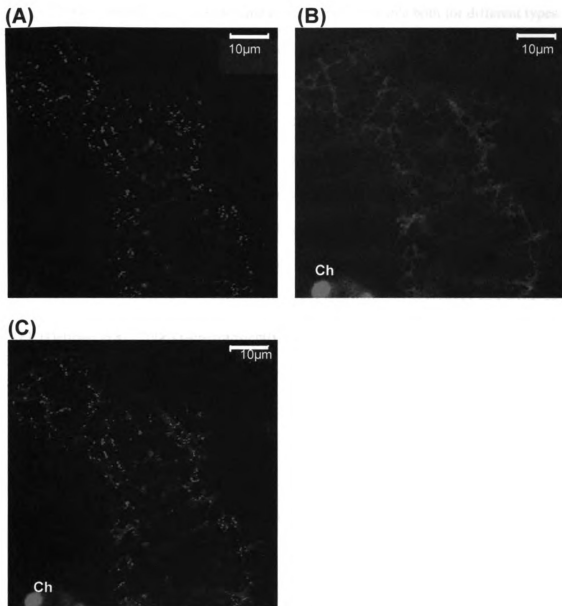


Figure 2-6. Dual localization result of HopM1-GFP and ST-RFP with BFA treatment. HopM1-GFP (A), ST-RFP (B) and their merged image (C) are shown. The induction of HopM1-GFP was by spraying of DEX solution with 0.01% of Tween-20. All images are from single focal planes of the epidermal cell layer of *N. tabacum*, 5-6 hours after DEX treatment. Ch: chloroplast.

et al., 2008). Currently known endosome markers are available both for different types of endosomes and/or for different portions of an endosome subgroup (Otegui and Spitzer, 2008; Robert et al., 2008; Robinson et al., 2008).

VHA-a1, a marker for TGN, was selected first for dual localization with HopM1 fusion proteins. Tanaka et al (2009) recently showed that AtMIN7, a member of *Arabidopsis* ARF-GEF family and a cellular target of HopM1 (Nomura et al., 2006), is co-localized with VHA-a1. Moreover, like HopM1-GFP observed in this study, the localization of VHA-a1-GFP does not show significant change upon BFA treatment, although some aggregation was noted (Dettmer et al., 2006). YFP-HopM1 and VHA-a1-RFP (Dettmer et al., 2006) were transiently co-expressed in tobacco leaves, and the expression of YFP-HopM1 was induced by DEX for 3 or 4 hours. The confocal microscopy result showed that YFP-HopM1 and VHA-a1-RFP were largely co-localized (Figure 2-7: Christy Mecey and Sheng Yang He, unpublished). Next, *Arabidopsis* RabF1 (ARA6), another early endosome marker (Ueda et al., 2001; Kotzer et al., 2004; Haas et al., 2007), was selected in co-localization study. The confocal microscopic observation was performed at early time points (before 5 hours) and later time points (after 5 hours) after the DEX-induction of YFP-HopM1. YFP-HopM1 and ARA6-CFP were co-localized at earlier time points (Figure 2-8: Christy Mecey and Sheng Yang He, unpublished), but they did not co-localize at later time point (Figure 2-8).

Localization of truncated HopM1 fusion proteins

Next, the localization of truncated HopM1 proteins fused to GFP or YFP was studied: the truncated HopM1 proteins included HopM1-N-GFP, YFP-HopM1-N, and

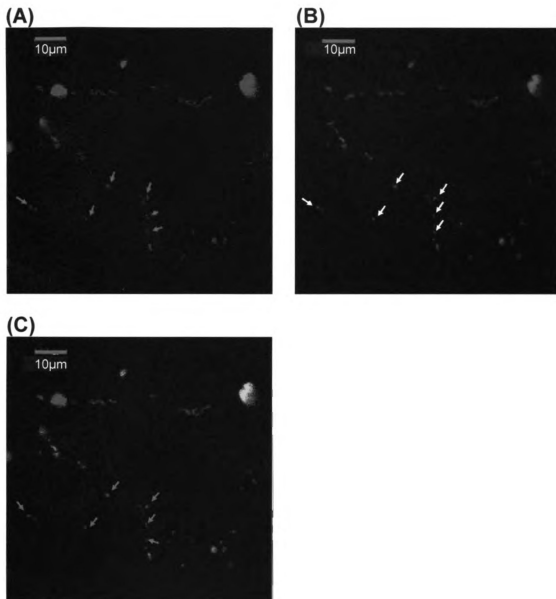
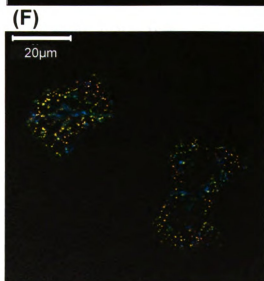
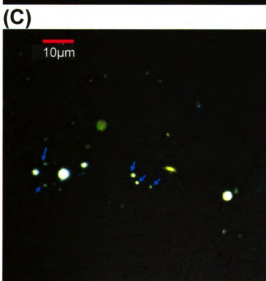
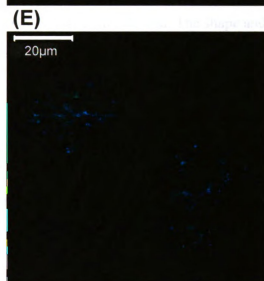
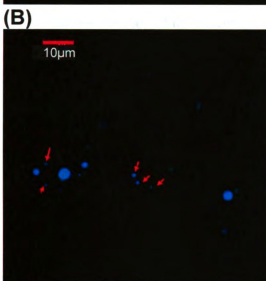
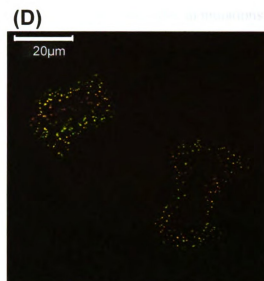
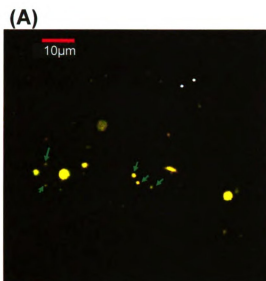


Figure 2-7. Dual localization results of YFP-HopM1 and VHA-a1-RFP. The fluorescence from YFP-HopM1 (indicated with red arrows) (A), VHA-a1-RFP (indicated with white arrows) (B) and their merged image (co-localized punctate structures are marked with blue arrows) (C) within 5 hours after dabbing DEX solution on the leaf surface. All of the images are from Z-stack, from the epidermal cell layer of *N. tabacum*.

Figure 2-8. Dual localization results of YFP-HopM1 and ARA6-CFP. The fluorescence from YFP-HopM1 (A), ARA6-CFP (B) and their merged image (C) within 5 hours after DEX treatment; the fluorescence from YFP-HopM1 (D), ARA6-CFP (E) and their merged image (F) 5 hours after DEX treatment. Images A, B and C were from the leaf sample which was dabbed with DEX solution without Tween-20. Image D, E and F were from the leaf sample which was sprayed with DEX solution containing 0.01% Tween-20. YFP-HopM1-associated punctate structures are yellow (A, C, D and F) and ARA6-CFP are blue (B, C, E and F). YFP-HopM1 in panel A and ARA6-CFP in panel B are indicated with green arrows and red arrows, respectively. Co-localized YFP-HopM1 and ARA6-CFP are marked with blue arrows (C). All images are from single focal planes of the epidermal cell layer of *N.tabacum*.



YFP-HopM1-C (HopM1-C-GFP was excluded from localization study due to mutations introduced during cloning). The confocal microscopic observations were performed at both early time point (within 5 hours) and later time point (between 5 and 6 hours) after DEX-induction. At early time point, HopM1-N-GFP and YFP-HopM1-N were found in small, punctate structures, which were similar to those observed with full-length HopM1 fusion proteins. YFP-HopM1-C was shown in unidentified structures which were round with uneven size (Figure 2-9). In later time point, however, all truncated HopM1 fusion proteins were found dispersed in the cells, instead of punctate structures (Figure 2-9).

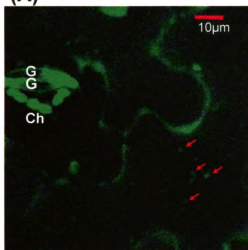
The localization of the N-terminus of HopM1 was further studied. The shape and size of the punctate structures of YFP-HopM1-N at the early time point were similar to those of full-length HopM1 fusion proteins. This result suggested that YFP-HopM1-N might be localized in the same subcellular structures in which full-length HopM1 fusions are localized. To test this possibility, YFP-HopM1-N was co-expressed with VHA-a1-RFP into tobacco leaves, which were examined by confocal microscopy. As shown in Figure 2-10, YFP-HopM1-N and VHA-a1-RFP co-localized, indicating that YFP-HopM1-N is localized in TGN. This result provides evidence that the N-terminal 300 amino acids of HopM1 contain all the information for localization to TGN.

Transgenic expression of HopM1 fusions in *Arabidopsis*

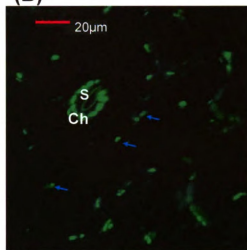
HopM1 fusions which were constructed and examined by confocal microscopy in transient assays were transformed into *Arabidopsis* by floral dipping (Clough and Bent, 1998), to establish stable transgenic *Arabidopsis* plants. The T₁ plants of each HopM1 fusion were sprayed with BASTA solution. Surviving plants were obtained from T₁ seeds

Figure 2-9. Localization of truncated HopM1 fusion proteins. The fluorescence from (A) HopM1-N-GFP at early time point (marked with red arrows); (B) YFP-HopM1-C at early time point (marked with blue arrows); (C) HopM1-N-GFP at later time point; (D) YFP-HopM1-N at later time point; (E) YFP-HopM1-C at later time point. All images are from single focal planes. Panels A and B are from the leaf samples which were dabbed with DEX solution and examined within 5 hours. Panels C, D, and E are from the leaf samples which were sprayed with DEX solution with 0.01% Tween-20 and observed 5 hours after DEX induction. S: Stomate. Ch:chloroplast. G: guard cell.

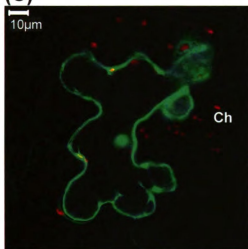
(A)



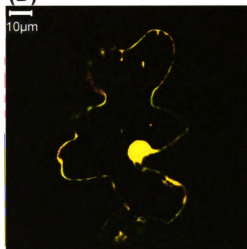
(B)



(C)



(D)



(E)

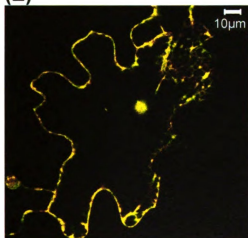
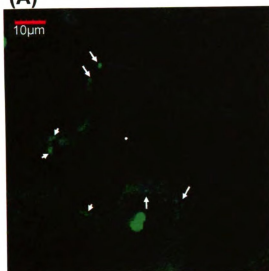
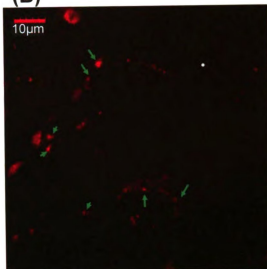


Figure 2-10. Dual localization results of YFP-HopM1-N and VHA-a1-RFP. The fluorescence from YFP-HopM1-N (indicated with white arrows) (A), VHA-a1-RFP (indicated with green arrows) (B) and their merged image (co-localized punctate structures are marked with blue arrows) (C) within 5 hours after dabbing DEX solution on the leaf surface. All of the images are from Z-stack, from the epidermal cell layer of *N.tabacum*.

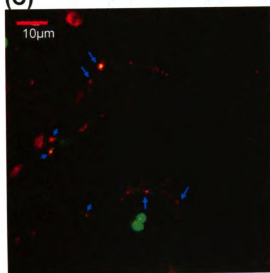
(A)



(B)



(C)



for four constructs in Col-0 background (Table 2-4). One leaf of each plant was detached, dipped in DEX solution, and examined by confocal microscopy after 24 hours (Table 2-4; Figure 2-11A-D). Full-length HopM1 fusions were found in punctate structures, and truncated HopM1 fusion proteins were shown dispersed in the cell (Figure 2-11A-D). These localization patterns were consistent with those in transient assay conducted at later time point after DEX treatment (Figure 2-4 and 2-9). The HopM1 constructs were transformed into the *atmin7* mutant, and the T₁ plants transformed with YFP-HopM1 and YFP-HopM1-N were obtained. YFP-HopM1 in the *atmin7* background was examined by confocal microscopy (Figure 2-11E); it was shown in small, punctate structures, which were similar to those in Col-0 background.

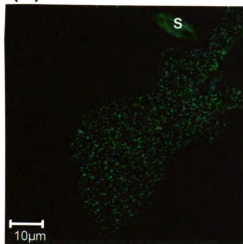
Table 2-4. Summary of transgenic *Arabidopsis* expressing HopM1 fusions.

HopM1 fusion name	<i>Arabidopsis</i> background	Line number
HopM1-GFP	Col-0	#1 [*] , 11, 12
YFP-HopM1	Col-0	#2 [*] , 3, 6
HopM1-N-GFP	Col-0	#1 [*] , 3
YFP-HopM1-N	Col-0	#4 [*] , 10
YFP-HopM1	<i>atmin7</i>	#3 [*]
YFP-HopM1-N	<i>atmin7</i>	#100, 101, 102, 103, 104

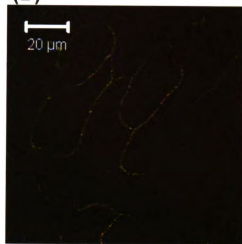
* indicates the transgenic lines which were examined by confocal microscopy (Figure 2-11)

Figure 2-11. HopM1 fusion proteins in *Arabidopsis* (Col-0 and *atmin7* background). The fluorescence of (A) HopM1-GFP in Col-0 (line#1), (B) YFP-HopM1 in Col-0 (line#2), (C) HopM1-N-GFP in Col-0 (line#1), (D) YFP-HopM1-N in Col-0 (line#4), and (E) YFP-HopM1 in *atmin7* (line#3). All images are from single focal planes of leaf samples except A, which was from z-stack. Leaf samples were dipped in DEX solution for 24 hours prior to confocal microscopy.

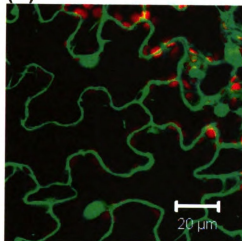
(A)



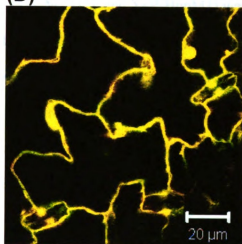
(B)



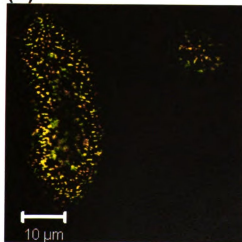
(C)



(D)



(E)



DISCUSSION

To determine the subcellular localization of HopM1 in plant cells, full-length and truncated versions of HopM1 were fused with selected fluorescence protein tags (sGFP and EYFP), and they were analyzed using transient expression assays in tobacco leaves and stable expression in *Arabidopsis* plants. All HopM1 fusions were induced by DEX. Under this condition, the expression of all HopM1 fusions can be regulated based on the induction time and DEX concentration.

When full-length HopM1 fusions (HopM1-GFP and YFP-HopM1) were transiently expressed in tobacco, the leaf tissues began to lose turgor approximately 8 hours after DEX induction, and were dead 48 hours after DEX induction. Tissue death was also induced by 6xHis-HopM1 expressed from pTA7002-6xHis-HopM1. The tissue death induced by HopM1 in *Arabidopsis* was previously reported (DebRoy et al., 2004; Nomura et al., 2006), but the tissue death induction by HopM1 (and HopM1 fusions) in a nonhost plant (tobacco) has not been reported before this study. The characteristics of the tissue death in tobacco plants induced by 6xHis-HopM1, HopM1-GFP and YFP-HopM1 are not clearly defined in this study. Badel et al. (2006) showed that another TTSS effector, AvrE, induced tissue death in *N. tabacum*. AvrE-induced tissue death was interpreted as a kind of nonhost hypersensitive response (HR), but experiments for determining the molecular characteristics of the tissue death were not performed (Badel et al., 2006). Considering that AvrE and HopM1 are both encoded in the CEL of *Pst* DC3000 and that they have redundancy in function (DebRoy et al., 2004), it is possible that the tissue death induced by AvrE and HopM1 (or HopM1 fusion proteins) share the

similar mechanism in tobacco plants. The tissue death caused by DEX-induced HopM1-GFP or YFP-HopM1 limited the DEX-induction time for confocal microscopy and protein sampling for immunoblot analyses. In this thesis, the confocal microscopy was performed within 6 hours after DEX spray, and protein sampling for western blot analysis was done 8 hours after DEX induction.

Confocal microscopy in this study was performed at two different time points: an early time point which was between 3 hours and 4 hours after DEX-induction, and a later time point which was between 4 hours and 6 hours after DEX-induction. In the experiments at later time point, the DEX solution was sprayed onto the leaf surface, and the surfactant Tween 20 (0.01%) was added for enhanced uptake of DEX. Under this condition, the GFP or YFP signal of full-length or truncated HopM1 fusion proteins was intense, clearly distinguishable from the background. The density of the fluorescence of full-length HopM1 fusion was high as well. Because it is generally believed that bacteria deliver only small amounts of effectors into host cells, it would be ideal to express effectors at the lowest possible level that still allow microscopic observation. Therefore, in some experiments, the observation was performed between 3 hours and 5 hours after DEX application, and the DEX was dabbed onto the leaf surface without Tween-20. Under this condition the intensity and density of the GFP/YFP fluorescence were reduced compared to those obtained at later time point, but they were distinguished from the background signal.

Full-length HopM1 fusion proteins were found in small, punctate structures both in early and later time points. However, in later time point the density and intensity of GFP/YFP signal were higher than those in earlier time point. It is likely that, within the

time periods used in this study, the expression of full-length HopM1 fusion proteins is proportional to the DEX exposure time. The difference in DEX concentration between dabbing and spraying (with or without Tween-20, respectively) also could affect the expression of HopM1 fusions.

The dual localization experiments show that YFP-HopM1 co-localizes with VHA-a1-RFP (a marker for TGN) and ARA6-CFP (a marker for early endosome). The localization of HopM1 in TGN is similar to that of AtMIN7 (Tanaka et al., 2009), consistent with the previous report that HopM1 interacts with AtMIN7 (Nomura et al., 2006). This result also is consistent with the notion that HopM1 targets and interferes with vesicle trafficking to suppress host defenses. On the other hand, HopM1-GFP did not co-localize with ST-RFP (a Golgi marker) and did not relocalize after BFA treatment as ST-RFP did. These results indicate that HopM1 does not target Golgi apparatus for its function. Finally, the dual localization assay of HopM1-GFP and PTS1-dsRED2 (a marker for peroxisome: Gould et al., 1989; Reumann, 2004; Fan et al., 2005) showed that HopM1 is not localized to the peroxisome (Appendix 2-1).

Besides full-length HopM1 fusions, the localization of truncated HopM1 fusions (HopM1-N-GFP, YFP-HopM1-N and YFP-HopM1-C) was also studied. These truncated HopM1 fusion proteins did not induce tissue death in tobacco plants, which is correlated with a lack of virulence function of HopM1₁₋₃₀₀ and HopM1₃₀₁₋₇₁₂ in Arabidopsis. The localization of truncated HopM1 fusion proteins provides interesting information. At early time point of DEX treatment, the N-terminus (YFP-HopM1-N) was localized in small, punctate structures, whereas the C-terminus (YFP-HopM1-C) was found in bigger, irregular-sized structures. YFP-HopM1-N co-localized with VHA-a1-RFP and ARA-

CFP, indicating that the N-terminus of HopM1 is sufficient for the localization to the same endosomal compartments in which full-length HopM1 fusion protein is localized. In a previous study to determine the intramolecular regions important for the virulence function of HopM1, transgenic overexpression of the same N-terminus of HopM1 had a dominant-negative effect on full-length HopM1 delivered from bacteria during infection, suppressing the symptom development and multiplication of the Δ CEL mutant complemented with a HopM1-expressing plasmid (Nomura et al., 2006). It was suggested that the N-terminus of HopM1 might function as an independent domain, interfering with the virulence function of the full-length HopM1 in plant cells (Nomura et al., 2006). The same localization of the N-terminus of HopM1 and full-length HopM1 in the endosomal compartments suggests that the dominant-negative effect may be caused in part by competition for the same localization between the overexpressed, nonfunctional N-terminus of HopM1 and full-length, functional HopM1.

At later time point of DEX- treatment, the intensity and density of the fluorescence signal of full-length HopM1 fusion proteins increased, and the shape of the punctate structures of full-length HopM1 proteins became more irregular compared with that at early time point of DEX treatment. Dual localization with a Golgi marker suggests that full length HopM1 was not in the Golgi apparatus at later time points, but the precise location was not precisely determined. It is possible that increased expression of full-length HopM1 fusion proteins led to mislocalization to additional small organelles. Alternatively, the high-density punctate structures at the later time point were caused by the virulence action of full-length HopM1 in plant cells. In this case, by degrading AtMIN7, HopM1 might have induced abnormal structures from endosomal

compartments. The punctate structures were found both in the transient expression assays and in transgenic *Arabidopsis* plants, suggesting that the effect of HopM1 upon the endomembrane structures is similar in nonhost and host plants. This putative distortion of endomembrane structures could be related to the suppression of basal defense of *Arabidopsis* by HopM1 (DebRoy et al., 2004; Nomura et al., 2006).

The different localization patterns between early and later time points were more obvious for the fusion proteins of truncated HopM1: at later time point both the N-terminus and C-terminus of HopM1 were dispersed in the cell. The dispersed localization of truncated HopM1 fusion proteins is similar to that of GFP alone (Appendix 2-2), but this diffused localization is not likely caused by fortuitous degradation of fusion proteins, which could generate a free GFP or YFP tag: western blot analysis did not indicate a significant amount of GFP or YFP. Thus, it seems that the localization of the N-terminus of HopM1 in the endosomal compartments is transient, and that neither the N-terminus nor the C-terminus of HopM1 is sufficient for the long-term localization in the endosome.

The HopM1 fusions were transformed into *Arabidopsis* (Col-0 and *atmin7*) for establishing transgenic *Arabidopsis* plants. DEX-induction time was longer in *Arabidopsis* (up to 24 hours) than in tobacco, because the expression of HopM1 fusions was slower in *Arabidopsis*: for example, confocal microscopic examination of transgenic plants expressing HopM1-GFP in Col-0 showed that, between 4-6 hours after DEX induction, full-length HopM1 fusion was not detected. At least 8 hours were needed for detecting fluorescence above background, and at 24 hours after DEX induction the fluorescence was clearer. The localization patterns of various HopM1 fusions in transgenic *Arabidopsis* were consistent with those in transient assays with tobacco at later

time point of DEX treatment: HopM1-GFP and YFP-HopM1 were associated with small, punctate structures, whereas HopM1-N-GFP and YFP-HopM1-N were dispersed in *Arabidopsis* cells.

The transgenic *Arabidopsis* plants expressing full-length or truncated HopM1 fusion proteins need to be further characterized. First, it would be important to confirm tissue death of transgenic *Arabidopsis* plants expressing HopM1-GFP or YFP-HopM1 after DEX induction: this experiment is needed to determine whether full-length HopM1 fusion proteins act like untagged HopM1, which induces tissue death in *Arabidopsis* (Nomura et al., 2006). Second, the localization of the HopM1 fusion proteins should be determined at early time point and with a reduced DEX concentration to avoid potential problems associated with overexpression of fusion proteins.

REFERENCES

- Alfano, J.R., Charkowski, A.O., Deng, W.L., Badel, J.L., Petnicki-Ocwieja, T., van Dijk, K., and Collmer, A. (2000) The *Pseudomonas syringae* Hrp pathogenicity island has a tripartite mosaic structure composed of a cluster of type III secretion genes bounded by exchangeable effector and conserved effector loci that contribute to parasitic fitness and pathogenicity in plants. *Proc Natl Acad Sci U S A.* **97**: 4856-4861.
- Anders, N. and Jürgens, G. (2008) Large ARF guanine nucleotide exchange factors in membrane trafficking. *Cell Mol Life Sci* **65**: 3433-3445.
- Aoyama, T. and Chua, N.H. (1997) A glucocorticoid-mediated transcriptional induction system in transgenic plants. *Plant J* **11**: 605-612.
- Assaad, F.F., Qiu, J.L., Youngs, H., Ehrhardt, D., Zimmerli, L., Kalde, M., Wanner, G., Peck, S.C., Edwards, H., Ramonell, K., Somerville, C.R., and Thordal-Christensen, H. (2004) The PEN1 syntaxin defines a novel cellular compartment upon fungal attack and is required for the timely assembly of papillae. *Mol Biol Cell* **15**: 5118-5129.
- Badel, J.L., Nomura, K., Bandyopadhyay, S., Shimizu, R., Collmer, A., and He, S.Y. (2003) *Pseudomonas syringae* pv. *tomato* DC3000 HopPtoM (CEL ORF3) is important for lesion formation but not growth in tomato and is secreted and translocated by the Hrp type III secretion system in a chaperone-dependent manner. *Mol Microbiol* **49**: 1239-1251.
- Badel, J.L., Shimizu, R., Oh, H.S., and Collmer, A. (2006) A *Pseudomonas syringae* pv. *tomato* avrE1/hopM1 mutant is severely reduced in growth and lesion formation in tomato. *Mol Plant-Microbe Interact* **19**: 99-111.
- Bassham, D.C., Brandizzi, F., Otegui, M.S., and Sanderfoot, A.A. (2008) The secretory system of Arabidopsis: September 30, 2008. The *Arabidopsis* Book. Rockville, MD: American Society of Plant Biologists.
<http://www.aspb.org/publications/arabidopsis/>
- Brandizzi, F., Snapp, E.L., Roberts, A.G., Lippincott-Schwartz, J., and Hawes, C. (2002) Membrane protein transport between the endoplasmic reticulum and the Golgi in tobacco leaves is energy dependent but cytoskeleton independent: evidence from selective photobleaching. *Plant Cell* **14**: 1293-1309.
- Buell, C.R., Joardar, V., Lindeberg, M., Selengut, J., Paulsen, I.T., Gwinn, M.L., Dodson, R.J., Deboy, R.T., Durkin, A.S., Kolonay, J.F., Madupu, R., Daugherty, S., Brinkac, L., Beanan, M.J., Haft, D.H., Nelson, W.C., Davidsen, T., Zafar, N., Zhou, L., Liu, J., Yuan, Q., Khouri, H., Fedorova, N., Tran, B., Russell, D., Berry,

- K., Utterback, T., Van Aken, S.E., Feldblyum, T.V., D'Ascenzo, M., Deng, W.-L., Ramos, A.R., Alfano, J.R., Cartinhour, S., Chatterjee, A.K., Delaney, T.P., Lazarowitz, S.G., Martin, G.B., Schneider, D.J., Tang, X., Bender, C.L., White, O., Fraser, C.M., and Collmer, A. (2003) The complete genome sequence of the *Arabidopsis* and tomato pathogen *Pseudomonas syringae* pv. *tomato* DC3000. *Proc Natl Acad Sci U S A* **100**: 10181-10186.
- Campbell, R.E., Tour, O., Palmer, A.E., Steinbach, P.A., Baird, G.S., Zacharias, D.A., and Tsien, R.Y. (2002) A monomeric red fluorescent protein. *Proc Natl Acad Sci U S A* **99**: 7877-7882.
- Chiu, W., Niwa, Y., Zeng, W., Hirano, T., Kobayashi, H., and Sheen, J. (1996) Engineered GFP as a vital reporter in plants. *Curr Biol* **6**: 325-330.
- Clough, S.J. and Bent, A.F. (1998) Floral dip: a simplified method for *Agrobacterium*-mediated transformation of *Arabidopsis thaliana*. *Plant J* **16**: 735-743.
- Collins, N.C., Thordal-Christensen, H., Lipka, V., Bau, S., Kombrink, E., Qiu, J.L., Huckelhoven, R., Stein, M., Freialdenhoven, A., Somerville, S.C., and Schulze-Lefert, P. (2003) SNARE-protein-mediated disease resistance at the plant cell wall. *Nature* **425**: 973-977.
- DebRoy, S., Thilmony, R., Kwack, Y.B., Nomura, K., and He, S.Y. (2004) A family of conserved bacterial effectors inhibits salicylic acid-mediated basal immunity and promotes disease necrosis in plants. *Proc Natl Acad Sci U S A* **101**: 9927-9932.
- Dettmer, J., Hong-Hermesdorf, A., Stierhof, Y.D., and Schumacher, K. (2006) Vacuolar H⁺-ATPase activity is required for endocytic and secretory trafficking in *Arabidopsis*. *Plant Cell* **18**: 715-730.
- Emanuelsson, O., Brunak, S., von Heijne, G., Nielsen, H. (2007) Locating proteins in the cell using TargetP, SignalP, and related tools. *Nature Protocols* **2**: 953-971.
- Fan, J., Quan, S., Orth, T., Awai, C., Chory, J., and Hu, J. (2005) The *Arabidopsis* PEX12 gene is required for peroxisome biogenesis and is essential for development. *Plant Physiol* **139**: 231-239.
- Gillingham, A.K. and Munro, S. (2007) The small G proteins of the Arf family and their regulators. *Annu Rev Cell Dev Biol* **23**: 579-611.
- Goodin, M.M., Dietzgen, R.G., Schichnes, D., Ruzin, S., and Jackson, A.O. (2002) pGD vectors: versatile tools for the expression of green and red fluorescent protein fusions in agroinfiltrated plant leaves. *Plant J* **31**: 375-383.
- Gould, S.J., Keller, G.A., Hosken, N., Wilkinson, J., and Subramani, S. (1989) A conserved tripeptide sorts proteins to peroxisomes. *Journal of Cell Biology*

108: 1657–1664.

Jürgens, G. and Geldner, N. (2002) Protein secretion in plants: from the trans-Golgi network to the outer space. *Traffic* **3**: 605-613.

Haas, T.J., Sliwinski, M.K., Martínez, D.E., Preuss, M., Ebine, K., Ueda, T., Nielsen, E., Odorizzi, G., and Otegui, M.S. (2007) The *Arabidopsis* AAA ATPase SKD1 is involved in multivesicular endosome function and interacts with its positive regulator LYST-INTERACTING PROTEIN5. *Plant Cell* **19**: 1295-1312.

Hauck, P., Thilmony, R., and He, S.Y. (2003) A *Pseudomonas syringae* type III effector suppresses cell wall-based extracellular defense in susceptible *Arabidopsis* plants. *Proc Natl Acad Sci U S A* **100**: 8577-8582.

Kalde, M., Nuhse, T.S., Findlay, K., and Peck, S.C. (2007) The syntaxin SYP132 contributes to plant resistance against bacteria and secretion of pathogenesis-related protein 1. *Proc Natl Acad Sci U S A* **104**: 11850-11855.

Kotzer, A.M., Brandizzi, F., Neumann, U., Paris, N., Moore, I., and Hawes, C. (2004) AtRabF2b (Ara7) acts on the vacuolar trafficking pathway in tobacco leaf epidermal cells. *J Cell Sci* **117**: 6377-89.

Lam, S.K., Siu, C.L., Hillmer, S., Jang, S., An, G., Robinson, D.G., and Jiang, L. (2007) Rice SCAMP1 defines clathrin-coated, trans-golgi-located tubular-vesicular structures as an early endosome in tobacco BY-2 cells. *Plant Cell* **19**: 296-319.

Memon, A.R. (2004) The role of ADP-ribosylation factor and SAR1 in vesicular trafficking in plants. *Biochim Biophys Acta* **1664**: 9-30.

Nakai, K. and Kanehisa, M. (1991) Expert system for predicting protein localization sites in gram-negative bacteria. *Proteins* **11**: 95-110.

Nomura, K., Debroy, S., Lee, Y.H., Pumplin, N., Jones, J., and He, S.Y. (2006) A bacterial virulence protein suppresses host innate immunity to cause plant disease. *Science* **313**: 220-223.

Otegui, M.S. and Spitzer, C. (2008) Endosomal functions in plants. *Traffic* **9**: 1589-1598.

Reumann, S. (2004) Specification of the peroxisome targeting signals type 1 and type 2 of plant peroxisomes by bioinformatics analyses. *Plant Physiol* **135**: 783–800.

Ritenthaler, C., Nebenführ, A., Movafeghi, A., Stussi-Garaud, C., Behnia, L., Pimpl, P., Staehelin, A., and Robinson, D.G. (2002) Reevaluation of the effects of brefeldin A on plant cells using tobacco bright yellow 2 cells expressing Golgi-targeted green fluorescence protein and COPI antisera. *Plant Cell* **14**: 237-261.

- Robert, S., Chary, S.N., Drakakaki, G., Li, S., Yang, Z., Raikhel, N.V., and Hicks, G.R. (2008) Endosidin1 defines a compartment involved in endocytosis of the brassinosteroid receptor BRI1 and the auxin transporters PIN2 and AUX1. *Proc Natl Acad Sci U S A* **105**: 8464-8469.
- Robinson, D.G., Jiang, L., and Schumacher, K. (2008) The Endosomal system of plants: charting new and familiar territories. *Plant Physiol* **147**: 1482-1492.
- Saint-Jore, C.M., Evins, J., Batoko, H., Brandizzi, F., Moore, I., and Hawes, C. (2002) Redistribution of membrane proteins between the Golgi apparatus and endoplasmic reticulum in plants is reversible and not dependent on cytoskeletal networks. *Plant J* **29**: 661-678.
- Tanaka, H., Kitakura, S., De Rycke, R., De Groodt, R., and Friml, J. (2009) Fluorescence imaging-based screen identifies ARF-GEF component of early endosomal trafficking. *Curr Biol* **19**: 391-397.
- Ueda, T., Yamaguchi, M., Uchimiya, H., and Nakano, A. (2001) Ara6, a plant-unique novel type Rab GTPase, functions in the endocytic pathway of *Arabidopsis thaliana*. *EMBO J* **20**: 4730-4741.
- Ueda, T., Uemura, T., Sato, M.H., and Nakano, A. (2004) Functional differentiation of endosomes in *Arabidopsis* cells. *Plant J* **40**: 783-789.
- Wang, D., Weaver, N.D., Kesarwani, M., and Dong, X. (2005) Induction of protein secretory pathway is required for systemic acquired resistance. *Science* **308**: 1036-1040.
- Wee, E.G.T., Sherrier, D.J., Prime, T.A., and Dupree, P. (1998) Targeting of active sialyltransferase to the plant Golgi apparatus. *Plant Cell* **10**: 1759-1768.

CHAPTER 3

Studies of the roles of several *Arabidopsis* ARF-GEFs in the defense against bacteria and their interaction with HopM1

Kinya Nomura contributed to Figure 3-9.

ACKNOWLEDMENTS

I appreciate the help of Dr. Kinya Nomura, who contributed to the Figure 3-9, and gave me numerous and valuable advices during my Ph.D.

ABSTRACT

AtMIN7, an adenosine-diphosphate ribosylation factor-guanine nucleotide-exchange factors (ARF-GEF) gene of *Arabidopsis*, has a role in defense against the Δ CEL mutant of *Pst* DC3000. *AtMIN7* interacts with N-terminus of HopM1 (HopM1₁₋₃₀₀) and it is degraded by full-length HopM1. In addition to *AtMIN7*, there are seven more *ARF-GEF* genes in *Arabidopsis*. To determine whether any of these genes have a role in defense, the multiplication of the Δ CEL mutant was quantified in the T-DNA insertion lines, and the yeast two-hybrid system was used for testing the interactions between HopM1 and these ARF-GEFs.

I was able to obtain T-DNA insertion lines for three of the seven ARF-GEF genes, *BIG2*, *BIG3* and *BIG4*. The T-DNA insertion mutants of *BIG2* (salk_033446) and *BIG4* (salk_082249) were knockouts, and the *BIG3* (salk_044617) insertion line was a knock-down. Unlike *atmin7* plants the multiplication of the Δ CEL mutant in these T-DNA insertion mutants was not significantly higher than wild type *Arabidopsis* (Col-0), suggesting that none of the three genes have significant role in the defense against the Δ CEL mutant as *AtMIN7* did.

The C-terminal portions of four ARF-GEFs (*BIG1*, *BIG3*, *GNL1* and *GNL2*) were studied by yeast two-hybrid assay to determine whether they interacted with HopM1₁₋₃₀₀. The C-terminus of *GNL2* did not interact with HopM1₁₋₃₀₀. The interactions between HopM1₁₋₃₀₀ and the C-termini of *BIG1*, *BIG3* and *GNL1* were not determined because of the failure to express the proteins in yeast.

INTRODUCTION

Previous research results showed that twenty one *Arabidopsis* proteins interact with the first 300 amino acids of the TTSS effector HopM1 from the bacterial pathogen *Pseudomonas syringae* pv. *tomato* (*Pst*) DC3000. These proteins were named AtMINs (*Arabidopsis thaliana* HopM1 interactors). At least eight AtMINs were destabilized by full-length HopM1 in plants and in yeast. Among them, *AtMIN7* was shown to be important for *Arabidopsis* defense against the Δ CEL mutant of *Pst* DC3000 (Nomura et al., 2006). In the Δ CEL mutant the conserved effector locus (CEL), encoding HopM1 and three other effectors, is deleted. As a result, the Δ CEL mutant does not cause symptoms and its multiplication level is reduced in host plants (Alfano et al., 2000; Badel et al., 2003; DebRoy et al., 2004). In the *atmin7* plants, however, the multiplication of the Δ CEL mutant is increased and the symptom development is partially restored (Nomura et al., 2006). In addition, the *atmin7* mutant the Δ CEL mutant is compromised in callose deposition (a defense response) after the inoculation of the Δ CEL mutant compared with wild-type Col-0 plants (Nomura et al., 2006).

AtMIN7 is one of the eight members of *Arabidopsis* gene family encoding adenosine-diphosphate ribosylation factor-guanine nucleotide-exchange factors (ARF-GEFs; Anders and Jürgens, 2008; Figure 3-1). ARF-GEFs regulate adenosine-diphosphate ribosylation factor (ARF) GTPase by promoting nucleotide exchange from its inactive GDP-bound state to the active GTP-bound state. It has been shown that ARF-GTPases function in vesicle budding necessary for intracellular vesicle trafficking, and ARF-GEF-dependent activation of ARF is critical for promoting the vesicle formation

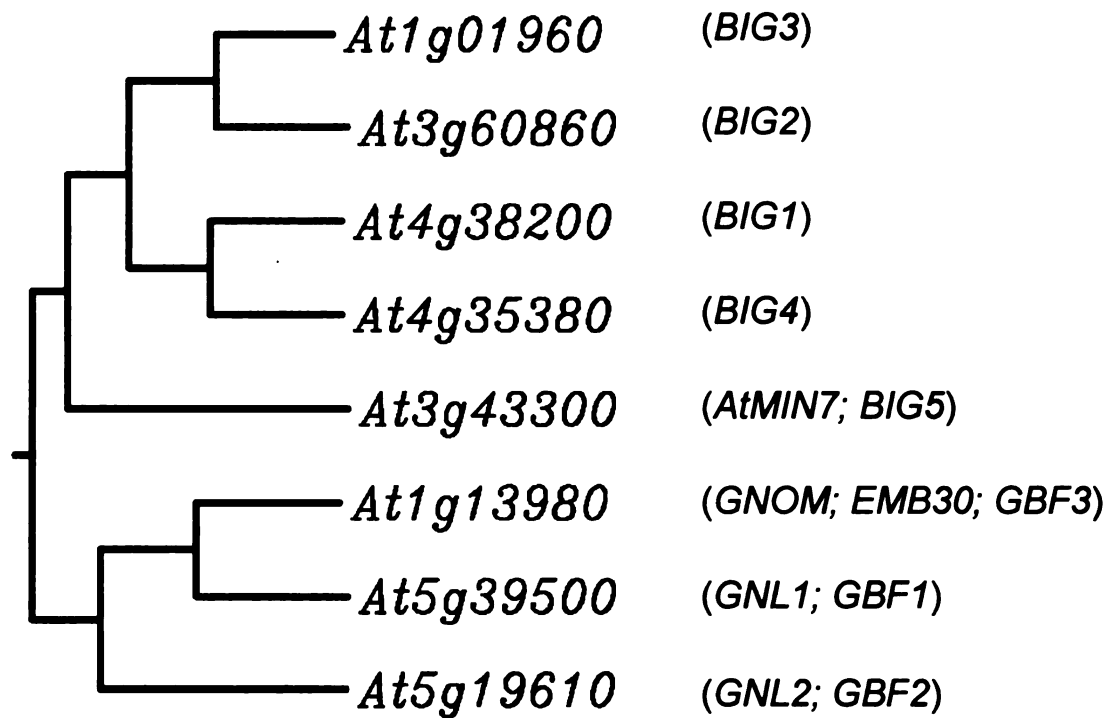


Figure 3-1. A phylogenetic tree of *Arabidopsis* ARF-GEF genes with their names in parenthesis (modified from Nomura et al., 2006).

and budding in trafficking pathways (Memon, 2004; Gillingham and Munro, 2007; Casanova, 2007; Anders and Jürgens, 2008; Bassham et al., 2008). ARF-GEF proteins share a conserved Sec7 domain that is sufficient to catalyze GTP/GDP exchange on ARFs (Chardin et al., 1996; Jackson and Casanova, 2000; Gillingham and Munro, 2007). The Sec7 domains of some ARF-GEFs are sensitive to a fungal toxin Brefeldin A (BFA). BFA binds to the ARF-GDP complex and interferes with the exchange of GTP for GDP (Anders and Jürgens, 2008).

The eight *ARF-GEF* genes including *AtMIN7* are grouped into two subfamilies: Sec7/BIG-type and Gea/GNOM/GBF-type (Cox et al., 2004; Gillingham and Munro, 2007). *AtMIN7* is in the Sec7/BIG-type subfamily. The *Arabidopsis* *ARF-GEF* genes are closely clustered in a larger phylogenetic tree containing all ARF-GEF genes, and their Sec7 domains show highly similarity (Cox et al., 2004). Currently, *AtMIN7* is the only *ARF-GEF* gene which has been studied in plant-pathogen interactions. Two other *ARF-GEF* genes have been characterized in growth and development of *Arabidopsis*: GNOM (Steinmann et al., 1999; Geldner et al., 2003), and GNOM-LIKE 1 (GNL1: Richter et al., 2007; Teh and Moore, 2007). GNOM is found in endosome/prevacuolar compartments (PVCs) of the *Arabidopsis* cells, and it is involved in the polarized targeting of PIN1 which is critical for polar auxin transport (Steinmann et al., 1999; Geldner et al., 2003). GNL1 is detected in the Golgi stack and has overlapping cellular functions with GNOM (Richter et al., 2007; Teh and Moore, 2007).

Although the multiplication of the Δ CEL mutant is higher in *atmin7* mutant plants compared with that in wild-type Col-0 plants, it does not reach the level of *Pst* DC3000 growth in *Arabidopsis*, suggesting that *AtMIN7* is not the only host target of HopM1

(Nomura et al., 2006). Second, in preliminary experiments the product of another *ARF-GEF* encoding gene (*AtBIG2* [Cox et al., 2004]) had a weak yeast two-hybrid interaction with HopM1 (Kinya Nomura and Sheng Yang He, unpublished). Third, BFA treatment of *Arabidopsis* Col-0 leaves restored the multiplication of the Δ CEL mutant to the level of *Pst* DC3000, indicating that there are other host targets of HopM1 which are BFA-sensitive, possibly including additional ARF-GEFs (Nomura et al., 2006). These observations suggest that other ARF-GEFs may also have a role in the defense of *Arabidopsis* and their products may be targeted by HopM1.

Nomura et al. (2006) tested the C-termini of three *ARF-GEF* genes (*BIG2*, *BIG4* and *GNOM*) in yeast two-hybrid system with HopM1₁₋₃₀₀; none of them showed an interaction with HopM1₁₋₃₀₀. However, not all *Arabidopsis ARF-GEF* genes were tested. Additionally, no study has been reported to directly determine the role of individual *ARF-GEF* genes in *Arabidopsis* defense against the Δ CEL mutant.

In this chapter, *Arabidopsis ARF-GEF* genes that had not been previously studied were analyzed with two approaches. First, to determine a possible role of other *ARF-GEF* genes in *Arabidopsis* defense against the Δ CEL mutant, the growth of the Δ CEL mutant in the T-DNA insertion mutants of *ARF-GEF* genes were compared with that of *atmin7* plants. Second, yeast two-hybrid assays were performed to examine possible physical interactions between these ARF-GEFs with HopM1₁₋₃₀₀.

MATERIALS AND METHODS

Identification of homozygous T-DNA insertion mutants for *Arabidopsis ARF-GEF* genes

The T-DNA insertion mutant of *AtMIN7* (salk_012013) was previously characterized by Nomura et al. (2006) and it was used in this chapter. The genomic sequences and putative T-DNA insertions of the *ARF-GEF* mutants were examined in The *Arabidopsis* Information Resource (TAIR: www.arabidopsis.org), and the mutants with putative T-DNAs located in exons were selected (Table 3-1). The seeds of the selected T-DNA insertion mutants were purchased from *Arabidopsis* Biological Resource Center (ABRC, The Ohio State University, Columbus, OH).

Plants were grown in soil for 4-5 weeks. Genomic DNA was extracted from leaf tissue of each plant and prepared following the protocol provided with the SIGMA REDExtract-N-AmpTM Plant PCR kit (Sigma-Aldrich, St. Louis, MO). The primers for genomic PCR are summarized in Table 3-2. For each T-DNA insertion mutant, two pairs of primers were used. One pair consists of two gene-specific primers that are before and after the putative insertion site of T-DNA. The second primer set includes a gene-specific primer and the primer designed from the left border of the T-DNA (5'-GACCGCTTGCTGCAACTCTCTC-3'). The locations of the primers in each *ARF-GEF* gene sequence are shown in the appendix (Appendix 3-1 to 3-7). Ten microliters of each PCR product was run on a 1% agarose gel containing SYBR® Safe DNA gel stain (1:10,000 dilution: Invitrogen, Carlsbad, CA). Gels were photographed with Quantity One software (Bio-Rad Laboratories, Hercules, CA), and the images were processed with

Table 3-1. The *Arabidopsis ARF-GEF* genes, their selected T-DNA insertion mutants, and the putative insertion site of T-DNA of each mutant.

<i>Arabidopsis ARF-GEF</i> gene	T-DNA insertion mutants	Insertion site
At4g38200 (<i>BIG1</i>)	salk_066766	1st exon
At3g60860 (<i>BIG2</i>)	salk_033446	8th exon
At1g01960 (<i>BIG3</i>)	salk_044617	7th exon
At4g35380 (<i>BIG4</i>)	salk_082249	8th exon
At1g13980 (<i>GNOM;EMB30;GBF3</i>)	salk_103014	1st exon
At5g39500 (<i>GNL1;GBF1</i>)	salk_067415	1st exon
At5g19610 (<i>GNL2;GBF2</i>)	salk_021757	3rd exon

Table 3-2. Primer sets designed for screening homozygous T-DNA insertion mutants for *ARF-GEF* genes.

<i>ARF-GEF</i> gene	T-DNA mutants	Primer sets
At1g01960 (<i>BIG3</i>)	salk_044617	Forward primer: 5'-GGAGGAAGAAGGAACTATCTACAAGATGC-3' Reverse primer: 5'-GTTATAATTGCGCAACTCTTCCCGCTC-3'
At3g60860 (<i>BIG2</i>)	salk_033446	Forward primer: 5'-GTCATTGTTATGCGTAGAAGTAATGATGTTGAGAT-3' Reverse primer: 5'-GCGTAAGGTATCAAACATAATCTGTAGTGC-3'
At4g38200 (<i>BIG1</i>)	salk_066766	Forward primer: 5'-CGTGAGAAGTCGAATATGCGTTAGATGTC -3' Reverse primer: 5'-GAGCATGATCTGAGCCAGCACAGATTTA -3'
At4g35380 (<i>BIG4</i>)	salk_082249	Forward primer: 5'- CTGTTGCAATATTTGTCATGGACTCGCTT-3' Reverse primer: 5'- CTGGGAGAATGCTAGAGCTGAAGATTCCA-3'
At1g13980 (<i>GNOM;EMB30;GBF3</i>)	salk_103014	Forward primer: 5'-GGAGGTCGATACATGTCTGGTGATGATC-3' Reverse primer: 5'-CAGAGCCATACGGAGTCCCAAGTATG-3'
At5g39500 (<i>GNL1;GBF1</i>)	salk_067415	Forward primer: 5'-GAATCATCCTTCGGAAGTAACTCGTTCC-3' Reverse primer: 5'-CTCATGCATTGTGTGGCGAGCTATAC -3'
At5g19610 (<i>GNL2;GBF2</i>)	salk_021757	Forward primer: 5'-GCATTATCTAACGTCCACCG-3' Reverse primer: 5'-GGAGACTAATGTGGTATGTGG-3'

Adobe Photoshop Element version 5.5 or 7.0.

Confirmation of gene knockout of T-DNA insertion mutants by reverse transcription and polymerase chain reaction (RT-PCR)

Homozygous T-DNA insertion mutants identified by PCR (salk_033446, salk_044617, and salk_082249) were analyzed by RT-PCR to confirm the loss of transcript. Total RNA sample of each salk line was extracted from 100 mg of *Arabidopsis* leaf tissue with the RNeasy® Plant Mini Kit (QIAGEN, Valencia, CA), followed by genomic DNA removal using RQ1 RNase-free DNaseI (Promega, Madison, WI). RNA was quantified with a NanoDrop ND-1000 Spectrophotometer (NanoDrop, Wilmington, DE).

RT-PCR was performed using the RNA LA PCR Kit (AMV), Ver. 1.1 (TaKaRa, Japan). The reverse transcription reaction mixture was prepared following the modified protocol of RNA LA PCR Kit (AMV), Ver. 1.1 (5mM MgCl₂, 1 × RNA PCR Buffer, 1 mM dNTP mixture, 1 unit/μl RNase Inhibitor, 0.25 units/μl AMV Reverse Transcriptase, 0.125 μM Oligo-dT Adaptor Primer, RNase-free water and 200-300 ng total RNA). The reverse transcription reaction was performed in a total volume of 50 μl, and incubated for 30 minutes at 45°C, followed by 5 minutes at 99°C and 5 minutes at 5°C. This cDNA sample was used as template in the PCR reaction with gene-specific primer pairs (Table 3-3). The sequences of these primers were chosen after the putative T-DNA insertion sites (Appendix 3-1 to 3-7). Each primer was checked by Basic Local Alignment Search Tool (BLAST: <http://blast.ncbi.nlm.nih.gov/blast.cgi>), to determine whether the primer shares sequence identity with an unrelated area of the *Arabidopsis* genome. Only the

Table 3-3. Primers for RT-PCR for T-DNA insertion mutants of selected *ARF-GEF* genes.

Primer Name	Sequence
Forward primer for Actin8 (<i>ACT8</i> , At1g49240)	5'- CTACATTGCTCCCTCTGTGC-3'
Reverse primer for Actin8 (<i>ACT8</i> , At1g49240)	5'- AGGAATGACCTGTGACGAGTG-3'
Forward primer E for salk_044617 (<i>BIG3</i> , At1g01960)	5'- GTTGACAATGTCAAGTCGGGATGGAAGAG -3'
Reverse primer E for salk_044617 (<i>BIG3</i> , At1g01960)	5' -CGTATGAGAAGTCAGGGGATGTAGCA -3'
Forward primer H for salk_082249 (<i>BIG4</i> , At4g35380)	5'-GCGTTGCATAGAAGTATTGTTCCACATTCTG-3'
Reverse primer H for salk_082249 (<i>BIG4</i> , At4g35380)	5'-GTAACCATGTCTTGGAGGACATCATGTAGG-3'
Forward primer D3 for salk_033446 (<i>BIG2</i> , At3g60860)	5'-CGCCTGGCTCTACGAGACCT-3'
Reverse primer D3 for salk_033446 (<i>BIG2</i> , At3g60860)	5'-CTTGCATCTGTGTCATGGGTCCTAGC-3'

primers which showed identity only with the selected *ARF-GEF* gene were used for RT-PCR. The locations of the selected primers in each *ARF-GEF* gene sequence are shown in the appendix. RT-PCR was performed using *Arabidopsis ACT8* gene-specific primers as a control (Table 3-3).

The second PCR reaction contained 2.5 mM MgCl₂, 1 X LA PCR Buffer II, 0.2 µM of each primer, sterilized distilled water and 10 µl of the previous reverse transcription reaction sample in a final volume of 50 µl. The reaction was performed as follows: 94°C, 2 minutes (1 cycle), 94°C, 30 seconds, 53°C, 30 seconds, 72°C, 1 -2 minutes (25 cycles, 30 cycles, 40 cycles or 50 cycles) and 72°C, 10 minute (1 cycle). Ten µl of the PCR reactions were loaded on a 1% agarose gel containing SYBR® Safe DNA gel stain (1:10,000 dilution: Invitrogen, Carlsbad, CA). Gels were photographed with Quantity One software (Bio-Rad Laboratories, Hercules, CA), and the images were processed with Adobe Photoshop Element version 5.5 or 7.0.

Construction of *ARF-GEF* gene clones for yeast two-hybrid assays

Four *ARF-GEF* genes (*BIG1*, *BIG3*, *GNL1* and *GNL2*) were cloned for the yeast two-hybrid assay. The 3' ends downstream of the putative Sec7 domains were selected for cloning, following the cloning procedure of the 3' end of *AtMIN7* (Nomura et al., 2006): the sequences of the ORFs of four selected ARF-GEF genes were aligned with other *Arabidopsis ARF-GEF* genes by CLUSTALW (<http://align.genome.jp/>), and the putative Sec7 domain and the C-terminus after the Sec7 domain was determined in each ORF. The putative amino acid sequence of the C-terminus of each ARF-GEF is in Figure 3-2. The 3'ends were obtained by PCR with primers in Table 3-4. The diagrams of

Table 3-4. Primer sequences for obtaining clones of selected *ARF-GEF* genes for yeast two-hybrid assay with the N-terminus of HopM1.

<i>ARF-GEF</i> gene	Template	Primer
<i>BIG1</i> (At4g38200)	cDNA	Forward primer : <i>EcoRI</i> 5'- CGT <u>GAATTC</u> CATAGAGCATTTGCAATTATTGGGCGAGG-3' Reverse primer: <i>Clal</i> 5' <u>GTTATCGATT</u> TATTCATCCATCATTGCACCCATACATG TATGG-3'
<i>BIG3</i> (At1g01960)	cDNA	Forward primer: <i>EcoRI</i> 5'-CGC <u>GAATTC</u> TTTGAGCATCTTCATCTCTTGGGGGAAG- 3' Reverse primer: <i>EcoRI</i> 5'-CTA <u>GAATTC</u> TTAGCAGCAAGAGCGGAGGAGAA-3'
<i>GNL1</i> (At5g39500)	Genomic DNA	Forward primer: <i>XmaII</i> 5'-TAT <u>CCCGGG</u> AGCCTCAACAACTCCACATTTTACCA- 3' Reverse primer: <i>XhoI</i> 5'-GAA <u>CTCGAG</u> TCAGACCTCATTTCCCGGTACCG-3'
<i>GNL2</i> (At5g19610)	Genomic DNA	Forward primer: <i>EcoRI</i> 5'CTA <u>GAATTC</u> AAACTTAGGAAGCTTCAGCTTCTTCCACA -3' Reverse primer: <i>XhoI</i> 5'GAA <u>CTCGAG</u> GCTAAATCTCTTCATCGGGAAATAACTCA TCCTTGAG-3'

The restriction sites inserted in the primers for subcloning are shown as bold and underlined.

Figure 3-2. Predicted amino acid sequences of the ARF-GEFs for yeast two-hybrid assays. Green-colored letters indicate amino acids for the putative Sec7 domain, and yellow-colored letters indicate amino acids for the C-terminus of an ARF-GEF. Asterisks(*) denote the stop codons.

[illegible]

MASTEVDLSRLGRVVPALDKVIKNASWRKXSLAHECKSVIERLRSPENSSPVADSESGSSIPGLPHDGGGA
AEYSLAESEIILSPLINASSTGVLKIVDPAVDCIQKLIAGHYVRGEADPTGGPEALLLSKLIETICKCHEL
DDEGLELLVLKTLTAVTSISLRHGDSSLQIVRTCYGIYLGSRNVVNQATAKASLVQMSVIVFRMEADS
STVPIQPIVVAELMEPMDKSESDPSTTQSVQGGFITKIMQDIDGVFNASANAGTFFGGHDGAFETSLPGTANP
TDLLDSTDKDMLDAKYWEISMYKSALEGRKGELADGEVEKDDDESEVQIGNKLRRDAFLVFRALCKLSMKTP
PKEDPELMRGKIVALELLKILLENAGAVFRTSDRFLGAIKQYLCLSLKNSASNLMIIFQLSCSILLSLV
RFRAGLKAEGIVFFPMVILRVLENVAQPFQOKMIVLFLDKLCLVDSQILVDIFINYDCDVNSSNIFERMV
NGLLKTAGQVPPGTVTLLPPQEAAAMKLEAMKVLAVLRSMGDWVNKQLRLPDYPYSAKMLEIVDRNLEEGS
HPVENGGKDGHHGGFFERSDSQSELSSGNSDALIEQRRRA
SFEFQGMFEDEATRAFLRGFRLPGEAQKIDR
EKFAERFCKCNPKDESSADTAYVLAYSVILLNTDAHNPMVKSMTADGETRNNRGIDDGKDLPEYLRA
ERISRNE KMKDDGLGPQQKQPTNSSRLLGLDTILNIVVPRRGDDMMNMTSDDLIRHMQERFEKARKSE
SVYYAASDVIIILRFMVEVCWAPMLAAFSVPLDQSDDAVITTLCLEGFHHAIHVTSMVSLKTHRDFAVTSLA
KFTSLHSPADIKQKNIEAIIKAIKVLAAEEEGNYLQDAWEHILTCVSRFEHLHLLEGAPPDATFFAFPQTES
GNSPLAKPNVSPAIKERAPKGLQYAAASAMRISGYSVGAGKASIAHTVNSEQMNNLISNLNLEQVGDMSRI
FTRSQRNLNSEAIDFVKALCKVSMDELRSMPDSRPFVSLTKIVEIAIHYNNMRLIRLVWSSIIHWLSDFFVTIG
CSDNLSIAIFAMDSLRQLSMKFLEREELANYNFQNEFMKPFVVVMRKSGAVEIRELIIRCVSQMVLSRVDN
VKSGWKSMMFIITTAADHAHNIVFLSFEMVEKIIIRDYFPHITETETTTFTDCVNCLVAFTNCKFEKDILS
QAI AFLQYCARKLAEGYVGSSLRNPPLSPQGGKIGKQDSGKFLESDEHLYSWFPLLAGLSLSFDPRAEI
RKVALKVLFDTLRNHGDHFSALWERVESVLFRIFDYVRQDVPSEDDSTDQRGYNGEVDQESWLYETCS
LALQLVVDL FVN FYKTVNPLLKKVLM LFVSLIKRPHQSLAGAGIAALVRLMRDVGHQFSNEQWLEVWSCIK
EAADATSPDFS YVT SEDLMEDVSNEDETNDNSNDALRRNRQLHAVVTDAKSKASIQIFVIQAVTDIYDMY
RMSLTANHMLMLFDAMHSGRENSNAHKINADLLRSRLQELGSSLESQEAPLLRLNENESFQTCMTFLDNLISD
QPVGNEAIEIESHLSIGREVLEFYINISCSKEQSSRAWVPSGSGKKELTARAPLVAAIQT LGNMGESL
FKKNLPELFPLIATLISCEHGSGEVOVALSDMLQTSMSGPVLLRSCC*

***GNL1* (At5g39500)**

***GNL2* (At5g19610)**

102

Figure 3-2 (continued).

NVFLVYLEQIVESAEFRTFWLGVLRMDTCMKADLGEYGDNKLQEVVPELLTMMIGTMKEKEILLVQKEDDD
LWEITYIQWIA PALKDELFPDEEI *

ARF-GEF genes are in Figure 3-3. The genomic DNA or cDNA from *Arabidopsis* Col-0 ecotype was used as a template for PCR, depending on whether introns are present in the region to be cloned (Table 3-4). Each PCR was performed with *PfuTurbo*[®] DNA polymerase (Stratagene, La Jolla, CA). PCR products were subcloned into pB42AD-L vector (pB42AD vector (Clontech, Mountain View, CA) with multicloning sites) and sequenced. Mutation-free clones were transformed into yeast strain EGY48 p8oplacz according to the manufacturer's protocol (frozen-EZ Yeast Transformation II[™] kit, Zymo Research Corporation, Orange, CA).

Yeast two-hybrid assay

Twenty µl of each yeast culture expressing HopM1₁₋₃₀₀ and the C-termini of *ARF-GEF* genes or containing an empty vector (pBD42AD-L) were grown on the solid SD+Glu-Ura-His-Trp medium (13.35g of minimal SD base, 0.35g of -Ura-His-Trp DO supplement, 10g of Agar in 500 ml water: Clontech, Mountain View, CA) at 30 °C for two days. A single colony of the each yeast was used to inoculate in 2 ml of SD+Glu-Ura-His-Trp liquid medium (6.675g of minimal SD base, 0.175g of -Ura-His-Trp DO supplement in 250 ml water: Clontech, Mountain View, CA) and cultured at 30 °C with shaking for approximately 24 hours. One milliliter of this liquid culture was used to inoculate into 6 ml of SD+Glu-Ura-His-Trp liquid medium, and re-cultured overnight (20 µl of each culture was spotted on the SD+Glu-Ura-His-Trp solid medium again, and incubated at 30 °C for two days). One ml of each culture was collected and centrifuged at the room temperature for 4 minutes at 500xg. The pellet was washed with 10 ml of Tris-EDTA buffer. The washed pellet was resuspended with 6 ml of SD+Gal-Ura-His-Trp

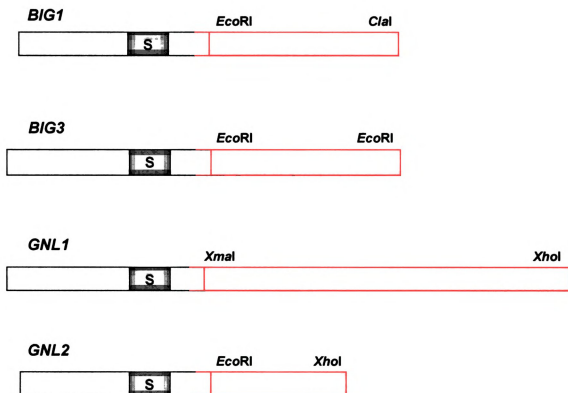


Figure 3-3. Diagrams of four *ARF-GEF* genes analyzed by yeast two-hybrid assay. Green box with S denotes the putative Sec7 domain of each gene. Yellow box indicates the C-terminus of each gene that was used for yeast two-hybrid assay. *EcoRI*, *ClaI*, *XmaI* and *XhoI* indicate the restriction enzyme sites added for subcloning.

liquid medium (9.25g of minimal SD base Gal/Raf and 0.175g of -Ura-His-Trp supplement in 250 ml water: Clontech, Mountain View, CA), and 20 μ l of each resuspended sample was spotted on the SD+Gal-Ura-His-Trp solid medium containing X-gal and BU salts (9.25g of minimal SD base Gal/Raf, 0.175g of -Ura-His-Trp DO supplement, 5g of agarose, 25 ml of 10 X BU salt solution (0.26 M of $\text{Na}_2\text{HPO}_4 \cdot 7\text{H}_2\text{O}$ and 0.25 mM of $\text{NaH}_2\text{PO}_4 \cdot \text{H}_2\text{O}$), and 1ml of 20mg/ml X-gal solution in 225 ml water: Clontech, Mountain View, CA) incubated at 30 °C for 5 days.

Total proteins extracted from yeast were separated on sodium dodecyl sulfate polyacrylamide gels (7.5%), then transferred onto Immobilon-P membrane (Millipore, Billerica, MA) using a semi-dry transfer apparatus (SEMIPHOR, Hoefer Scientific Instruments, San Francisco, CA). Immunoblot analyses were performed with a LexA-antibody for HopM1 or a HA-antibody for ARF-GEF proteins. For determining the approximate sizes of proteins, PageRuler™ Prestained Protein Ladder Plus (Fermentas International Inc, Ontario, Canada) was used.

Growth curve assay for determining multiplication of *Pst* DC3000 and its mutants in *Arabidopsis*

Arabidopsis plants for bacterial growth curve assay were grown in pots in growth chambers (a 12 h dark/12 h light cycle, 100 μ E, 20°C), until they were approximately 5 weeks old. The bacteria selected for growth curve assay were cultured in low-sodium Luria-Bertany (LB) medium (10g/l Tryptone, 5g/l Yeast Extract, 5g/l NaCl) plus appropriate antibiotics, at 30°C with shaking at 250 rpm. Bacterial liquid culture was incubated to the mid- to late-logarithmic phase. Bacteria were collected by centrifugation

(3,000xg, room temperature, 30 minutes) and resuspended in sterile, de-ionized water with 0.03% Silwet L-77 (OSI Specialties, Friendship, WV). The bacterial inoculum was 1×10^8 colony forming units (CFUs)/ml, unless otherwise indicated. Plants were inoculated by dipping, and bacteria in leaf samples were quantified according to the protocol described in Katagiri et al. (2002).

Crossing *atmin7* knockout mutant (salk_012013) and knockout mutant of *BIG2* (salk_033446)

For constructing double knockout mutant lines of *AtMIN7* and *BIG2*, homozygous T-DNA insertion mutant of *AtMIN7* (salk_012013; Nomura et al., 2006) and that of *BIG2* (salk_033446) were grown on pots until they were flowering. The pollens from the mature stamens of salk_033446 were collected and applied to the stigmas of semi-mature flowerbuds of salk_012013. The artificially pollinated stigmas of salk_012013 were sealed with plastic wrap, and the whole plants were put into the growth chamber (under a 12 h dark/12 h light cycle, 100 μ E, 20°C), until the artificially pollinated stigmas had developed into siliques. F₁ seeds were collected from mature siliques and germinated on the soil, and F₁ plants were analyzed by genomic PCR (Table 3-2). F₁ plants which had T-DNA insertion for both *AtMIN7* and *BIG2* were selected, and their F₂ seeds were collected. F₂ plants were analyzed by genomic PCR, and homozygous knockouts for *AtMIN7* and *BIG2* were selected. F₃ or F₄ plants were used for further analyses.

RESULTS

Identification of homozygous T-DNA insertion mutants for *Arabidopsis* ARF-GEF genes

To determine a possible role of *ARF-GEF* genes other than *AtMIN7* in *Arabidopsis* defense against the Δ CEL mutant, I attempted to identify T-DNA insertion mutants of seven *Arabidopsis* *ARF-GEF* genes. Based on the genomic PCR results, homozygous T-DNA insertion mutants of three genes (*BIG2*, *BIG3* and *BIG4*) were obtained (salk_033446, salk_044617, and salk_082249, respectively: Figure 3-4). These homozygous mutants did not have visible phenotypes in growth and development. Homozygous T-DNA insertion mutants of four ARF-GEF genes (*AtBIG1*, *GNOM*, *GNL1* and *GNL2*) were not isolated and only heterozygote plants were observed by genomic PCR (Wei-Ning Huang and Sheng Yang He, unpublished). Three heterozygous mutants of the four ARF-GEF genes (salk_066766 of *AtBIG1*, salk_067415 of *GNL1* and salk_103014 of *GNOM*) had shrunken seeds in their siliques and their germination rate were low (Wei-Ning Huang and Sheng Yang He, unpublished). The heterozygous T-DNA insertion mutants were not included in further analyses.

Confirmation of gene knockout in the homozygous T-DNA insertion mutants by RT-PCR

The homozygous salk lines chosen by genomic PCR were examined by RT-PCR to determine whether they were true knockouts. RT-PCR was performed with the primers which are specific for each *ARF-GEF* gene. After 25 cycles of PCR, transcript was not

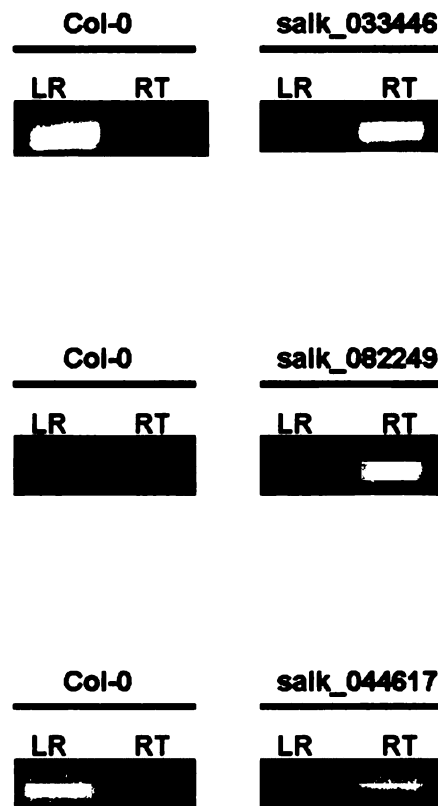


Figure 3-4. Genomic PCR results of homozygous T-DNA insertional mutants for three *ARF-GEF* genes (*BIG2*, *BIG3* and *BIG4*). LR indicates the reactions performed with gene-specific primer surrounding the T-DNA insertion site. RT indicates the reactions performed with a gene-specific primer and the T-DNA left border primer.

detected for salk_033446, indicating that it was a knockout mutant of *BIG2*. On the contrary, transcript was detected in salk_044617 plant. However, the amount of transcript was significantly less than that of Col-0. This indicates that salk_044617 is not a knockout of *BIG3*, but the transcript level was reduced (Figure 3-5A).

Neither Col-0 nor *big4* (salk_082249) samples had detectable transcript after 25 cycles (Figure 3-5A). However, after increasing the number of the PCR cycles to 30, 40, and 50 cycles, transcript was detected in Col-0 but not in salk_082249 (Figure 3-5B). This result indicates that salk_082249 is a *BIG4* knockout mutant.

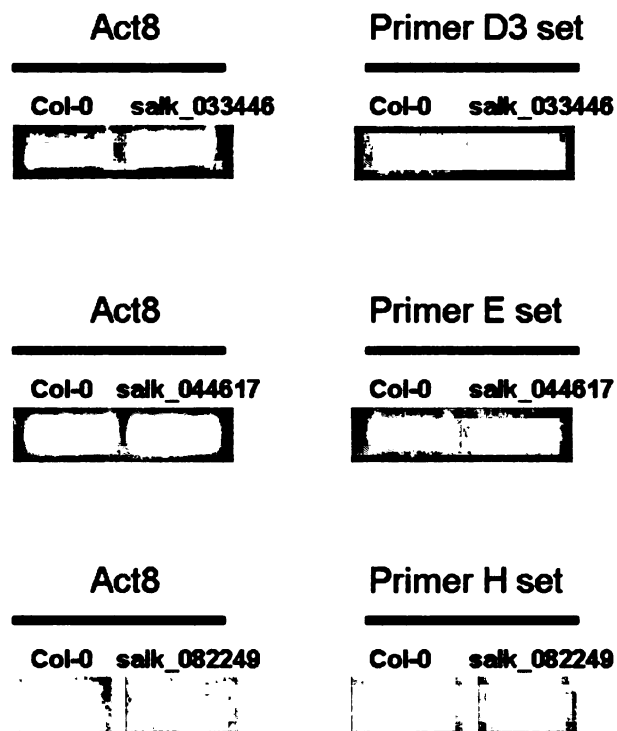
Determination of the multiplication of the Δ CEL mutant in the selected T-DNA insertion mutants

The multiplication of the Δ CEL mutant in the three homozygous T-DNA insertion mutants was examined. For comparison, the multiplication of *Pst* DC3000 (wild type; fully virulent) and the *hrcC* mutant (defective in the TTSS; nonpathogenic) were also investigated. Besides selected salk lines, Col-0 and *atmin7* plants were included as controls. Repeated assay results showed that none of the T-DNA insertion mutants showed enhanced growth of Δ CEL as seen in *atmin7* plants (Figure 3-6). This result indicates that knockout of *AtBIG2* and *AtBIG4* and knockdown of *AtBIG3* did not increase the multiplication of the Δ CEL mutant.

Determination of the multiplication of the Δ CEL mutant in the double knockout mutant of *AtMIN7* and *BIG2*

The C-terminus of *BIG2* (the product of At3g60860) had shown a weak

(A)



(B)

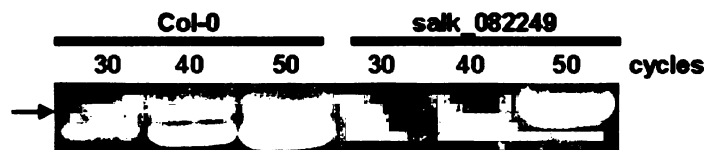


Figure 3-5. RT-PCR results of selected T-DNA insertional mutants of *AtBIG2*, *AtBIG3* and *AtBIG4*. (A) RT-PCR results of salk-033446, salk_044617, and salk_082249 after 25 cycles. (B) RT-PCR result of salk_082249 after 30, 40 and 50 cycles. PCR products from genomic DNA were detected (arrow) in addition to those from cDNA.

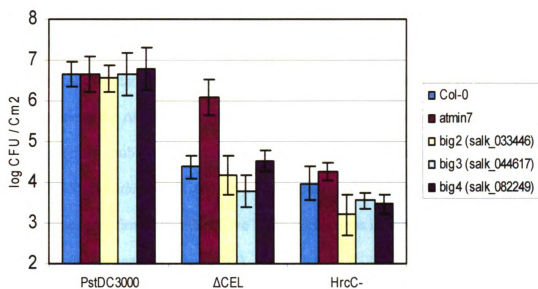


Figure 3-6. Multiplication of *Pst* DC3000, the Δ CEL mutant and the *hrcC*⁻ mutant in Col-0, *atmin7* and *ARF-GEF* T-DNA insertion lines. Results are displayed as means of 4 leaves with standard errors.

interaction with HopM1₁₋₃₀₀ in the yeast two-hybrid assay (Kinya Nomura and Sheng Yang He, unpublished). Although the T-DNA insertion mutant of *BIG2* (salk_033446) did not show an enhanced susceptibility to the Δ CEL mutant, it is still possible that the role of *BIG2* in defense may be partially redundant to and masked by *AtMIN7*. If so, a double knockout mutant of *AtMIN7* and *AtBIG2* might support a higher level of multiplication of the Δ CEL mutant than either *atmin7* or *atbig2* single mutant,. To test this hypothesis, a double knockout mutant was constructed by crossing *atmin7* (salk_012013) and *atbig2* (salk_033446). The F₃ and F₄ plants were tested by genomic PCR and it was confirmed that they have T-DNA insertions in both genes. Line #6-3 was selected for further analysis (Figure 3-7).

The multiplications of *Pst* DC3000, Δ CEL mutant, and *hrcC* mutant in the F₄ plants of line #6-3 were compared (Figure 3-8). The *atmin7/big2* plants showed higher multiplication of Δ CEL mutant than in Col-0, but it was not significantly higher than that of *atmin7* mutant. Therefore, the double knockout of *AtMIN7* and *BIG2* did not fully complement the Δ CEL mutation.

Yeast two- hybrid assay of selected Arabidopsis ARF-GEF genes with HopM1

Nomura et al. (2006) reported that the C-terminus of *AtMIN7* interacted with HopM1₁₋₃₀₀, whereas the corresponding C-termini of three other ARF-GEFs, *BIG2*, *GNOM* and *BIG4*, did not in the yeast two-hybrid assay. It is not known whether any of the four remaining ARF-GEFs, *BIG1*, *BIG3*, *GNL1* and *GNL2*, interacts with HopM1₁₋₃₀₀. In this study, the sequences of the ORFs of these four genes were aligned with other

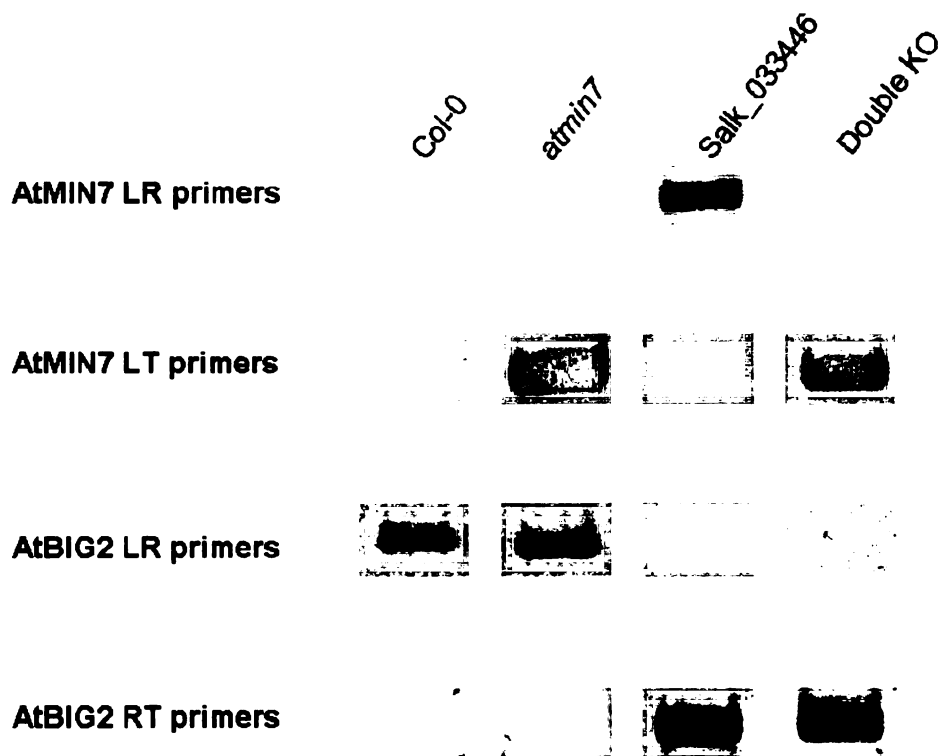


Figure 3-7. Genomic PCR results confirming the double knockout of *AtMIN7* and *BIG2*. LR primers are the forward and reverse primers for the genomic PCR products of *AtMIN7* or *BIG2*. Primer sets LT and RT denote the reactions performed with a gene-specific primer and a T-DNA-specific primer. LR indicates the reactions performed with gene-specific primers surrounding the insertion site. The double knockout plant was from the F₃ generation of line #6-3.

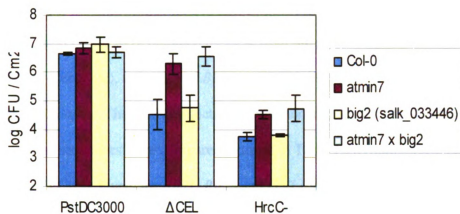
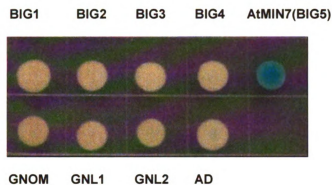


Figure 3-8. Multiplication of *Pst* DC3000, the Δ CEL mutant and the *hrcC*⁻ mutant in Col-0, *atmin7*, *big2*, and the double knockout of *AtMIN7* and *AtBIG2*. Results are displayed as means of 4 leaves with standard errors.

Arabidopsis ARF-GEF genes by CLUSTALW (<http://align.genome.jp/>), and the predicted C-terminus after the putative Sec7 domain of each gene was determined (Figure 3-2), following the previous experimental design (Nomura et al., 2006). The 3'-coding regions of *GNL1* and *GNL2* were obtained by PCR from the genomic DNA of *Arabidopsis* (Col-0 ecotype), and those of *BIG1* and *BIG3* were obtained by PCR from the cDNA of *Arabidopsis*. The PCR products were subcloned into pB42AD-L vector and sequenced, and the sequences were compared to those in TAIR (www.arabidopsis.org). The sequences of PCR products for *BIG1*, *BIG3* and *GNL1* were confirmed to be identical to those in the TAIR database, but the PCR product *GNL2* had mismatches, resulting in two amino acid changes (Appendix 3-8). However, these two changed amino acids were found in two independent sets of PCR, and were therefore not likely to be mutations introduced during PCR procedures.

The PCR products were cloned into pB42AD-L vector and the recombinant plasmids were introduced into yeasts. Previously characterized ARF-GEF clones (*BIG2*, *BIG4*, *AtMIN7* and *GNOM*; Nomura et al., 2006) were included in yeast two-hybrid assay with *HopM1*₁₋₃₀₀. Among the four newly made ARF-GEF clones, *BIG1*, *BIG3* and *GNL1* were not expressed in yeast, and only *GNL2* clone was expressed (Figure 3-9B). *GNL2* did not show interaction with *HopM1*₁₋₃₀₀ (Figure 3-9A). In these experiments, *BIG2* clone which had previously been demonstrated to have a weak interaction with *HopM1*₁₋₃₀₀ (Kinuya Nomura and Sheng Yang He, unpublished) also did not interact with *HopM1*₁₋₃₀₀ (Figure 3-9A).

(A)



(B)

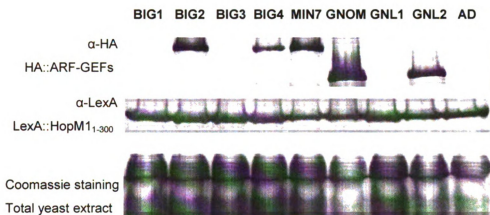


Figure 3-9. Yeast two-hybrid assay result of the C-termini of selected ARF-GEFs with HopM1₁₋₃₀₀. (A) Yeast two-hybrid assay between the C-termini of ARF-GEFs and HopM1₁₋₃₀₀. AD is the empty pB42AD-L vector. (B) Immunoblot analyses of ARF-GEF clones expressed in yeast. ARF-GEFs were detected by an HA antibody, and HopM1₁₋₃₀₀ was detected by a LexA antibody.

DISCUSSION

In this chapter *Arabidopsis ARF-GEF* genes were studied to determine whether they have roles in the defense against the Δ CEL mutant and whether their products interact with HopM1.

To determine the roles of the *ARF-GEF* genes in *Arabidopsis* defense against the Δ CEL mutant of *Pst* DC3000, homozygous T-DNA insertion mutants of seven *ARF-GEF* genes were collected. Homozygous T-DNA insertion mutants of three *ARF-GEF* genes (*BIG2*, *BIG3* and *BIG4*) were confirmed by PCR. RT-PCR results showed that the homozygous T-DNA insertion mutants of *BIG2* (salk_033446) and *BIG4* (salk_082249) were knockout mutants and that the T-DNA insertion mutant of *BIG3* (salk_044617) had a reduction in transcript level. However, salk_044617 was included in further experiments because it was the only available salk line for *BIG3* (TAIR, www.arabidopsis.org). The RT-PCR result of salk_082249 needed more PCR cycles than those of the two other salk lines (25 cycles), indicating that the transcription level of the *BIG4* is low. It is consistent with the information available from the Bio-Array Resource for *Arabidopsis* Functional Genomics. The expression of *BIG4* is very low in vegetative organs but high in anthers (the information of the expression of each *ARF-GEF* gene in different tissue is in the Appendix 3-9: Winter et al., 2007; <http://www.bar.utoronto.ca/efp/cgi-bin/efpWeb.cgi>).

The multiplication of the Δ CEL mutant was quantified in the selected T-DNA insertion mutants, and compared to those in Col-0 and in *atmin7* plants. In addition to the Δ CEL mutant (a mutant with an intact TTSS, but a partially deleted CEL), *Pst* DC3000 (a

wild type pathogen with an intact TTSS) and the *hrcC*⁻ mutant (a mutant without a functional TTSS) were also tested. The multiplication of the ΔCEL mutant in the T-DNA insertion mutants was similar to that seen in Col-0, and none of the mutants showed increased multiplication of the ΔCEL mutant equivalent to the multiplication in *atmin7* plants. These data show that the mutation of *BIG2* and *BIG4* do not result in enhanced multiplication of the ΔCEL mutant, and that these *ARF-GEF* genes do not have a role in *Arabidopsis* defense against the ΔCEL mutant.

A prior yeast two-hybrid assay showed a weak interaction between *BIG2* and HopM1₁₋₃₀₀, suggesting that *BIG2* may contribute to *Arabidopsis* defense against the ΔCEL mutant (Kinya Nomura and Sheng Yang He, unpublished). The double knockout mutant of *AtMIN7* and *BIG2* may therefore support increased multiplication level of the ΔCEL mutant above that shown in *atmin7*. However, the multiplication of the ΔCEL mutant in the double knockout mutant was not significantly different than that in *atmin7* mutant. In addition, the yeast two-hybrid interaction between *BIG2* and HopM1₁₋₃₀₀ was not reproduced. Based on these data, it can be interpreted that *BIG2* does not significantly contribute to *Arabidopsis* defense against the ΔCEL mutant and it is not a host target of HopM1.

BIG4 is not likely to contribute to *Arabidopsis* defense against the ΔCEL mutant based on the ΔCEL mutant multiplication level in the T-DNA insertion mutant (salk_082249). *BIG4* also did not interact with HopM1₁₋₃₀₀ in the yeast two-hybrid assay (Nomura et al., 2006), indicating that it is not a host target of HopM1. From its anther-specific expression (Appendix 3-9 [Winter et al., 2007]), *AtBIG4* may have roles in organ development rather than in defense.

The role of *BIG3* in *Arabidopsis* defense against the Δ CEL mutant remains unclear. The T-DNA insertion mutant of *BIG3* (salk_044617) was not a complete knockout mutant. It did not support the multiplication of the Δ CEL mutant, and this may be due to the presence of residual *BIG3* transcript. The yeast two-hybrid assay between *BIG3* and HopM1₁₋₃₀₀ could not be performed, because the C-terminus of *BIG3* was not expressed in yeast for unknown reasons.

Homozygous T-DNA insertion mutants for *BIG1*, *GNOM*, *GNL1* and *GNL2* were not isolated although heterozygous mutant plants were obtained (Wei-Ning Huang and Sheng Yang He, unpublished). These heterozygous mutants were not further analyzed. The heterozygous mutants of *BIG1*, *GNOM* and *GNL1* had abnormal seed development in the siliques (Wei-Ning Huang and Sheng Yang He, unpublished), suggesting that these *ARF-GEF* genes may function in seed or embryo development. Indeed, *GNOM* functions in embryo development, and its heterozygous mutant produces embryo-lethal seeds (Mayer et al., 1993; Vielle-Calzada et al., 2000).

The C-termini of *BIG1*, *GNOM*, *GNL1* and *GNL2* were tested by yeast two-hybrid assay to determine whether they interact with HopM1₁₋₃₀₀. *GNL2* was successfully expressed in yeast, but it did not interact with HopM1₁₋₃₀₀ suggesting that *GNL2* is not likely to be targeted by HopM1. However, the C-termini of three of the *ARF-GEFs*, *BIG1*, *GNOM*, *GNL1*, were not expressed in yeast. This could be due to the toxicity generated by those C-termini to the yeast or structural defects in the truncated *ARF-GEF* proteins. As a result, the interaction between *AtBIG1*, *GNOM* or *GNL1* with HopM1₁₋₃₀₀ could not be tested in the yeast two-hybrid assay.

In this chapter it was confirmed that *AtBIG2* and *AtBIG4* do not have a significant

influence in *Arabidopsis* defense against the Δ CEL mutant. It was also demonstrated that GNL2 does not interact with HopM1₁₋₃₀₀. The role of *GNL2* in defense against the Δ CEL mutant was not determined. However, thus far, we have been unable to demonstrate that any ARF-GEFs other than *AtMIN7* function in the defense against the Δ CEL mutant or that they are targeted by HopM1. However, it still cannot be concluded that *AtMIN7* is the only ARF GEF that is important for *Arabidopsis* defense and the only ARF-GEF target of HopM1.

REFERENCES

- Alfano, J.R., Charkowski, A.O., Deng, W.L., Badel, J.L., Petnicki-Ocwieja, T., van Dijk, K., and Collmer, A. (2000) The *Pseudomonas syringae* Hrp pathogenicity island has a tripartite mosaic structure composed of a cluster of type III secretion genes bounded by exchangeable effector and conserved effector loci that contribute to parasitic fitness and pathogenicity in plants. *Proc Natl Acad Sci U S A*. **97**: 4856-4861.
- Anders, N. and Jürgens, G. (2008) Large ARF guanine nucleotide exchange factors in membrane trafficking. *Cell Mol Life Sci* **65**: 3433-3445.
- Badel, J.L., Nomura, K., Bandyopadhyay, S., Shimizu, R., Collmer, A., and He, S.Y. (2003) *Pseudomonas syringae* pv. *tomato* DC3000 HopPtoM (CEL ORF3) is important for lesion formation but not growth in tomato and is secreted and translocated by the Hrp type III secretion system in a chaperone-dependent manner. *Mol Microbiol* **49**: 1239-1251.
- Bassham, D.C., Brandizzi, F., Otegui, M.S., and Sanderfoot, A.A. (2008) The secretory system of Arabidopsis: September 30, 2008. The *Arabidopsis* Book. Rockville, MD: American Society of Plant Biologists.
<http://www.aspb.org/publications/arabidopsis/>
- Casanova, J.E. (2007) Regulation of Arf activation: the Sec7 family of guanine nucleotide exchange factors. *Traffic* **8**: 1476-1485.
- Chardin, P., Paris, S., Antonny, B., Robineau, S., Béraud-Dufour, S., Jackson, C.L., Chabre, M. (1996) A human exchange factor for ARF contains Sec7- and pleckstrin-homology domains. *Nature* **384**: 481-484.
- Cox, R., Mason-Gamer, R.J., Jackson, C.L., and Segev, N. (2004) Phylogenetic analysis of Sec7-domain-containing Arf nucleotide exchangers. *Mol Biol Cell* **15**: 1487-1505.
- DebRoy, S., Thilmony, R., Kwack, Y.B., Nomura, K., and He, S.Y. (2004) A family of conserved bacterial effectors inhibits salicylic acid-mediated basal immunity and promotes disease necrosis in plants. *Proc Natl Acad Sci U S A* **101**: 9927-9932.
- Geldner, N., Anders, N., Wolters, H., Keicher, J., Kornberger, W., Muller, P., Delbarre, A., Ueda, T., Nakano, A., and Jürgens, G. (2003) The *Arabidopsis* GNOM ARF-GEF mediates endosomal recycling, auxin transport, and auxin-dependent plant growth. *Cell* **112**: 219-230.
- Gillingham, A.K. and Munro, S. (2007) The small G proteins of the Arf family and their

- regulators. *Annu Rev Cell Dev Biol* **23**: 579-611.
- Jackson, C.L. and Casanova, J.E. (2000) Turning on ARF: the Sec7 family of guanine-nucleotide-exchange factors. *Trends Cell Biol* **10**: 60-67.
- Mayer, U., Buttner, G., and Jürgens, G. (1993) Apical-basal pattern formation in the *Arabidopsis* embryo: studies on the role of the *Gnom* gene. *Development* **117**: 149-162.
- Memon, A.R. (2004) The role of ADP-ribosylation factor and SAR1 in vesicular trafficking in plants. *Biochim Biophys Acta* **1664**: 9-30.
- Nomura, K., Debroy, S., Lee, Y.H., Pumplin, N., Jones, J., and He, S.Y. (2006) A bacterial virulence protein suppresses host innate immunity to cause plant disease. *Science* **313**: 220-223.
- Richter, S., Geldner, N., Schrader, J., Wolters, H., Stierhof, Y.D., Rios, G., Koncz, C., Robinson, D.G., and Jürgens, G. (2007) Functional diversification of closely related ARF-GEFs in protein secretion and recycling. *Nature* 2007 **448**: 488-492.
- Steinmann, T., Geldner, N., Grebe, M., Mangold, S., Jackson, C.L., Paris, S., Gälweiler, L., Palme, K., and Jürgens, G. (1999) Coordinated polar localization of auxin efflux carrier PIN1 by GNOM ARF GEF. *Science* **286**: 316-318.
- Teh, O.K. and Moore, I. (2007) An ARF-GEF acting at the Golgi and in selective endocytosis in polarized plant cells. *Nature* **448**: 493-496.
- Vielle-Calzada, J.P., Baskar, R., and Grossniklaus, U. (2000) Delayed activation of the paternal genome during seed development. *Nature* **404**: 91-94.
- Winter, D., Vinegar, B., Nahal, H., Ammar, R., Wilson, G.V., and Provart, N.J. (2007) An "electronic fluorescent pictograph" browser for exploring and analyzing large-scale biological data sets. *PLoS One* **2**: e718.

CHAPTER 4

***In vivo* Subcellular Localization Imaging of Several *Arabidopsis* Proteins That Are Putative Cargoes of Defense-Associated Cellular Trafficking**

ABSTRACT

Confocal microscopy has been used for the visualization of plant-pathogen interactions in living plant cells and enabled the understanding of the characteristics of defense-associated proteins in the context of the cellular processes. In this chapter, three known or predicted extracellular *Arabidopsis* proteins (PR1, a putative lipid transfer protein (LTP) encoded by At2g10940 and FLA9, a putative arabinogalactan protein (AGP) encoded by At1g03870) were fused with GFP, and they were examined in *Arabidopsis* by western blot analyses and confocal microscopy. The immunoblot analysis results of PR1-GFP and At2g10940-GFP did not show any sign of degradation or modification of fusion proteins. The FLA9-GFP fusion was not expressed in *Arabidopsis*. PR1-GFP was localized in the intercellular space both in Col-0 and *atmin7* backgrounds. At2g10940-GFP was localized in the intercellular space in Col-0 background, but in *atmin7* background, unidentified round intracellular structures were observed. These results suggest that the localization of At2g10940-GFP may be dependent on AtMIN7-mediated vesicle trafficking pathway(s), whereas the localization of PR1-GFP is not.

INTRODUCTION

Microscopic visualization of the components of pathogens or plants during infection has been one of the most powerful experimental approaches in the study of plant-pathogen interactions. In recent years, confocal microscopic analyses of cellular proteins fused to fluorescence proteins (such as GFP and its derivatives) have revolutionized the field of plant cell biology, in large part because confocal microscopy enables monitoring the localization and dynamic changes of GFP fusion proteins in living cells or organisms (Brandizzi et al., 2004).

The interactions between *Arabidopsis* and its pathogens have been also studied by confocal microscopy. For instance, pathogens such as *Pst* DC3000 or cauliflower mosaic virus (CaMV) were tagged with GFP and used for the microscopic detection of their behaviors during infection (Badel et al., 2002; Love et al., 2007). Also, numerous defense-associated proteins of *Arabidopsis* have been studied by confocal microscopy for determining their localization in the cell.

Several known defense-associated proteins in *Arabidopsis* are components of the cellular trafficking system. PEN1 (SYP121), a protein having a role for the defense against fungal pathogens, is a SNARE protein which acts in vesicle targeting and fusion (Collins et al., 2003; Assaad et al., 2004; Mayer et al., 2009). SYP122, the closest homologue of PEN1, is also involved in the regulation of defense-associated signaling pathways (Assaad et al., 2004; Zhang et al., 2007). AtMIN7 plays a role in the defense against the Δ CEL mutant of *Pst* DC3000, and it is a putative ARF-GEF which activates ARF protein required for vesicle formation and budding (Nomura et al., 2006). Another

Arabidopsis protein, RabE1.d, which physically interacts with the type III secretion system (TTSS) effector AvrPto, is a small GTPase functioning in vesicle targeting. The constitutively active form of RabE1.d enhances the resistance against *Pst* DC3000 (Speth et al., 2009). All of these proteins were studied by confocal microscopy and their subcellular localizations were determined: PEN1 and SYP122 are localized in the plasma membrane (Collins et al., 2003; Assaad et al., 2004), AtMIN7 is localized in the trans-Golgi network (Tanaka et al., 2009) and RabE1.d is localized in the Golgi and plasma membrane (Speth et al., 2009). In addition to *Arabidopsis*, NbSYP132, a SNARE protein in *N.benthamiana* has role in defense (Kalde et al., 2007).

Accumulating evidence suggests that *Pst* DC3000 affects the components of defense-associated cellular trafficking pathways of *Arabidopsis* via its TTSS effectors. For instance, AtMIN7 and RabE1.d are targeted by HopM1 and AvrPto, respectively. AtMIN7 is degraded by HopM1, and the localization of RabE1.d is changed in transgenic *Arabidopsis* expressing AvrPto (Nomura et al., 2006; Speth et al., 2009; Elena Bray Speth and Sheng Yang He, unpublished). Furthermore, global gene expression analysis of *Arabidopsis* upon infection of *Pst* DC3000 showed that there was a biased suppression of genes encoding putatively secreted proteins in a TTSS-dependent manner (Hauck et al., 2003; Thilmony et al., 2006). The TTSS-dependent effect on the host vesicle traffic is also observed in other bacterial pathogens. For example, a TTSS effector of *Xanthomonas campestris*, XopJ, when expressed in tobacco, interfered with the secretion of GFP which was introduced in tobacco (Bartetzko et al., 2009).

Despite these intriguing observations, it is still poorly understood how the bacterial TTSS effector system alters the dynamic and spatial patterns of host vesicle

traffic during infection. In the case of AtMIN7, currently neither the cargoes nor the functional components of AtMIN7-dependent vesicle trafficking pathway have been elucidated. The only clue for understanding the characteristics of AtMIN7-mediated vesicle trafficking is that the *atmin7* plant has reduced and altered callose deposition in cell wall-associated PTI (Nomura et al., 2006).

In this chapter, the localization of three known or predicted extracellular *Arabidopsis* proteins were studied by confocal microscopy: PR1 encoded by At2g14610 (Laird et al., 2004), a putative protease inhibitor/seed storage/lipid transfer protein (LTP) family protein encoded by At2g10940 (Hauck et al., 2003), and a putative fasciclin-like arabinogalactan 9 protein (FLA9) encoded by At1g03870 (Hauck et al., 2003; Johnson et al., 2003). *PR1* is a representative gene which is induced in plant defense and has been extensively used as a marker for the establishment of local and systemic plant resistance. *PR1* is induced in both incompatible and compatible *Arabidopsis*-*P.syringae* interactions (Uknes et al., 1992; Laird et al., 2004) and by SA or SA analogues such as 2,6-dichloroisonicotinic acid (INA) or a benzothiadazole derivative (BTH) (Uknes et al., 1992; Lawton et al., 1996). PR1 is localized in the intercellular space of *Arabidopsis* based on the analysis of apoplastic fluid (Uknes et al., 1992), but its localization has not been studied by confocal microscopy. The functions of PR1 in plant resistance against bacterial pathogens are not known despite its known contributions to the resistance against fungi or oomycetes (Alexander et al., 1993; Niderman et al., 1995).

At2g10940 (a putative protease inhibitor/seed storage/lipid transfer protein (LTP) family protein) and At1g03870 (a putative fasciclin-like arabinogalactan 9 protein (FLA9)) were also selected in this study. The expression of both of them was suppressed

in a TTSS-dependent manner (Hauck et al., 2003; Roger Thilmony and Sheng Yang He, unpublished), in contrast to the expression of *PR1*, which was induced in a TTSS-dependent manner. The products of these genes were suggested as putative cargoes of a defense-associated secretion pathway or a defense-associated cell wall component in *Arabidopsis* (Hauck et al., 2003): it was suggested that the TTSS-dependent suppression the two genes is the reflection of the effect to the secretion of the gene products by TTSS effectors.

These proteins were fused with GFP, and the GFP fusions were introduced into *Arabidopsis*. Their expression and localization were studied by immunoblot analysis and confocal microscopy, and their localization in Col-0 and the *atmin7* plants was compared.

MATERIALS AND METHODS

Construction of GFP fusions and their subcloning into plant expression vector

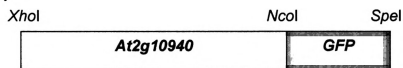
The predicted amino acid sequences of *PR1*, At2g10940 and *FLA9* were examined using the SignalP 3.0 software (<http://www.cbs.dtu.dk/services/SignalP/>) (Bendtsen et al., 2004; Nielsen et al., 1997) to identify putative signal sequences at their N-termini. Based on these analyses, fusions were designed to have GFP attached at the C-termini of the proteins (Figure 4-1, Appendix 4-1 to 4-3).

The ORF of *PR1* was amplified by PCR using a *PR1* clone in pBluescript II KS (+) (He laboratory culture collection #742) as the template. The ORFs of At2g10940 and *FLA9* were amplified by PCR using genomic DNA of Col-0 as a template. TaKaRa LA Taq (TaKaRa BioInc, Japan) was used for PCR. The primers used for PCR are in table 4-1. The PCR products were cloned into pCR[®]2.1-TOPO (Invitrogen, Carlsbad, CA), and their sequences were determined. The ORFs were transferred to pBluescript II KS (+) containing a *sGFP* ORF (Chiu et al., 1996), in which the *sGFP* ORF is followed by the NOS terminator. In all cases, the 3' end of the ORF was attached to the 5' end of the *sGFP* ORF. Mutation-free *PR1-GFP*, At2g10940-*GFP* and *FLA9-GFP* fusions (including the NOS terminator) were subcloned into the *XhoI/SpeI* sites of the pBD vector (a gift From Dr. Jeff Dangl laboratory, University of North Carolina, Chapel Hill, NC), a binary vector carrying a kanamycin resistance gene for selection in bacteria, a resistance gene for herbicide BASTA (glufosinate), and a rat glucocorticoid hormone dexamethasone (DEX [Aoyama and Chua, 1997])-inducible promoter.

(A)



(B)



(C)

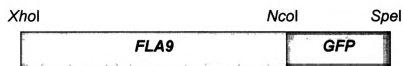


Figure 4-1. Diagrams of the PR1-GFP (A), At2g10940-GFP (B) and FLA9-GFP (C) fusions. *XhoI*, *NcoI*, *EcoRI*, *HindIII*, *Sall* and *SpeI* are the restriction enzyme sites.

Table 4-1. Primers used for PCR to construct GFP fusions of selected *Arabidopsis* genes.

Gene	Primer
<i>PR1</i>	Forward primer : <i>Xho</i> I 5'-CGG <u>CTCGAG</u> GCTCTAGAAAAAATGAATTT-3'
	Reverse primer: <i>Nco</i> I 5'-GTAT <u>CCATGG</u> CGTATGGG TTCTCGTT-3'
<i>At2g10940</i>	Forward primer: <i>Xho</i> I 5'-CGC <u>CTCGAG</u> CACTCTACTCAACATG-3'
	Reverse primer: <i>Nco</i> I 5'- TACA <u>CCATGG</u> CTATGGAACAAGTGTAGC-3'
<i>FLA9</i>	Forward primer: <i>Xho</i> I 5'-GCC <u>CTCGAG</u> ACTAAGCAAACCAATAATGG -3'
	Reverse primer: <i>Nco</i> I 5'-CGCA <u>CCATGG</u> CAAAGAGAAATTTCAAACATAAG -3'

The restriction sites which were inserted in the primers for subcloning are shown as bold and underlined.

Transformation of recombinant plasmids into *Agrobacterium*

The pBD derivatives containing fusion ORFs were transformed into *E.coli* strain DH5 α , and kanamycin-resistant colonies were obtained on solid Luria-Bertani (LB) medium supplemented with kanamycin (50 mg/ml). These recombinant plasmids were then introduced into *Agrobacterium* strain C58C1 (resistant to rifampicin and tetracycline) by tri-parental mating with the *E.coli* helper strain pRK2013.

Production of transgenic *Arabidopsis* lines expressing GFP fusions

PR1-GFP, At2g10940-*GFP* and *FLA9-GFP* gene fusions cloned in pBD vector and transformed in *Agrobacterium* were transformed into *Arabidopsis*. pBD-*PR1-GFP* and pBD-At2g10940-*GFP* were introduced into both Col-0 and the *atmin7* knockout plant, and *FLA9-GFP* gene fusion was introduced into Col-0 only. The transformation was performed following the protocol of floral dipping (Clough and Bent, 1998). Ten to fourteen-day-old T₁ plants were sprayed with 0.2 % BASTA solution (glufosinate-ammonium, trade name Finale, AgroEvo Environmental Health, Montvale, NJ) to select putative T₁ transformants. The leaf samples of BASTA-resistant T₁ plants were dipped in 30 μ M DEX solution and they were examined by confocal microscopy. T₁ plants showing GFP fluorescence, an indication of GFP fusion expression, were chosen for further analysis. Plants of T₂ or later generations in each transgenic line were used for confocal microscopy and western blot analyses.

Confocal microscopy

Leaf samples were prepared from stable transgenic *Arabidopsis* plants. Prior to

confocal microscopic observation the leaf samples were dipped into DEX solution (30 μ M, 24 hours), to induce the expression of GFP fusions. Leaf pieces were cut and mounted in water, followed by imaging with LSM510 META inverted confocal laser scanning microscope (Zeiss). A 40x oil immersion objective was used.

The GFP fusions were excited at 488 nm from an argon laser, and the emission light was filtered with a 505-530 nm band-pass filter to acquire the GFP signal. The autofluorescence from chloroplasts of mesophyll cells was filtered by a 615 nm long-pass filter. All images were examined and processed with Carl Zeiss AIM Version 3.2. Some images were adjusted using Adobe Photoshop Element version 5.5 or 7.0 in brightness and contrasts.

Plasmolysis of leaf samples

Leaf samples were dipped in 1M Tris-HCl solution (pH 7.5) for up to 30 minutes prior to confocal microscopic observation. The samples were mounted on slides in Tris-HCl solution (pH 7.5) or water.

Protein extraction and western blot analyses

Total protein samples were extracted from transgenic *Arabidopsis* plants expressing GFP fusions. A leaf from each transgenic plant was detached and dipped in the DEX solution (30 μ M). After 24 hours, 20 mg of each leaf sample (fresh weight) was ground in 200 μ L of the 2X SDS buffer [100 mM Tris-HCl pH 6.8, 200 mM DTT, 4% SDS, 20% glycerol]. Extracts were immediately heated at 90°C for 10 minutes and then frozen at -20°C.

Prior to the loading of each protein sample on protein gels, extracts were thawed at room temperature, heated at 90°C for 3 minutes, and centrifuged at $10,000\times g$ for 1 minute. Ten to 20 μL of the supernatant of each sample was used for SDS-PAGE electrophoresis (the volumes of different samples were the same in an immunoblot analysis). Total proteins were separated on precast gradient gels (4-20%, ISC BioExpress, Kaysville, UT) or hand-made SDS-PAGE gels (7.5, 10, or 12% gels), then transferred to Immobilon-P membrane (Millipore, Billerica, MA) using a semi-dry transfer apparatus (SEMIPHOR, Hoefer Scientific Instruments, San Francisco, CA). Immunoblot analyses were performed with a GFP-specific antibody (Santa Cruz Biotechnology, Inc., Santa Cruz, CA). For estimating the sizes of proteins, PageRuler™ Prestained Protein Ladder Plus (#SM1811, Fermentas International Inc, Ontario, Canada) was used.

RESULTS

Production of transgenic *Arabidopsis* expressing GFP fusion proteins

The ORF of *sGFP* (Chiu et al., 1996) was attached to the 3' ends of the selected *Arabidopsis* genes (Figure 4-1). These fusion ORFs were introduced into *Arabidopsis*, and BASTA-resistant T₁ plants were selected. More than 10 different T₁ plants transformed with pBD-*PR1-GFP* or pBD-*At2g10940-GFP*, respectively, survived after BASTA spray. T₁ plants showing the GFP-fluorescence were collected. From these plants, two independent PR1-GFP or At2g10940-GFP lines were selected for further experiments (Table 4-2, Table 4-3 and Appendix 4-4 and 4-5). On the other hand, fluorescence was not detected in any of BASTA-resistant T₁ plants transformed with pBD-*FLA9-GFP*. pBD-*PR1-GFP* and pBD-*At2g10940-GFP* were transformed into the *atmin7* mutant as well. Among the BASTA-resistant T₁ plants transformed with *PR1-GFP* or *At2g10940-GFP*, two independent PR1-GFP or At2g10940-GFP lines showing GFP fluorescence were selected for further experiments (Table 4-2, Table 4-3 and Appendix 4-4 and 4-5).

The transgenic *Arabidopsis* expressing PR1-GFP or At2g10940-GFP were analyzed by western blot analysis. The western blot analysis results showed that the protein bands of the expected sizes for both PR1-GFP (approximately 44 kDa) and At2g10940-GFP (approximately 58 kDa) fusion proteins were detected in both Col-0 and in the *atmin7* mutant backgrounds using the GFP-specific antibody (Figure 4-2). Besides the protein bands corresponding to PR1-GFP protein and At2g10940-GFP fusion proteins, there were additional bands corresponding to the size of GFP. The intensity of the GFP-

Table 4-2. Summary of transgenic *Arabidopsis* expressing PR1-GFP fusion protein.

Genetic background of <i>Arabidopsis</i>	Line number	Generations used for analyses
Col-0	#1	T ₂
	#3	T ₆
<i>atmin7</i>	#1	T ₃
	#5	T ₂

The lines described in this chapter are marked with red color.

Table 4-3. Summary of transgenic *Arabidopsis* expressing At2g10940-GFP fusion protein.

Genetic background of <i>Arabidopsis</i>	Line number	Generations used for analyses
Col-0	#9	T ₆
	#16	T ₃
<i>atmin7</i>	#41	T ₂
	#71	T ₂

The lines described in this chapter are marked with red color.

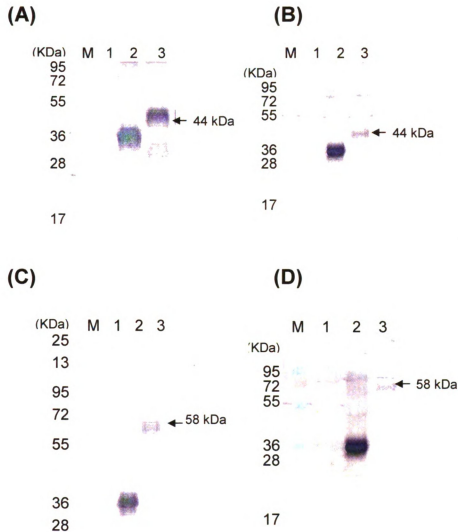


Figure 4-2. Immunoblot analysis of PR1-GFP and At2g10940-GFP in *Arabidopsis* using a GFP antibody. (A) PR1-GFP in Col-0 background (line #1). M is marker, lane 1: Col-0, lane 2: pEGAD transiently expressed in tobacco leaf, and lane 3: PR1-GFP in line #1. (B) PR1-GFP in *atmin7* background (line #1). M is marker, lane 1: the *atmin7* plant, lane 2: pEGAD transiently expressed in tobacco leaf, and lane 3: PR1-GFP in Col-0 (line #1). (C) At2g10940-GFP in Col-0 (line #9). M is marker, lane 1: Col-0 plant, lane 2: pEGAD transiently expressed in tobacco leaf, and lane 3: At2g10940-GFP in Col-0 background (line #9). (D) At2g10940-GFP in *atmin7* background (line #41). M is marker, lane 1: Col-0 plant, lane 2: pEGAD transiently expressed in tobacco leaf, and lane 3: line #41.

sized bands was variable in different leaf samples (Figure 4-2). The transgenic *Arabidopsis* plants which were transformed with the FLA9-GFP plasmid did not show any GFP-specific bands in western blot analysis.

The subcellular localization of PR1-GFP in *Arabidopsis*

Confocal microscopic examination showed that PR1-GFP was located along the cell edge in the Col-0 genetic background (Figure 4-3A and B) in independent transgenic lines. To determine whether the cell-edge fluorescence represents localization of PR1-GFP fusion at the plasma membrane or in the intercellular space between cells, I performed plasmolysis to separate the plasma membrane from the cell edge. Under this condition, PR1-GFP was clearly observed in the intercellular space (Figure 4-3C and D). This intercellular localization of PR1-GFP is consistent with its localization based on the intercellular wash fluid analysis, as previously reported (Uknes et al., 1992). Besides the intercellular space, PR1-GFP was also shown along the putative *Arabidopsis* cell wall. Almost all epidermal cells after plasmolysis showed localization of PR1-GFP in the intercellular space including the putative cell wall (Figure 4-3C). The examination of mesophyll cells showed a similar localization pattern (Figure 4-3D), but the intensity of fluorescence from the intercellular space was often lower than that along the putative cell wall.

The localization of PR1-GFP was also examined in transgenic lines with the *atmin7* background. PR1-GFP was found along the cell edge, like that in the Col-0 background (Figure 4-4A and B). After plasmolysis PR1-GFP was found in the intercellular space and the putative cell wall as shown in epidermal cells and mesophyll

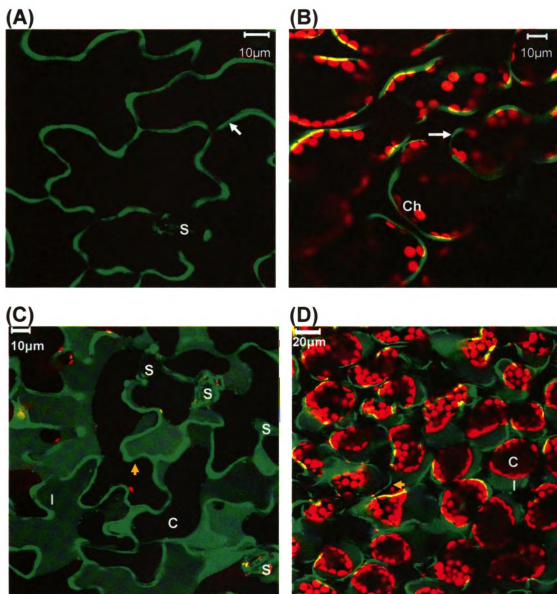


Figure 4-3. Localization and expression of PR1-GFP in *Arabidopsis*, line #1 (Col-0). (A) and (C): Localization of PR1-GFP in epidermal cell layer before and after plasmolysis, respectively. (B) and (D): Localization of PR1-GFP in mesophyll cells before and after plasmolysis, respectively. White arrows in panel A and B indicate PR1-GFP signal before plasmolysis. Yellow arrows in panel C and D indicate putative cell wall. C indicates cytoplasm which was shrunk after plasmolysis. Note that the shrunk cytoplasm of mesophyll cells in panel D contains chloroplasts. Ch indicates chloroplast with red autofluorescence. I indicates the intercellular space. S indicates stomate.

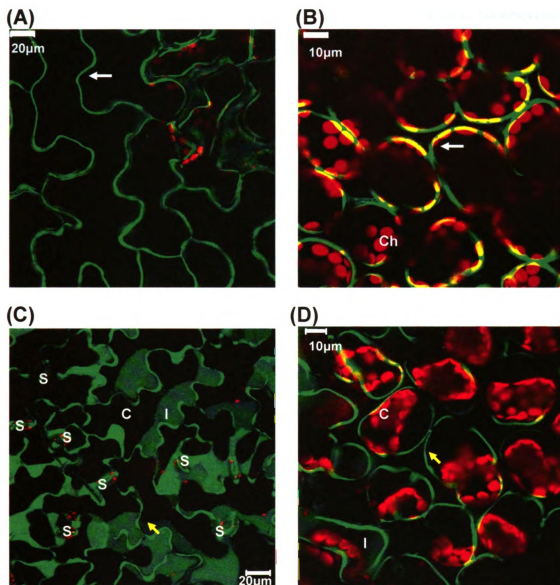


Figure 4-4. Localization of PR1-GFP in *Arabidopsis*, line#1 (in *atmin7* mutant background). (A) and (C): Localization of PR1-GFP in epidermal cell layer before and after plasmolysis, respectively. (B) and (D) are the localization of PR1-GFP in mesophyll cells before and after plasmolysis, respectively. White arrows in panel A and B indicate PR1-GFP before plasmolysis. Yellow arrows in panel C and D indicate putative cell wall. C indicates cytoplasm which was shrunken after plasmolysis. Note that the shrunken cytoplasm of mesophyll cells in panel D contains chloroplasts. Ch indicates chloroplast with red autofluorescence. I indicates the intercellular space. S indicates stomate.

cells of the Col-0 background (Figure 4-4C and D). Again, the intensity of fluorescence from the intercellular space was often lower than that along the putative cell wall. Thus, the localization of PR1-GFP in Col-0 and *atmin7* knockout background did not appear to be different.

The subcellular localization of At2g10940-GFP in *Arabidopsis*

The localization of At2g10940-GFP fusion protein in independent transgenic *Arabidopsis* lines was examined by confocal microscopy. At2g10940-GFP was found along the cell edge (Figure 4-5A and B), which was similar to the localization of PR1-GFP. After plasmolysis At2g10940-GFP was detected in the intercellular space and along the putative cell wall (Figure 4-5C and D). In mesophyll cells, the intensity of fluorescence of At2g10940 from the intercellular space was often lower than that along the putative cell wall.

Next, the localization of At2g10940-GFP in the *atmin7* background was examined in independent lines. Compared to that in Col-0 background, the At2g10940-GFP was found in not only along the cell edge, but also in the unidentified, round structures (Figure 4-6). This localization pattern was shown in two independent lines (Appendix 4-4 and 4-5).

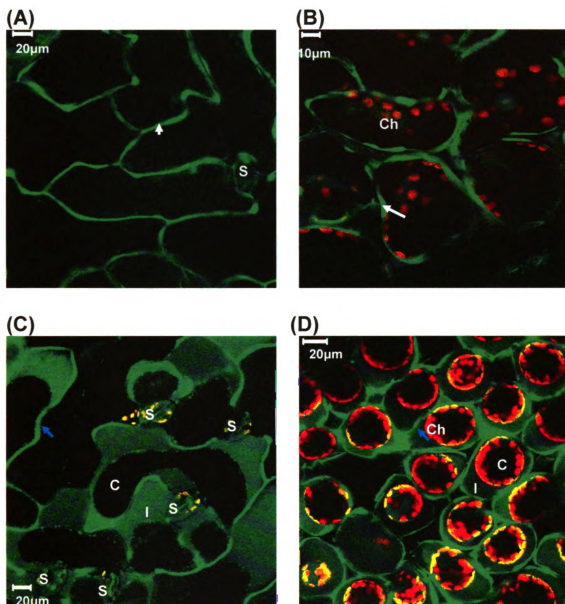


Figure 4-5. Localization of At2g10940-GFP in *Arabidopsis*, line #9 (in Col-0 background). (A) and (C): Localization of At2g10940-GFP in epidermal cell layer before and after plasmolysis, respectively. (B) and (D): Localization of PR1-GFP in mesophyll cells before and after plasmolysis, respectively. White arrows in panel A and B indicate At2g10940-GFP before plasmolysis. Blue arrows in panel C and D indicate putative cell wall. C indicates cytoplasm which was shrunken after plasmolysis. Note that the shrunken cytoplasm of mesophyll cells in panel D contains chloroplasts. Ch indicates chloroplast with red autofluorescence. I indicates the intercellular space. S indicates stomate.

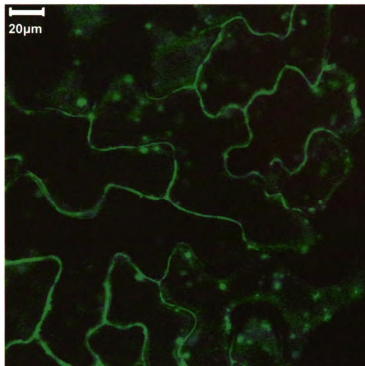


Figure 4-6. The localization of At2g10940-GFP in the *atmin7* background (line#41). The image was from the epidermal cell layer.

DISCUSSION

In this chapter, as part of an effort to establish a GFP fusion-based, *in planta* imaging system for long-term study of the dynamic effects of pathogen infection on vesicle trafficking and/or protein secretion in *Arabidopsis*, the subcellular locations of GFP fusions of two *Arabidopsis* extracellular proteins were examined by confocal microscopy and stable transgenic plants expressing these proteins were produced. These proteins were selected based primarily on the hypothesis that they might be related to extracellular defense or putative cargoes of defense-associated secretion pathways.

Numerous studies have shown that PR1 is an extracellular protein associated with various forms of plant disease resistance, although transgenic *Arabidopsis* plants stabling expressing a PR1-GFP fusion has not yet been reported. Although direct evidence for an association of At2g10940 and At1g03870 to plant defense is lacking, the products of these genes, a putative protease inhibitor/seed storage/lipid transfer protein (LTP) family protein and a putative fasciclin-like arabinogalactan 9 protein (FLA9), respectively, were suggested as putative cargoes of a defense-associated secretion pathway or a defense-associated cell wall component in *Arabidopsis*.

Both PR1-GFP and At2g10940-GFP were detected by western blot analysis in transgenic plants. The detected bands were of expected sizes, without significant degradation. This result indicates that both GFP fusion proteins were successfully expressed in the transgenic *Arabidopsis*, and the GFP fluorescence detected by the confocal microscopy reflected fusion proteins. There were additional bands corresponding to the approximate size of GFP in several protein samples, but the

intensity of the GFP-sized bands was variable in different leaf samples. There was no correlation between a specific transgenic line and the presence or intensity of the GFP-sized band, suggesting that appearance of such bands is likely caused by sample preparation. Consistent with this possibility, these bands were not detected in every examined sample. I examined the images acquired by confocal microscopy to see whether there is fluorescence in the cytoplasm, in which GFP alone is known to reside (Appendix 2-2), but there was no significant fluorescence detected in the cytoplasm.

The results from confocal microscopic analyses coupled with plasmolysis showed that both PR1-GFP and the At2g10940-GFP were localized in the intercellular space of *Arabidopsis* (Col-0). Such localization is consistent with their predicted localization based on the presence of a putative N-terminal signal sequence, and, in the case of PR1-GFP, to that based on the apoplastic fluid analysis (Uknes et al., 1992). The plasmolysis condition which was applied to the leaves expressing PR1-GFP and At2g10940-GFP was the same as that applied to the leaves expressing the PIPA2-GFP fusion, which is known to be localized in the *Arabidopsis* plasma membrane (EGAD line Q8: Cutler et al, 2000). It was previously shown that after plasmolysis PIP2A-GFP remains in the plasma membrane (Speth et al., 2009), which looked clearly different from PR1-GFP or At2g10940-GFP fusions found primarily in the intercellular space after plasmolysis.

I noticed that after plasmolysis, both PR1-GFP and At2g10940-GFP were found not only in intercellular space but also in the putative cell wall. This result suggests that PR1 and the LTP encoded by At2g1940 may have interaction with the cell wall. Further experiments may be performed with plasmolysis plus cell wall-specific marker or detector, such as propidium iodide, which stains the plant cell wall (Chen et al., 2009). It

is possible that the putative cell wall localization is caused by transgenic overexpression of GFP fusions. If so, future experiments should be performed to reduce the expression of fusion proteins by reducing DEX concentration or induction time.

The localization of PR1-GFP and At2g10940-GFP was also determined in the *atmin7* knockout mutant. PR1-GFP was shown in the intercellular space and along the putative cell wall, similar to its localization in Col-0. This result is supported by the observation that PR1 in the *atmin7* plants was detected in the intercellular wash fluid sample of those transgenic plants by the immunoblot analysis (Kinya Nomura and Sheng Yang He, unpublished). Together these results indicate that either PR1 is not delivered to the intercellular space and/or the cell wall via the AtMIN7-mediated vesicle trafficking pathway, or PR1 could be transported by multiple vesicle trafficking pathways including that mediated by AtMIN7.

In contrast, the At2g10940-GFP fusion protein expressed in the *atmin7* mutant showed interesting dual localization: multiple, round structures were found inside the cells, besides the localization along the cell edge. It is unlikely that those round structures were from the nonspecific aggregation or degradation of At2g10940-GFP, considering that the western blot analysis result revealed a protein with the expected size. It is also not likely that those round structures were from an aggregation of the putative GFP, which was detected in western blot analysis, because the fluorescence from the GFP alone does not show such distinct localization pattern (Appendix 2-2). Also, there was no significant fluorescence in the cytoplasm, in which GFP is known to reside (Appendix 2-2). The possibility that the overexpression of At2g10940-GFP caused the appearance of nonspecific structures can also be excluded, considering that the *Arabidopsis* plants

expressing PR1-GFP and At2g10940-GFP expressed in the Col-0 genetic background and the plants expressing PR1-GFP in the *atmin7* background did not show these intracellular structures. In addition, the round intracellular structures were shown in two independent transgenic lines in the *atmin7* mutant background (Appendix 4-5). Altogether, these results raise the possibility that the *atmin7* mutation affected secretion of the At2g10940-GFP, and, as a result, at least some At2g10940-GFP was retained in the cytoplasm.

Several further experiments need to be performed to confirm my localization study of At2g10940-GFP. Specifically, plasmolysis of the transgenic *atmin7* plant expressing At2g10940-GFP is needed. Some At2g10940-GFP was detected along the cell edge, but its exact localization was not determined. Without plasmolysis, it is difficult to distinguish the intercellular space from the plasma membrane or even the cytoplasm. If the cell-edge localization of At2g10940-GFP in *atmin7* plants represents the intercellular space, the result can be interpreted that the secretion of the At2g10940-GFP fusion protein was blocked only partially in the *atmin7* mutant and suggests existence of multiple pathways for the secretion of At2g10940-GFP. On the other hand, if the cell-edge localization of At2g10940-GFP represents the plasma membrane or the cytoplasm, the result would suggest a more significant block of At2g10940-GFP secretion in the *atmin7* background. The identity of the At2g10940-GFP-associated round structures is unknown and remains to be elucidated. They could represent nonspecific aggregations of At2g10940-GFP or can be some type of subcellular structures.

The fusion protein FLA9-GFP was not observed by confocal microscopy in any of the BASTA-resistant plants. Western blot analysis also did not show any specific band

detectable by GFP antibody. These results suggest that the expression of FLA9-GFP in T₁ plants was not successful. FLA9 is a member of fasciclin-like arabinogalactan protein (FLA) family of *Arabidopsis* (Johnson et al., 2003). FLA proteins possess a C-terminal hydrophobic domain, which is cleaved and replaced by a glycosylphosphatidyl inositol (GPI) anchor (Gaspar et al., 2001). Therefore, it is possible that the C-terminal GFP in FLA9-GFP was cleaved off, and as a result, FLA9-GFP fusion protein was not correctly expressed.

REFERENCES

- Alexander, D., Goodman, R.M., Gut-Rella, M., Glascock, C., Weymann, K., Friedrich, L., Maddox, D., Ahl-Goy, P., Luntz, T., Ward, E., and Ryal, J. (1993) Increased tolerance to two oomycete pathogens in transgenic tobacco expressing pathogenesis-related protein 1a. *Proc Natl Acad Sci U S A*. **90**: 7327-7331.
- Aoyama, T. and Chua, N.H. (1997) A glucocorticoid-mediated transcriptional induction system in transgenic plants. *Plant J* **11**: 605-612.
- Assaad, F.F., Qiu, J.L., Youngs, H., Ehrhardt, D., Zimmerli, L., Kalde, M., Wanner, G., Peck, S.C., Edwards, H., Ramonell, K., Somerville, C.R., and Thordal-Christensen, H. (2004) The PEN1 syntaxin defines a novel cellular compartment upon fungal attack and is required for the timely assembly of papillae. *Mol Biol Cell* **15**: 5118-5129.
- Badel, J.L., Charkowski, A.O., Deng, W.L., and Collmer, A. (2002) A gene in the *Pseudomonas syringae* pv. *tomato* Hrp pathogenicity island conserved effector locus, *hopPtoA1*, contributes to efficient formation of bacterial colonies *in planta* and is duplicated elsewhere in the genome. *Mol Plant-Microbe Interact* **15**: 1014-1024.
- Bartetzko, V., Sonnewald, S., Vogel, F., Hartner, K., Stadler, R., Hammes, U.Z., and Börnke, F. (2009) The *Xanthomonas campestris* pv. *vesicatoria* type III effector protein XopJ inhibits protein secretion: evidence for interference with cell wall-associated defense responses. *Mol Plant-Microbe Interact* **22**: 655-664.
- Bendtsen, J.D., Nielsen, H., von Heijne, G., and Brunak, S. (2004) Improved prediction of signal peptides: SignalP 3.0.J. *Molecular Biology* **340**: 783-795.
- Brandizzi, F., Irons, S.L., Johansen, J., Kotzer, A., and Neumann, U. (2004) GFP is the way to glow: bioimaging of the plant endomembrane system. *J Microsc* **214**: 138-158.
- Chen, X.Y., Liu, L., Lee, E., Han, X., Rim, Y., Chu, H., Kim, S.W., Sack, F., and Kim, J.Y. (2009) The *Arabidopsis* callose synthase gene *GSL8* is required for cytokinesis and cell patterning. *Plant Physiol* **150**: 105-113.
- Chiu, W., Niwa, Y., Zeng, W., Hirano, T., Kobayashi, H., and Sheen, J. (1996) Engineered GFP as a vital reporter in plants. *Current Biology* **6**: 325-330.
- Clough, S.J. and Bent, A.F. (1998) Floral dip: a simplified method for *Agrobacterium*-mediated transformation of *Arabidopsis thaliana*. *Plant J* **16**: 735-743.

- Collins, N.C., Thordal-Christensen, H., Lipka, V., Bau, S., Kombrink, E., Qiu, J.L., Huckelhoven, R., Stein, M., Freialdenhoven, A., Somerville, S.C., and Schulze-Lefert, P. (2003) SNARE-protein-mediated disease resistance at the plant cell wall. *Nature* **425**: 973-977.
- Cutler, S.R., Ehrhardt, D.W., Griffiths, J.S., and Somerville, C.R. (2000) Random GFP-cDNA fusions enable visualization of subcellular structures in cells of *Arabidopsis* at a high frequency. *Proc Natl Acad Sci U S A* **97**: 3718-3723.
- Gaspar, Y., Johnson, K.L., McKenna, J.A., Bacic, A., and Schultz, C.J. (2001) The complex structures of arabinogalactan-proteins and the journey toward understanding function. *Plant Mol Biol* **47**: 161-176.
- Hauck, P., Thilmony, R., and He, S.Y. (2003) A *Pseudomonas syringae* type III effector suppresses cell wall-based extracellular defense in susceptible *Arabidopsis* plants. *Proc Natl Acad Sci U S A* **100**: 8577-8582.
- Johnson, K.L., Jones, B.J., Bacic, A., and Schultz, C.J. (2003) The fasciclin-like arabinogalactan proteins of *Arabidopsis*. A multigene family of putative cell adhesion molecules. *Plant Physiol* **133**: 1911-1925.
- Kalde, M., Nühse, T.S., Findlay, K., and Peck, S.C. (2007) The syntaxin SYP132 contributes to plant resistance against bacteria and secretion of pathogenesis-related protein 1. *Proc Natl Acad Sci U S A* **104**: 11850-11855.
- Laird, J., Armengaud, P., Giuntini, P., Laval, V., and Milner, J.J. (2004) Inappropriate annotation of a key defence marker in *Arabidopsis*: will the real *PR-1* please stand up? *Planta* **219**: 1089-92.
- Lawton, K.A., Friedrich, L., Hunt, M., Weymann, K., Delaney, T., Kessmann, H., Staub, T., and Ryals, J. (1996) Benzothiadiazole induces disease resistance in *Arabidopsis* by activation of the systemic acquired resistance signal transduction pathway. *Plant J* **10**: 71-82.
- Love, A.J., Laval, V., Geri, C., Laird, J., Tomos, A.D., Hooks, M.A., and Milner, J.J. (2007) Components of *Arabidopsis* defense- and ethylene-signaling pathways regulate susceptibility to Cauliflower mosaic virus by restricting long-distance movement. *Mol Plant-Microbe Interact* **20**: 659-670.
- Meyer, D., Pajonk, S., Micali, C., O'Connell, R., and Schulze-Lefert, P. (2009) Extracellular transport and integration of plant secretory proteins into pathogen-induced cell wall compartments. *Plant J* **57**: 986-999.
- Niderman, T., Genet, I., Bruyère, T., Gees, R., Stintzi, A., Legrand, M., Fritig, B., and Mössinger, E. (1995) Pathogenesis-related PR-1 proteins are antifungal. Isolation and characterization of three 14-kilodalton proteins of tomato and of a basic PR-1

of tobacco with inhibitory activity against *Phytophthora infestans*. *Plant Physiol* **108**: 17-27.

- Nielsen, H., Engelbrecht, J., Brunak, S., and von Heijne, G. (1997) Identification of prokaryotic and eukaryotic signal peptides and prediction of their cleavage sites. *Protein Engineering* **10**: 1-6
- Nomura, K., DebRoy, S., Lee, Y.H., Pumplin, N., Jones, J., and He, S.Y. (2006) A bacterial virulence protein suppresses host innate immunity to cause plant disease. *Science* **313**: 220-223.
- Speth, E.B., Imboden, L., Hauck, P., and He, S.Y. (2009) Subcellular localization and functional analysis of the *Arabidopsis* GTPase RabE. *Plant Physiol* **149**: 1824-1837.
- Tanaka, H., Kitakura, S., De Rycke, R., De Groodt, R., and Friml, J. (2009) Fluorescence imaging-based screen identifies ARF-GEF component of early endosomal trafficking. *Curr Biol* **19**: 391-397.
- Thilmony, R., Underwood, W., and He, S.Y. (2006) Genome-wide transcriptional analysis of the *Arabidopsis thaliana* interaction with the plant pathogen *Pseudomonas syringae* pv. *tomato* DC3000 and the human pathogen *Escherichia coli* O157:H7. *Plant J* **46**: 34-53.
- Uknes, S., Mauch-Mani, B., Moyer, M., Potter, S., Williams, S., Dincher, S., Chandler, D., Slusarenko, A., Ward, E., and Ryals, J. (1992) Acquired resistance in *Arabidopsis*. *Plant Cell* **4**: 645-656.
- Zhang, Z., Feechan, A., Pedersen, C., Newman, M.A., Qiu, J.L., Olesen, K.L., and Thordal-Christensen, H. (2007) A SNARE-protein has opposing functions in penetration resistance and defence signalling pathways. *Plant J* **49**: 302-312.

CHAPTER 5

Conclusions and Future Perspectives

In the pathogenic interactions between *Arabidopsis* and *Pst* DC3000, one important question related to TTSS effector-associated virulence is how *Pst* DC3000 TTSS effector proteins affect cellular processes in the host plant. The recent study of HopM1, a TTSS effector of *Pst* DC3000, and AtMIN7, its host target and a putative ARF-GEF protein in *Arabidopsis*, supported the idea that one of the functions of TTSS effectors is to contribute to the virulence of *Pst* DC3000 by suppressing the vesicle trafficking in plant cells. This led to the research direction that combined the study of plant-pathogen interactions with a cell biological approach. In my dissertation the localization of HopM1 in plant cells was studied by confocal microscopy in order to understand how its action in host cells contributes to the virulence of *Pst* DC3000. I also attempted to determine the specificity of the defense-associated role of *AtMIN7* compared with that of other *ARF-GEF* gene family members. Finally, the localization of several putative cargo proteins of defense-associated protein secretion pathways were compared in Col-0 and the *atmin7* backgrounds.

The results in the localization study of HopM1 show that hopM1 is localized in TGN and early endosome. The N-terminus of HopM1 (HopM1₁₋₃₀₀) is also localized in the TGN and early endosome like the full-length HopM1, although it seems more transient compared to that of full-length HopM1. With the previous study showing that HopM1 interacts and destabilizes AtMIN7 (Nomura et al., 2006), this is another important clue for understanding the virulence-associated function of HopM1. A possible further research direction could be the study of HopM1 fusion proteins in *Arabidopsis*. After collecting transgenic *Arabidopsis* lines expressing all needed HopM1 fusion proteins and confirming the correct expression of the fusion proteins, I suggest the

following experiments. First of all, confocal microscopic examination of expression of HopM1 fusions over time is essential. Microscopic observation at early and later time points (within or after 5 hours post-DEX treatment) could be performed. It is also necessary to determine whether tissue death of transgenic *Arabidopsis* plants is induced by full-length HopM1 fusion proteins in a similar way as described for the full-length HopM1 without fluorescence protein tag (Debroy et al., 2004; Nomura et al., 2006).

Nomura et al (2006) showed that the multiplication of the Δ CEL mutant is enhanced in transgenic *Arabidopsis* expressing HopM1. They also showed that the first 300 amino acids of HopM1 expressed in *Arabidopsis* suppressed the multiplication of the Δ CEL mutant complemented with *hopM1* and *shcM* ORFs. These results could be reconfirmed in the transgenic *Arabidopsis* expressing full-length or truncated HopM1 fusion proteins. Compared to previous research results with HopM1 without fluorescence tag, it is possible to detect the localization change of HopM1 fusion proteins by confocal microscopy with time courses. Related to this, it would be interesting to determine the localization of HopM1 fusion proteins after the infiltration of the Δ CEL mutant complemented with *avrE* and its chaperone ORFs, considering that AvrE and HopM1 are both from the CEL of *Pst* DC3000 and are functionally redundant (Alfano et al., 2000; DebRoy et al., 2004).

HopM1 suppresses the SA-dependent callose deposition in the *Arabidopsis* cell wall (DebRoy et al., 2004), but the mechanism of this suppression was not determined in previous studies. With fluorescence protein-tagged HopM1, it is possible to detect the localization change of HopM1 (full-length or truncated) associated with this suppression: the GFP/YFP fusions of HopM1 can be compared before and after the application of SA

or its analogue, BTH. Also, considering that flg22 induces callose deposition in *Arabidopsis* (Gomez-Gomez et al., 1999; Underwood et al., 2007) and that PAMP/MAMP-triggered signaling pathway in *Arabidopsis* has positive interplay with SA-mediated signaling (Tsuda et al., 2008), it would be interesting to detect the localization of HopM1 fusion proteins upon the treatment of flg22. In addition, it would be also interesting to detect the potential change of specific marker proteins of endosomal compartments, including AtMIN7, after the infiltration of bacterial pathogens or in transgenic *Arabidopsis* expressing HopM1 or its fusion proteins.

The experimental design for determining the localization of HopM1 in plant cells is not a natural situation. It depends on the *in planta* overexpression of a specific TTSS effector (or its fusions) and the amount of the effector protein is unnaturally high compared to that translocated by the TTSS. The ideal approach is to introduce HopM1 fusions in *Pst* DC3000 and let it be delivered through the TTSS, but this approach was not successful in previous studies. In this study, instead, the timing of microscopic observation was limited, to avoid the overexpression of HopM1 fusion proteins as much as possible.

The results of the study of *Arabidopsis ARF-GEF* genes in this dissertation are not sufficient to obtain a clear determination of the role and importance of each *ARF-GEF* gene in defense. None of the studied *ARF-GEF* genes, however, showed the characteristics indicating that they are involved in *Arabidopsis* defense against the Δ CEL mutant. The possibility that *AtBIG2* has additive role in the defense against the Δ CEL mutant was not supported, based on the results from the multiplication of the Δ CEL mutant in the T-DNA insertional mutant and the yeast two-hybrid assay with HopM1.

From the multiplication result in the knockout mutant and from the yeast two-hybrid assay data, respectively, we can conclude that *AtBIG4* and *GNL2* are not important for defense against the Δ CEL mutant. The studies of T-DNA insertional mutants of several ARF-GEF genes suggest their possible roles in development and growth of *Arabidopsis* (Steinmann et al., 1999; Geldner et al., 2003; Teh and Moore, 2008; Richter et al., 2008; Tanaka et al., 2009), but this was not studied in this dissertation. Although the defense-associated functions of *Arabidopsis* ARF-GEF genes and their physical interactions with HopM1₁₋₃₀₀ were not completely determined in this chapter, it is still possible that these *ARF-GEF* genes are involved in the defense against other pathogens for *Arabidopsis* which are not *Pst* DC3000, such as fungal pathogens. It would be interesting to study the roles of these genes in defense against the non-bacterial pathogens.

The location of several *Arabidopsis* proteins which are putative cargoes of defense-associated protein secretion was studied by confocal microscopy. In this study the localization was determined in Col-0 and the *atmin7* backgrounds. PR1-GFP was localized in the intercellular space, and this localization was not changed in the *atmin7* background. On the other hand, At2g10940-GFP showed an interesting intracellular localization in the *atmin7* background, suggesting that its location is affected by the AtMIN7-mediated trafficking. It would be interesting to study the role of At2g10940 in *Arabidopsis* defense. Unfortunately, we do not have sufficient information for understanding the function of At2g10940 besides its expression pattern (induced by the *hrpS* mutant and suppressed by *Pst* DC3000 [Hauck et al., 2003; Roger Thilmony and Sheng Yang He, unpublished]). At2g10940 is annotated as a lipid transfer protein (LTP), but the nucleotide sequence of At2g10940 does not share high similarity with other LTP

genes (The Arabidopsis Information Resource, <http://www.arabidopsis.org>). Considering the altered papilla formation in *atmin7* mutant after the infiltration of the Δ CEL mutant (Nomura et al., 2006) and the old annotation of At2g10940 as a putative cell wall component (Hauck et al., 2003), At2g10940 might encode a putative component of papillae. This idea can be tested by the infiltration of mutant bacteria which induce cell wall-associated PTI into transgenic plants expressing Atg210940-GFP (the promoter can be substituted by its native promoter). The study of T-DNA insertional mutant of At2g10940 is challenging, because mutants containing T-DNA insertion in the ORF of At2g10940 are not available (The *Arabidopsis* Information Resource, <http://www.arabidopsis.org>). In the case of *FLA9*, this study does not provide data for its localization in *Arabidopsis* cells, possibly due to its structural characteristics. There is an example of GFP fusion design for an arabinogalactan protein (AGP), in which the GFP was inserted after the putative N-terminal signal sequence (Sun et al., 2004), but this approach requires an exact prediction of N-terminal signal sequence. Like At2g10940, *FLA9* is induced by *hrpS* mutant and suppressed by *Pst* DC3000 (Hauck et al., 2003), but other characteristics of *FLA9* are unknown, and there is no available mutant containing T-DNA in its ORF (The *Arabidopsis* Information Resource, <http://www.arabidopsis.org>).

The experimental system used in this study, (i.e., DEX-induced production of GFP fusions and confocal microscopy) has advantages in that GFP fusion construction enables the visualization of the localization of selected *Arabidopsis* proteins in living cells under different conditions. For instance, the factors affecting *Arabidopsis* defense such as the infiltration of different bacteria or application of chemical agents such as BTH or flg22 can be used for the localization study of GFP/YFP fusion proteins: some of

these suggested conditions were preliminarily applied to the transgenic *Arabidopsis* expressing PR1-GFP (Appendix 4-6 to 4-8). On the other hand, using a DEX-inducible promoter had advantages and limitations. It was useful to control the expression and timing of transgenes, which is advantageous compared to using a constitutive promoter. At the same time, the DEX-inducible promoter drives high expression of transgenes resulting in excessive amount of fusion proteins. This situation can make the localizations of fusion proteins incorrect by the “over-spill” of the overexpressed fusions into unrelated subcellular compartments (Crofts et al., 1999; Brandizzi et al., 2004). Also, compared to constitutive expression or native promoter-dependent expression, DEX-induction of transgenes depends on the uptake of the DEX into the plant tissue through stomata. The uptake of DEX in each experiment was not the same, so the expression level of GFP or YFP fusion proteins was not completely predictable.

REFERENCES

- Alfano, J.R., Charkowski, A.O., Deng, W.L., Badel, J.L., Petnicki-Ocwieja, T., van Dijk, K., and Collmer, A. (2000) The *Pseudomonas syringae* Hrp pathogenicity island has a tripartite mosaic structure composed of a cluster of type III secretion genes bounded by exchangeable effector and conserved effector loci that contribute to parasitic fitness and pathogenicity in plants. *Proc Natl Acad Sci U S A* **97**: 4856-4861.
- Brandizzi, F., Irons, S.L., Johansen, J., Kotzer, A., and Neumann, U. (2004) GFP is the way to glow: bioimaging of the plant endomembrane system. *J Microsc* **214**: 138-158.
- Crofts, A.J., Leborgne-Castel, N., Hillmer, S., Robinson, D., Phillipson, B., Carlsson, L.E., Ashford, D.A. and Denecke, J. (1999) Saturation of the endoplasmic reticulum retention machinery reveals anterograde bulk flow. *Plant Cell* **11**: 2233–2247.
- DebRoy, S., Thilmony, R., Kwack, Y.B., Nomura, K., and He, S.Y. (2004) A family of conserved bacterial effectors inhibits salicylic acid-mediated basal immunity and promotes disease necrosis in plants. *Proc Natl Acad Sci U S A* **101**: 9927-9932.
- Geldner, N., Anders, N., Wolters, H., Keicher, J., Kornberger, W., Muller, P., Delbarre, A., Ueda, T., Nakano, A., and Jürgens, G. (2003) The *Arabidopsis* GNOM ARF-GEF mediates endosomal recycling, auxin transport, and auxin-dependent plant growth. *Cell* **112**: 219-230.
- Gomez-Gomez, L., Felix, G., and Boller, T. (1999) A single locus determines sensitivity to bacterial flagellin in *Arabidopsis thaliana*. *Plant J* **18**: 277-284.
- Hauck, P., Thilmony, R., and He, S.Y. (2003) A *Pseudomonas syringae* type III effector suppresses cell wall-based extracellular defense in susceptible *Arabidopsis* plants. *Proc Natl Acad Sci U S A* **100**: 8577-8582.
- Nomura, K., DebRoy, S., Lee, Y.H., Pumplin, N., Jones, J., and He, S.Y. (2006) A bacterial virulence protein suppresses host innate immunity to cause plant disease. *Science* **313**: 220-223.
- Richter, S., Geldner, N., Schrader, J., Wolters, H., Stierhof, Y.D., Rios, G., Koncz, C., Robinson, D.G., and Jürgens, G. (2007) Functional diversification of closely related ARF-GEFs in protein secretion and recycling. *Nature* **2007** **448**: 488-492.
- Sun, W., Kieliszewski, M.J., and Showalter, A.M. (2004) Overexpression of tomato LeAGP-1 arabinogalactan-protein promotes lateral branching and hampers

reproductive development. *Plant J* **40**: 870-881.

Steinmann, T., Geldner, N., Grebe, M., Mangold, S., Jackson, C.L., Paris, S., Gälweiler, L., Palme, K., and Jürgens, G. (1999) Coordinated polar localization of auxin efflux carrier PIN1 by GNOM ARF GEF. *Science* **286**: 316-318.

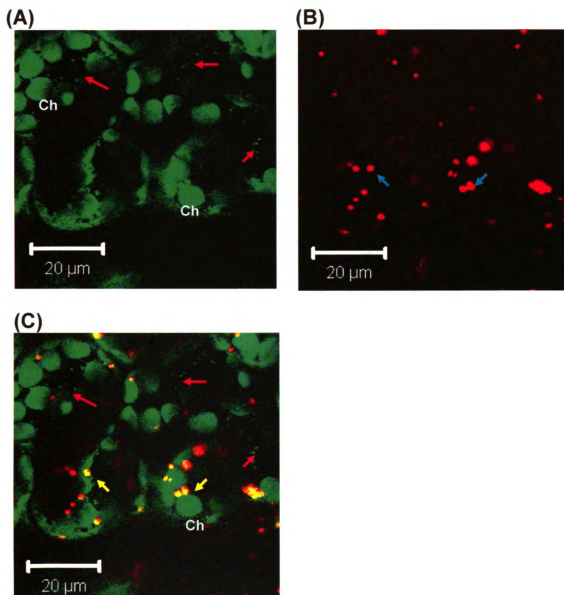
Tanaka, H., Kitakura, S., De Rycke, R., De Groodt, R., and Friml, J. (2009) Fluorescence imaging-based screen identifies ARF-GEF component of early endosomal trafficking. *Curr Biol* **19**: 391-397.

Teh, O.K. and Moore, I. (2007) An ARF-GEF acting at the Golgi and in selective endocytosis in polarized plant cells. *Nature* **448**: 493-496.

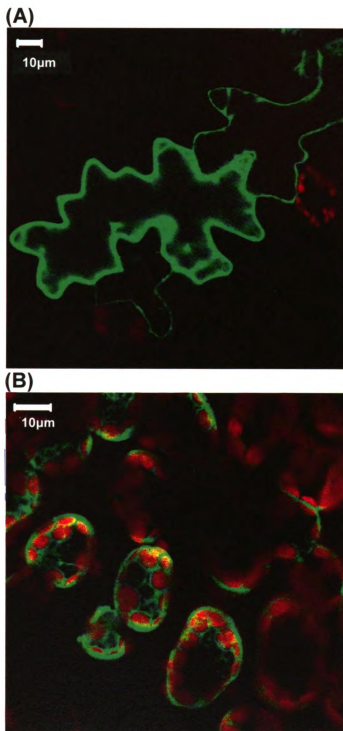
Tsuda, K., Sato, M., Glazebrook, J., Cohen, J.D., and Katagiri, F. (2008) Interplay between MAMP-triggered and SA-mediated defense responses. *Plant J* **53**: 763-775.

Underwood, W., Zhang, S., and He, S.Y. (2007) The *Pseudomonas syringae* type III effector tyrosine phosphatase HopAO1 suppresses innate immunity in *Arabidopsis thaliana*. *Plant J.* **52**: 658-672.

APPENDICES



Appendix 2-1. Dual localization result of HopM1-GFP and PTS1-dsRED2. (A) HopM1-GFP expressed in mesophyll cells of *N. benthamiana* (marked with red arrows). The autofluorescence from chloroplasts is also shown (Ch). (B) PTS1-dsRED2 expressed in mesophyll cells of *N. benthamiana* (marked with blue arrows). (C) Merged image. Note that PTS1-dsRED2 is excited by both 488 nm and 543 nm lasers (yellow punctuate structures pointed by yellow arrows).



Appendix 2-2. Transiently expressed of EGFP in pEGAD vector in *N.benthamiana*. (A) Fluorescence of the EGFP detected in (A) epidermal cells and (B) mesophyll cells. The leaf samples were examined 48 hours after *Agrobacterium* infiltration. All images were from single focal planes.

Appendix 3-1. The genomic sequence of *AtBIG1* (At4g38200). Start codon (ATG) and stop codon (TGA) are in red and bold letters. Exons are in yellow color and capitals, and introns are in violet and small letters. The partial 5'-UTR is indicated by black and small letters. The putative T-DNA insertion of salk_066766 is highlighted with green color. The forward and reverse primers for genomic PCR to screen homozygous salk_066766 are bold, underlined and blue-colored.

agaaacgcagcgcttctgcttgcacaaagtccccgggttctgggttgcccttttatcattttgaatgcgcgt
gagaagtgcgaatgatgcttagATGTCCTGCTGCAGAAAGCTTCTGGGGCCACAGATCGCGCGGGTGAT
TGGGCCATCTTTGGACAAGATCATAAAAAATCGCCGCTGGCGCAAGCACACCTTCCTGTTTTCGGCCTGTGA
AGTCTGTACTCGACAAGCTCGAAGCTCTCTCCGATCTCCCGATCTCTCGCTGCCTCTTCGGCTGTCACT
ACCTTCGGATCGAGATGCGCTTCTTCAGCCACTCTCTCTCTCTGTATGATACCGGTATGCTAAGGTTATTGA
GCTCTGCTCGAATTGCTCTTTTCAAGCTCTCTCTCTCTCTCCCTCCGCGGCGAGGTCCTGCTCTCGCGCG
CTGATTCTCTTCTCTACAAGCTCATCCATGCGATCTGCAAGGTTTTCGGGCATCGCGGAGGAGTCAAATGAG
CTGGCGGCTCTCTGCTGCTCTCTCGCGCGCGTCAAGATCTCTCGCATCTCAATCCGTGGCGATTGTTTGCT
CCATCTAGTCAGGAAGCTGCTCAATGTGTATCTCGCGGATTCACAGGGAACACAGATCTCGCGCTAAAT
CTGTGCTGGCTCAGATCATGCTCTGCTCTTCACAGATTCGAGGCGAATTCATGGATGCATCAGTCAAA
ACGGTTAATGTCAAGCACTTGTCTGCAATCACGGATAAGAAATGCAACAGAGGGAACCTGTTTATATTGT
TCAGGGATTGATTAACGACCTCATTAATGCGCGGGGAAGCAATCTCTCTCGGATTTCGGCTAGTCCAACT
CACTCAGAGGAAGGTGCTCTTCAATGAGGATGAAAGTACAGGAGCAAGATCAGGGAAGACGGTTTCTCT
CTCTTCAAAATCTCTGTGAAGTTCTCTATGAAGTTCTCTGTCAGAGAGAACCAGCATCAGATTCTGTG
GAGAGGCAAGACTTTCTCTCTGATTTGCTCAAAAGTCAATCATGATAAGCGCGGCCAATTGGCTCTCTG
ACGAAAGGCAAGTTGTTTTATCTTCAATTCACAGGTTAGTCTAGTCTCTCTCAAGTAGTAATGAACCTCA
AGAGCTCACTCTCCCTCGCCCAAAAATATGCAAGTTTCTAAATGCGCATCAAGCGATTGCTCTGTTGCTCG
TGTTAAAGATATAGCGCACTTTCTGGTATGTCTATTTTTCAAATTCAGTGTGCTATCTTCACAACCTTACTA
CGGAATATAGATCGGATGAAATCAGAAATAGGTATATTCTTCAGATGCTTGTCTCTCGGCTCCTTGA
AAATGTTCTCCAGCCTAAGTTCTGCAAGAAATGACCTGCTCTGCTTACTCGAGAACATTTGCCACGACC
CAAACTTAATCATTTACATATTTGTGAATTTGATGCGATGTTGAGGCTCTCCCAACATCTTCGAAAGTAT
tggagtttttttttataatctccccctagatagtttttggtttttttctcggaaatgattctcagatg
ttgtcagattacagttatttttagctgaaagtgttagagatcagagccaccagggttagcgtacgoggt
catattgatttccatagtggtgtgttacttttaataaagtgtattaaagcttataattctatcagatg
tttgcagttgttttcaacgcttctctgaaatctgtttagggcttctctggttgccttgcacaaatattgtcc
CCAATCCAGGATATTAATTTCTCGGCACTAATCTGTGAAGTGTCTGTTAGCATATTAAAGCAATGGGAAC
ATGSAATGGACCAATATGAGCTGGAGATTCATTTCTGCTTAAGAGCTTAGAAATGAGGCATGGCAAC
ACAATCATTTCAAACTCAATGAAGAGAGTGGAGCACTATAGATCATGCTTTCCACCAAGATTGGAATCCA
GAGTCTACAGAGCTGCAATCTTGAACAGAGAGGCGCATATAAAATTTGAAGCGGAGTcttattgttattt
tttttttagaagtgtgaatttcttattataaaatggaacattgttttataatctgctctggggaagggt
cttctatgacaaaaaaaattataaaagtattagctactacaacatactaaagtatttagaggatgcttag
gatagattagacatctgagaaccttgagcgagcagagctccacatctcttggcgttaagcagcagatgaaga
gagtgatatttatgtcgaggaatttcttatttgcatataaaagaactaaaaattgtccacacactcgatg
atatttagtagaatttgttttctctcttctggtcatgttaattgctttatcatcttctctggtttatgtgcagA
AAGGCGTCACTCTAATCAATAGAAAGCTGCAAGGATATGAGTTTCTATACGCTCTAAAAAGTTGGC
AACTCCCGGATGAGGTGGTGTCTGCTGAGGAATACCACTGGCTGAATGCAAGCATGATTGGTGAATTA
TTTGGGTGAAGAGAGCATTTTCCAATGAAAGTATGCTATGCTATGCTGGAATGTTGATTGATTCAAGGAGA
TGAATTTTGGTGAAGCAATTAAGTTTCTTAAAGGCGCTCGAGCTCTCTGGGGAAGCAGACAGAAATTTGAC
CGCATATGGAAGAAATTTGCTGAAGCGTTTTTCAAAATGCAACCAAAATTCATTGAGCAGTGCAGACAGC
ATATGTTCTTGCATCTCTTAATTAAGTGTAAACTGATGTCAGCAATATCATGGTTAAAGAGAGAGGTTT
gtctcttggctgtcaaaatttataccatccatgactgactagattttgagtgatttggcagattgtgttaact
tttttggctattctgtgctcagaaaatttgccttttgaatatttcaaatggagatgcttttttgggtgtaa
ggctcttacaagtgatttttaacgtctgtcttctggttttagacaatcagatGACCAAGCTGATTTTATCAG
AAATAACCGAGGCATGATGATGGCAAGAGATCTCCCAAGAGATATCTTGGTGCTTTATGACCAAGTTG
TCAATAAATGAATTAAGATGAGTTCTGATTCTTCAGCCCAAGAAAGCAGGAGTCCAAATGGCTGGAATAAA
CTACTGGGTCTGGAGCGGTATACCTCAATCTGGTTTATGGACAACAGACAGAGAGATGATTTGCTTTTCATGGCCAAATTCAA
TGGTCTCTTTATAAGGATATTCAGAGAAAGTTCAAGTGTGAATGCTCGAAATTCAGAGtaagctcgtttac
cttaaggtcttagtgtaagagatgcttattgagcgagtcaggttacctgcaaccttagcgaactaaagtga
accatcgtttctcttatacgttaataaaacctacttcccccttagtttcaagctttagttgttctgtcga
attgtgtattctctgagaattgagaacctactcttttaaaaggatttaatttagacaatcccggtgacggaat
gttaggatttatactataaaccttagctctaaggaactggatttttttggctttagatTCAGCTTATAC
ATGTAGTCACAGAGTTTGCATATTTGCTTTATATGTTGAAATTTCTCGGAGCAACATGCTTGGCGATTC
AGCGTGACATTTGATGAGATGATGACAGGCTTGTGTGAGTTGAATGCTTACGAGGCTTTTGGTATGCACT
TCATGTGACAGCTGATTTGGTATATGCAAAAGCAAGAGATGATTTGCTTTTCATGGCCAAATTCAA
ATCTCCATTCGGCAGGAGATATGAGCAAAAGAAATATCGATGCTGTTAAAGtaagtttcttacttcttcca
tattataatcgcgtgttcagaatgaaggagttgttctctctgtgttttcttctctcgcactgattttt
atgtatacagagagatgaagcattctgagcactactgaccttaagtattcatatgttttcaattttctgttt

Appendix 3-1 (continued).

[illegible]

Appendix 3-2. The genomic sequence of *AtBIG2* (At3g60860). Start codon (ATG) and stop codon (TGA) are in red and bold letters. Exons are in yellow color and capitals, and introns are in violet and small letters. The putative T-DNA insertion of salk_033446 is highlighted with green color. The forward and reverse primers for genomic PCR to screen homozygous salk_033446 are bold, underlined and black-colored. The forward and reverse primers for RT-PCR are in bold, underlined and blue letters.

Appendix 3-2 (continued).

GTGAAGCTATATAGACTTTGTTAAAGCTCTGTGCAAACTTTCTATGGATGAGTTGGCGTCTCCTTCTAAT
 CCACGCCGTTTTTAAAGCTTCACAAAGATTTGTGAGATAGCGtaagaatctcctagtttcgttctctctgttc
 tctcctatctactgcctatcaagagacgttctctgttctcttagcaactttaagtagtagtctgcacaaatcttctgt
 ttgttcattttgtgacagTCATTTATAAATATTAATGCTATAAGCTTGTGTGGTCAAGCATCTGGTAAGTGT
 ATCAGGTTTCTTTGTGACCATGGATGCTCAGATAATCTTTTATTGCAATATTTGCAATGGATTCTCTCC
 GCCAGTTGTCTCAATTAATTTCTGGAACGGAAGGAGTTGGCTAATTACAACCTTCCAAAATGAATTTATGACA
 CCTTTT**GTCATTGTTATCGGTAGAACTAATGATGTTGAGAT**AGAGAACTTATCATCAGATGTGTTCTCA
 GATGGTATTGTCACTGTAAATAATGTTAACTCAGGATGGAAAGCATGTTTATGgttaggcattttattgta
 attttctggtaaccacatttaatttaagaattttttggttttactcacaatgtgtttctctccgttgcagGTT
 TTTACCCACAGCGGCATATGACGACCACAAAAATATTGTGTTTTTGTCTCTTGAATAATTACGAGAAGATTAT
 TCGAGAATATTTCCCATACATCACTGAGACAGAAACCAACCACTTTTACAGATTGTGTGAATTGCCAGTTG
 CATTCACCAATAACAGATTTAGCAAGGATATCAGTCTCAGTTCTATAGCTTTCTCCCGGATTATTGCAACA
 AAGCTTGCAGAAGGAGATCTTAACTCGCCATCAACAAACAAATACAAGGGAACCTCTGGAAAGATTCTCTCA
 CTCATCTCTCCACAGTGGAAAAAGTGGGAAACAGAGAACGGAGAGATTGTAAACAA**CAATCACTTTTATT**
 TTTGGTTTTCCCTTTACTATCAGgtataacactataattttatcgagaagattactttaagttgaagattctat
 tcatgtgttttcacacctctctctgtctaatgtgcaagJTTTATCAGAGCTTAGTTTCGATCCAGACCAGAAAT
 CAGGAAAAG**CGACTACAGATTATGTTTGATACCTTACCGCA**CCATGGCCATTTATTTTCTCTGCCGTTAT
 GGGAAAAAGTATTGCACTCTATTAATTCCTATATTGAGACACGTACGCCATTCTATTGATCCCTTTCTGGG
 GAAGACGAATCTCTGATCAAGGAAATTTCTGGTGGTGAAGTGATGAGCTAGATATGA**CGCCTGGCTCTA**
CGAGACCTATCATTAGCACTACAGCTTATAGTGGATCTCTTTCTCAAATTTTACACTACAGTAAATCCAC
 TTCTAGAGAAAGTACTAATGCTTTTGTGAAGCTTATAAAGGAGACTTCAACAGAGCCTTGAGGAATTTGGT
 ATTGCTGGGTTTGTCTGTGATGAGCGATGCTGATGGCTTTCTCTGAAGAAAAGTGGTTAGAGGTGGT
 GTCAGCTTTAAAGAAAGTGGCGAAAAACAATTTGCCAGATTTTTCGATTTCTTAGCGAAGAAATATGTAG
 CAAGAAGCCAGAGAGTGTCTCAACATTCAAAACAGTAATGCTGAGTCTGTGCTGCCAAGTGTACCGAT
 GGCAATGAAGAGAGTCAAGAGAACGCAACCCATCTTTACGGTGTATCTCTGATGCTAAGTGGCGAGCCGC
 TGTTCACCTTTTGTGATTCAGgttagttctctcgaagccttacatttatgtattataataatgtgtgttc
 ctccaattgaaccagacaaattttattctttaatacaaatgtctttgttaaatgataactcaaaaggca
 aacgcaaacagagagggaactttggagttcttttccgtttacaattttacaaaaaaagtaaatgcaa
 tttgtgtgtgtgtgtattttagtaaatgtttctatttttttcagTCGTGTATGGAGATTATCAACATGTA
 CAGACTCAGCTTTTACGTGAAAAAACAATTAGTCTCTGTAGTGCATTGACGGTGTAGCTTTACATGCTC
 ACGGAATAACAGTAACATAATACTTCTGTTCAAGACTACAAAG**GCTAGGACCCATGACACAGATCGAAG**AT
 CCTCTCACTACTCTCTTTGAAAAAGAGTCTTATCAAAATCTGCTGACATCTTACAGATCTTTGTGCAGA
 CAAACCCAAAAAGAGAAAGAAAGAGAGAGGAAATAGTATCACTTGTCAACATCTGTCAAGAAG
 TTCTCAACTTTTACATCGAGACTTCTCTCTGCAAAAAATACAATCAGAAATCATACGGGCCACGCGAA
 TACCGATGGAGAATACCTTTGGTATCAGGAAGAGAGAGAGCTATCAGCAAGAGCTCCTCTTATAGTTGC
 AACACTTCAAGCAATGTGTAATTTGATGAGGTCATCTTTGAAGAAGCTTGAATGTCTATTCCACTTC
 TGGCTAACTTGATTAAGTGCAGAACGGCTCTACCGAGGTTAGACTGCTCTGTGTGACATGCTTGGCTTA
 TCGGTTGGCCGGTTTTACTCCAAGTGGT**TGA**

Appendix 3-3. The genomic sequence of *AtBIG3* (At1g01960). Start codon (ATG) and stop codon (TGA) are in red and bold letters. Exons are in yellow color and capitals, and introns are in violet and small letters. The putative T-DNA insertion of salk_044617 is highlighted with green color. The forward and reverse primers for genomic PCR to screen homozygous salk_044617 are bold, underlined and black-colored. The forward and reverse primers for RT-PCR are in bold, underlined and blue letters.

171

TGCGGGGAAGAGTTGGCGAATTATAAC

TGTCAAGTTCGGGATGGAAGAG

TGCTACATCCCCTGACTTC

TCATACG

TAA

Appendix 3-4. The genomic sequence of *AtBIG4* (At4g35380). Start codon (ATG) and stop codon (TGA) are in red and bold letters. Exons are in yellow color and capitals, and introns are in violet and small letters. The putative T-DNA insertion of salk_082249 is highlighted with green color. The forward and reverse primers for genomic PCR to screen homozygous salk_082249 are bold, underlined and black-colored. The forward and reverse primers for RT-PCR are in bold, underlined and blue letters.

Appendix 3-4. The genomic sequence of *AtBIG4* (At4g35380). Start codon (ATG) and stop codon (TGA) are in red and bold letters. Exons are in yellow color and capitals, and introns are in violet and small letters. The putative T-DNA insertion of salk_082249 is highlighted with green color. The forward and reverse primers for genomic PCR to screen homozygous salk_082249 are bold, underlined and black-colored. The forward and reverse primers for RT-PCR are in bold, underlined and blue letters.

aagtaacacacacacacatttctcaatataatataccatctttgaatatgttttcaatgatctgtgttttag
 [REDACTED]
 [REDACTED]
 gttacaacaagatattgcttattgtgttllacacataagttatatccctctgttttggttaaataatttgagt
 attttttattttgttcag CGGTTCCATAGA
AGTATTGTTCCACATTCTG TGGAATCTTCAGCT
CTATCATTCTCCAG
 ccaaggactctgttttgaactctctgtctctctctcttstaagccaatgactctgttcttgactcctctgt
 tctttttacag CCTACATGATGTTCCCTCCAAGACATGGTTAC
 [REDACTED]

Appendix 3-5. The genomic sequence of *GNOM* (At1g13980). Start codon (ATG) and stop codon (TGA) are in red and bold letters. Exons are in yellow color and capitals, and introns are in violet and small letters. The putative T-DNA insertion of salk_103014 is highlighted with green color. The forward and reverse primers for genomic PCR to screen homozygous salk_103014 are bold, underlined and black-colored.

[illegible]

Appendix 3-5 (continued).

Appendix 3-6. The genomic sequence of *GNL1* (At5g39500). Start codon (ATG) and stop codon (TGA) are red and bold letters. Exons are in yellow color and capitals, and introns are in violet and small letters. The putative T-DNA insertion of salk_067415 is highlighted with green color. The forward and reverse primers for genomic PCR to screen homozygous salk_067415 are bold, underlined and black-colored.

Appendix 3-6 (continued).

Appendix 3-7. The genomic sequence of *GNL2* (At5g19610). Start codon (ATG) and stop codon (TGA) are in red and bold letters. Exons are in yellow color and capitals, and introns are in violet and small letters. The putative T-DNA insertion of salk_021757 is highlighted with green color. The forward and reverse primers for genomic PCR to screen homozygous salk_021757 are bold, underlined and black-colored.

ATG iATCGTATCGGCCGTAAGAGCAAAAGCGAAAGAGGTTAGGATATATATCGATGCTTAAACACGGAGGTTGG
 TGCATGCTTTGCGCTCAATTGCTAGACGGCTTTAGAGAGGTTACCTTCTCTCCCAAGAAACAGACACTGTGT
 AITATCGTGCACCAATCTCTTAATCTCTTAAGCTCTTATTTTCAATCCGCAACAAGTTCTGGCGCCAC
 ATAGATCTCTTGGGTTTATCTTTCTCTTCTCGAAGTTATTTCAAAGCGATGATGATTCGCGCTAGCGCCAC
 AGCTGTGCGCTTTCTCTCTCATCTTAAGAGCTCTTAATAATCGAGATCTTTGATGAGAGAAACCTGTGTGCAA
 AAGATGCTATGAATCTCATTTGTCTCCGGGATTAAGTTGTCTTTGGAAGAAACAGATTGGTGTGTGAA
 GATGCTTAATGATGAGGATTTCTCAAGTTTAAACCGGAATCATGAAACATCCATCTCTGTacggttcatt
 aactataatcttttactacaagtgttattttgtcctcttttaagacagtaataaagtattgtattaa
 aacagaggttatTAAGAGATCAAGCGTTTGCACATAGTCAATACATGTTTCCAAGTAGTGCACATATCT
 ACCGTAGATGAGATTTGTCTCAACCGAAATGTAAGATATCAATTCATGAGCTGATTCAGATCATTTCTCT
 CAGATTACCTGATTTTGAGGTGAGATGAGATGAAGTGTGTGAGATTTAGAATCTGATACGACGAAATCG
 ACAATGAGCGCGGATATGAATTCGATGTGCAATGAATCTTTCATTTCTTATGTCGTGTGCTCAATGTT
 GTTAAAGTTGTGAGAACTTAGAAGTGACAAAGCTTCAAGCTGAGAGAGAGATGTCAGATGATTTTGTCTT
 AGTTTAATAAAATAGCGCATTTAGTTAAGTGTGTGATGTGATCGGCAATACCTAAGCTCTTCTGAGGT
 TTCAGAGATGATCTTTCAATCATTTAATTCATCATGGAGCTTCTTCAAGCTCTCTTTGTGCTATCAATGATCT
 TGTAGTTGTATCTAATCAATATCACTTCTCTCGCAAGtaagtcctgtttttatacaactaaaacct
 aaaactctgttttattctcaacttttgtctaacaacaatgtgttgatttattagTTCATGAGCTTCAATCT
 GAATCTTCTCTCTCTCTGCTGTGTGTGAGATTAACAGCTTTCAAGGCTTCTCTCTGTTAAGAAGATGCT
 TCTTGAAGGCTAATTAAGATTTTGTGACAACTGCTTTCATAGTGAAGCTTAGATGAAATACGATGTGT
 ATCGATGATGTGAGAAATATATTTGAAGAGAGCGGAAAGTTCTATGTCAGACATACATCTTCACTCTGTGT
 CCTTTAAGCTCTATACAAATGCAAGCTTTTGAAGGCTTTGTGATCTTGAACATCAACATCTGCAACATAT
 GGAATGAGAGAGGATGAGGCTTAATGAAGAGATGATAATAACTGGAATGTGATTAAGCTGAGGCTGTGTG
 AGATCATGAGTATACATCTCTTGGATAGATGAAGCAAGAGAGATTTGAGAGCTGGGATGATCATATA
 AGATGAAGGAAGCTCAAGAGAGAGAGCTAGCGATGCTTCAATCATTTCAACAGATGAGAGAGAGAGG
 TTTGAGATATTTAGATTAATCACTTACTTGTCTGAGATCTCTTGTATCCATGGCATTAAGCTTCTCTTCA
 GATTCACACCGGGTTTGGATAAGACAATGATTGAGATTAATTTGAGAGCTCTGATGAATTAATCTTCACT
 GTTATTAGAAGCTTTACATACATTTAGTTTCACTGGTATGAATCTTGTATCCGCACTTGAAGACATTTCT
 TGAATCATTTCTGTGTACGGGATGCTTCAAGAGATGAGATGATGATGAGCTTCTCTGAGAGATTTCT
 ATGATCAACATCATCTGATATTTTGAAGCAAGAGATAGCTTTCATATTTGTGTACTGTCTTATAATG
 CTCACAGCTGATCAATTAACCTCTCAATAGAGAGAAATGATGAGAGATGAGTTGATTTGCAACAGAG
 GGTATTAACGCGGAAAGAGCTTTCAAGAGATATCTGAGCTTTTTCATGCTCATGCAATCAAGAAAG
 CATCTGCTTTATCGACACATTCGTGTCTGCGGAAATGAATCCAAACAGATGAGTTGAGCTTAATGAACAG
 ACAAGATTAACACACCTTTATATTTATGTAGTGTGATCTGAGAAATGAAGGGATGATTTGCAACCAT
 TGCAGGTCTCATCAATAGCAATTTTCTGATCTTTGAGCATGATGATGATGAGCTCTCATGAAT
 GTGTGATGCTATGATCTATAGCAAGAGTTGCTCAGTATGGCTTGAAGACTCTTTGATGAGCTCATTT
 GCTTCTTTTGTAAATTCACAAAGTTGTTAAACCTCTTCACTACATCTGAGAGACTTTTGTTCATTTAG
 TCAAGATATGAACCGCGAATGGCTACTCTGCGCTTTTCAAGCTCTCTTAACCATTTGGTGATTTCTATCA
 GAGAGGGTGGAGGAACATTTGATTTGCTTTTGAACCTTAGAAGTTTCAAGCTTCTCTCAAGCTGTGT
 ATTTAGTTTGAATTAATGAAGAAATGGCGATCAGAAATGAGATGAAATGTTTGAAGCGAGGACGA
 AAAATTTAAACGATACAACTTTAGTTTAATGGGCTGCTTTTCACTTTCTGTGCAATAGCAAGCTGG
 AAGATCTGTAATCTTGAAGTGAGTGAGTTTGAAGAAAGCTTTAAATCTATAAACAATCAAGATGGGT
 CAATATTCAGCAAAAGCTTGTGTGTGCGGATTTGTGTGTGATTTTGGTGTCTTTAATCTATG
 AGCTGCTGGGAAAGGACGAAGTTTATGACAGCTATCGAAGAGAGAGACGGTTAAGTTTGTGGGAT
 TGAATCAACCATTT**GCATTATCTAACGTCACCGG**TTCAACATGTTTGGCAAGTTTACCATGATATCTA
 TCAACCTTCAAACTTTCTGCTCTTTTCAACCATTTCCGTTTGTGCAAAAGAGGCTCCCGGGTTTATTAG
 GGTATGATGATGATGATGCTCTTCAACCTTCAAGACCATCTACAGAGAGATTTGATTTTATGCTCTTGA
 CATATATGTGGAAGATAGACAAAGAAATCATTTGAACATGTTATGACACATTAACAGAGCTTTGTGACGAAG
 ATCATTTATAGACTACTCTGCGAATCTGCATACCAATATAGGGTGGAAAGAGTTTATACAACTACTCTTT
 ATGTGGAAGACCTCCAGAGACAAAGAGCAAGCGGTGATGCTCTCATCGGTTTAAATGTCATTTAAGCAG
 TCGCATCTTCCGAGTCAAGCTACGCTTATTGCTATCGATTGCGGCTTCAGTTTGTGTGCTTTAAGAAATAGC
 TCTGTTGAGAGAAAGATTGAATAATTTGGATCTCATGGCAGATTGATGACAAATGTTTGGAAATGGTACAA
 AACGCTCTTATTTGATAGCTTTGAAGATGATAGCTCGGTAAGCAATTAAGAGCTTCTATGATGGAAG
 AAACCACTTGAGAGGGGTTAACTTTGTATCATCTCTTCTCTTAACTCTCTCGAGGTTTGTGAAGAAACG
 ACCTTTGCACGCGGAGAAAGATTAAGCAAGAGCTAGCTGAGCTCTCTAGAGAAATGTTTAACTGGGTCA
 TGAAGATCTTGGATTTACACCTTTCTGGTGTATATATCTGATAGACATGATGATTTCTTCAACATGATG
 ACTTGATGAGAAAGCTCTCTGACATTTAAGGCTGAAGAAATGGAAAGAGAGATGATGATGATGAGG
 ACGTTGAAGATGAGTATGAAGGTGCTATGAACCTTTCTTGTGTGTGTAACAAATTTGAAGAAATGCT

TAGacttttattattgtactatgtaattcatgat
ttaatgctcaaattatatgatcaacttcaagaagtcatgagattttggatatatatagcttctactaatc
catagagcaatcatcaattttatggcaaataatccatattaaatatatatacccttataagtctcattcaa
tta**ccacataccacattagtotcc**atttttttagacaacacattaactccatagaagagtgatttgaggca
a

Appendix 3-8. Comparison of the nucleotide sequences and amino acid sequences of the C-termini of GNL2. (A) The comparison of the nucleotide sequences of the C-termini of *GNL2* in TAIR (GNL1-T) and that of the clone used for yeast two-hybrid assay (GNL1-C). The different nucleotides are highlighted in yellow color. (B) The comparison of the amino acid sequences of the C-termini of GNL2 in TAIR (GNL1-T) and that of the clone used for yeast two-hybrid assay (GNL1-C). The different amino acids are highlighted in blue color.

(A)

GNL1-T AAACCTAGGAAGCTTCAGCTTCTTCCACAGTCTGTTATTGAGTTTGAGATAAATGAAGAA
GNL1-C AAACCTAGGAAGCTTCAGCTTCTTCCACAGTCTGTTATTGAGTTTGAGATAAATGAAGAA

GNL1-T AATGGCGGATCAGAATCCGACATGAACAATGTTTCGAGCCAGGACACAAAATTTAACC**GA**
GNL1-C AATGGCGGATCAGAATCCGACATGAACAATGTTTCGAGCCAGGACACAAAATTTAACC**GG**

GNL1-T CGACAAGGTTCTAGTCTAATGGGTCGGTTTTTCACACTTCTTGGCATTAGAC**CA**CGTGGAA
GNL1-C CGACAAGGTTCTAGTCTAATGGGTCGGTTTTTCACACTTCTTGGCATTAGAC**AG**CGTGGAA

GNL1-T GAATCTG**TAG**CTCTTGGAAATGAGTGAGTTTGAACAAAACCTTAAAGTCATAAAACAATGC
GNL1-C GAATCTG**TG**GCTCTTGGAAATGAGTGAGTTTGAACAAAACCTTAAAGTCATAAAACAATGC

GNL1-T AGGATCG**GT**CAAAATATTCAGCAAAAGCT**CAG**TGTTGCCGGATGTTGCCGGTGTGAATCTT
GNL1-C AGGATCG**GC**CAAAATATTCAGCAAAAGCT**CGG**TGTTGCCGGATGTTGCCGGTGTGAATCTT

GNL1-T GGTCCGTCTTTAATCTATGCAGCTGCTGGGAAAGGACAGAAGTTTAGTACAGCTA**TC**GAA
GNL1-C GGTCCGTCTTTAATCTATGCAGCTGCTGGGAAAGGACAGAAGTTTAGTACAGCTA**TA**GAA

GNL1-T GAAGAAGAGACGG**TTA**AGTTTTGTTGGGATTGATCATAACCATTGCATTATCTAACGTC
GNL1-C GAAGAAGAGACGG**TC**AAGTTTTGTTGGGATTGATCATAACCATTGCATTATCTAACGTC

GNL1-T CACCGGTTCAACATGT**TTT**GGCCAAGTTACCATGAATATCTACTCAACGTTGCAAACTTT
GNL1-C CACCGGTTCAACATGT**CTT**GGCCAAGTTACCATGAATATCTACTCAACGTTGCAAACTTT

GNL1-T CCGCTCTTTTCAACCATTCGGTTTGTGCGAAAAGGGCTCCCGGGTTTATTTAGGGTATGC
GNL1-C CCGCTCTTTTCAACCATTCGGTTTGTGCGAAAAGGGCTCCCGGGTTTATTTAGGGTATGC

GNL1-T ATCAAGATTCTTGCTTCTAACCTTCAAGACCATCTACCAGAGGAGTTGATTTTTAGGTCC
GNL1-C ATCAAGATTCTTGCTTCTAACCTTCAAGACCATCTACCAGAGGAGTTGATTTTTAGGTCC

GNL1-T TTGACAATAATGTGGAAGATAGACAAAGAAATCATTGAAACATGTTATGACACAATAACA
GNL1-C TTGACAATAATGTGGAAGATAGACAAAGAAATCATTGAAACATGTTATGACACAATAACA

GNL1-T GAGTTTGTGACGAAGATCATTATAGACTACTCTGCGAATCTGCATACCAATATAGGGTGG
GNL1-C GAGTTTGTGACGAAGATCATTATAGACTACTCTGCGAATCTGCATACCAATATAGGGTGG

GNL1-T AAAAGTGTTTTACAACACTTTCTTTATGTGGAAGACATCCAGAGACCAAAGAGCAAGCG
GNL1-C AAAAGTGTTTTACAACACTTTCTTTATGTGGAAGACATCCAGAGACCAAAGAGCAAGCG

GNL1-T GTGGATGCTCTCATCGGTTTAATGTGTCATTAAACGCATCGCATCTATCGCAGTCAAGCTAC
GNL1-C GTGGATGCTCTCATCGGTTTAATGTGTCATTAAACGCATCGCATCTATCGCAGTCAAGCTAC

GNL1-T GCTTATTGCATCGATTGCGCCTTCAGTTTTGTTGCTTTAAGAAATAGCTCTGTTGAGAAG
GNL1-C GCTTATTGCATCGATTGCGCCTTCAGTTTTGTTGCTTTAAGAAATAGCTCTGTTGAGAAG

GNL1-T AACTTGAAATATTTGGATCTCATGGCAGATTTCAGTGACAATGTTGGTAAATGGTACAAA
GNL1-C AACTTGAAATATTTGGATCTCATGGCAGATTTCAGTGACAATGTTGGTAAATGGTACAAA

GNL1-T ACTGCCTCTACTGATACCGCGAATAGCTATAGCCCGGCAAGCAACCAAGCAGTTTCATCA
GNL1-C ACTGCCTCTACTGATACCGCGAATAGCTATAGCCCGGCAAGCAACCAAGCAGTTTCATCA

GNL1-T TCCATGGAAGAAAAACAACTTGAGAGGGGTTAACTTTGTTTCATCATCTTTTCTCAAACCTC
GNL1-C TCCATGGAAGAAAAACAACTTGAGAGGGGTTAACTTTGTTTCATCATCTTTTCTCAAACCTC

Appendix 3-8 (continued).

GNL1-T TCCGAGGCTTTTCGAAAAACGACCTTGCACGCCGAGAAGAGATAAGGAACAGAGCAGTG
 GNL1-C TCCGAGGCTTTTCGAAAAACGACCTTGCACGCCGAGAAGAGATAAGGAACAGAGCAGTG

GNL1-T ACGTCTCTAGAGAAAAGTTTACCATGGGTCATGAAGATCTTGGATTACACCTTCTGGT
 GNL1-C ACGTCTCTAGAGAAAAGTTTACCATGGGTCATGAAGATCTTGGATTACACCTTCTGGT

GNL1-T TGTATATACTGCATAGACCATGTATATTTCCCAACAATCGATGACTTGCATGAGAAGCTT
 GNL1-C TGTATATACTGCATAGACCATGTATATTTCCCAACAATTGATGACTTGCATGAGAAGCTT

GNL1-T CTGGACTATTCAAGGCGCGAAAAACGCGGAAAGAGAGATGAGAAGCATGGAGGGGACGTG
 GNL1-C CTAGACTATTCAAGGCGCGAAAAACGCGGAAAGAGAGATGAGAAGCATGGAGGGGACGTATA

GNL1-T AAGATAGCTATGAAAGTGCTCATGAACGTTTTCTTGGTTTACTTGGAAACAAATTGTAGAA
 GNL1-C AAGATAGCTATGAAAGTGCTCATGAACGTTTTCTTGGTTTACTTGGAAACAAATTGTAGAA

GNL1-T AGTGCTGAGTTTAGAACTTTTTGGTTAGGAGTGTTGAGGAGAATGGATACGTGTATGAAG
 GNL1-C AGTGCTGAGTTTAGAACTTTTTGGTTAGGAGTGTTGAGGAGAATGGATACGTGTATGAAG

GNL1-T GCGGATTGGGAGAGTATGGAGATAACAACTTCAAGAGGTTGTCCTGAACTTTTGACC
 GNL1-C GCGGATTGGGAGAGTATGGAGATAACAACTTCAAGAGGTTGTCCTGAACTTTTGACC

GNL1-T ACCATGATTGGTACCATGAAGGAGAAAGAGATTTGGTGAGAGGAGACGATGACCTT
 GNL1-C ACCATGATTGGTACCATGAAGGAGAAAGAGATTTGGTGAGAGGAGACGATGACCTT

GNL1-T TGGGAGATTACGTATATTCAGATTCAATGGATTGCTCCAGCGCTCAAGGATGAGTTATTT
 GNL1-C TGGGAGATTACGTATATTCAGATTCAATGGATTGCTCCAGCGCTCAAGGATGAGTTATTT

GNL1-T CCCGATGAAGAGATTTAG
 GNL1-C CCCGATGAAGAGATTTAG

(B)

GNL1-T KLRKLQLLPQSVIEFEINEENGSESMDNNVSSQDTKFNRRQGSLSMGRFSHFALDVE
 GNL1-C KLRKLQLLPQSVIEFEINEENGSESMDNNVSSQDTKFNRRQGSLSMGRFSHFALDVE

GNL1-T ESVALGMSFEQNLKVIKQCRIGQIFSKSSVLPDVAVLNLRSLIYAAAGKGQKFSTAIE
 GNL1-C ESVALGMSFEQNLKVIKQCRIGQIFSKSSVLPDVAVLNLRSLIYAAAGKGQKFSTAIE

GNL1-T EETVKFCWDLIIITIALSNVHRFNMFWPSYHEYLLNVANFPLFSPIPFVEKGLPGLFRVC
 GNL1-C EETVKFCWDLIIITIALSNVHRFNMFWPSYHEYLLNVANFPLFSPIPFVEKGLPGLFRVC

GNL1-T IKILASNLQDHLPEELIFRSLTIMWKIDKEIIETCYDTITEFVSKIIIDYSANLHTNIGW
 GNL1-C IKILASNLQDHLPEELIFRSLTIMWKIDKEIIETCYDTITEFVSKIIIDYSANLHTNIGW

GNL1-T KSVLQLLSLCGRHPETKEQAVDALIGLMSFNASHLSQSSYAYCIDCAFSFVALRNSSEVK
 GNL1-C KSVLQLLSLCGRHPETKEQAVDALIGLMSFNASHLSQSSYAYCIDCAFSFVALRNSSEVK

GNL1-T NLKILDLMADSVTMLVKWYKTASTDTANSYSPASNTSSSSSMEENLRGVNFVHHLFLKL
 GNL1-C NLKILDLMADSVTMLVKWYKTASTDTANSYSPASNTSSSSSMEENLRGVNFVHHLFLKL

GNL1-T SEAFRKTTLLARREEIRNRAVTSLEKSFTMGHEDLGFTPSGCIYCIDHVIPTIDDLHEKL
 GNL1-C SEAFRKTTLLARREEIRNRAVTSLEKSFTMGHEDLGFTPSGCIYCIDHVIPTIDDLHEKL

Appendix 3-8 (continued).

GNL1-T LDYSRRENAEREMRSMEGTLKIAMKVL MNVFLVYLEQIVESAEFRTFWLGVLR RMDTCMK
GNL1-C LDYSRRENAEREMRSMEGTLKIAMKVL MNVFLVYLEQIVESAEFRTFWLGVLR RMDTCMK

GNL1-T ADLGEYGDNKLQEVVPELLTTMIGTMKEKEILVQKEDDDLWEITYIQI QWIAPALKDELF
GNL1-C ADLGEYGDNKLQEVVPELLTTMIGTMKEKEILVQKEDDDLWEITYIQI QWIAPALKDELF

GNL1-T PDEEIX
GNL1-C PDEEIX

Appendix 3-9. The expression patterns of *ARF-GEF* genes from the Bio-Array Resource for *Arabidopsis* Functional Genomics (Winter et al., 2007; <http://www.bar.utoronto.ca/efp/cgi-bin/efpWeb.cgi>).


<i>ARF-GEF</i> gene	Tissues with high expression of <i>ARF-GEF</i> gene
At4g38200 (<i>BIG1</i>)	All tissue
At3g60860 (<i>BIG2</i>)	All tissue
At1g01960 (<i>BIG3</i>)	All tissue
At4g35380 (<i>BIG4</i>)	Anther
At3g43300 (<i>BIG5</i> , <i>AtMIN7</i>)	All tissue
At1g13980 (<i>GNOM</i> ; <i>EMB30</i> ; <i>GBF3</i>)	All tissue
At5g39500 (<i>GNL1</i> ; <i>GBF1</i>)	All tissue
At5g19610 (<i>GNL2</i> ; <i>GBF2</i>)	Anther


 TCAAGATAGCCCACAAGATTATCTAAGGGTTCACAACCAGGCACGAGGAGCGGTAGGCGTAGGTC
 CCATGCAGTGGGACGAGAGGGTTGCAGCCTATGCTCGGAGCTACGCAGAACAATAAGAGGCAACTGCAGA
 CTCATACACTCTGGTGGGCCTTACGGGGAAAACCTAGCCTGGGGTAGCGGTGACTTGTCTGGCGTCTCCGC
 CGTGAACATGTGGGTAGCGAGAAGGCTAACTACAACCTACGCTGCGAACACGTGCAATGGAGTTTGTGGTC
 ACTACACTCAAGTTGTTTGGAGAAAGTCAGTGAGACTCGGATGTGCCAAAGTGAGGTGTAACAATGGTGGA
 ACCATAATCAGTTGCAACTATGATCCTCGTGGGAATTATGTGAACGAGAAGCCATACGGCATGGTGAGCAA
 GGGCGAGGAGCTGTTACCGGGGTGGTGCCCATCCTGGTCGAGCTGGACGGCGACGTAAACGGCCACAAGT
 TCAGCGTGTCCGGCGAGGGCGAGGGCGATGCCACCTACGGCAAGCTGACCCTGAAGTTCATCTGCACCACC
 GGCAAGCTGCCCCGTGCCCTGGCCCACCCTCGTGACCACCTTCACCTACGGCGTGCAAGTTCAGCCGCTA
 CCCCAGCCACATGAAGCAGCAGACTTCTTCAAGTCCGCCATGCCGAAGGCTACGTCCAGGAGCGCACCA
 TCTTCTTCAAGGACGACGGCAACTACAAGACCCGCGCCGAGGTGAAGTTCGAGGGCGACACCCTGGTGAAC
 CGCATCGAGCTGAAGGGCATCGACTTCAAGGAGGACGGCAACATCCTGGGGCACAAGCTGGAGTACAATA
 CAACAGCCACAACGTCTATATCATGGCCGACAAGCAGAAGAACGGCATCAAGGTGAACTTCAAGATCCGCC
 ACAACATCGAGGACGGCAGCGTGCAGCTCGCCGACCACTACCAGCAGAACACCCCCATCGGCGACGGCCCC
 GTGCTGCTGCCCCACAACCACTACCTGAGCACCCAGTCCGCCCTGAGCAAAGACCCCAACGAGAAGCGCGA
 TCACATGGTCCTGCTGGAGTTCGTGACCGCCGCCGGGATCACTCTCGGCATGGACGAGCTGTACAAG**TAA**

Appendix 4-1. The sequence of *PRI-GFP* fusion ORF. The *PRI* ORF is in black letters and the *GFP* ORF is in green letters. The start codons and stop codon are in red and bold letters. The three nucleotides connecting *PRI* ORF without stop codon and *GFP* ORF are underlined. The putative N-terminal signal sequence of *PRI* is highlighted with blue color.

ATGCGGCTCTTGCAACCCACGGAAGGGCGGAAAGCACTCCCCTAAAGCCCCTAAGCTACCAG
TTCCCTCCGGTGACCGTCCCTAAGCTACCAGTTCCCTCCGGTGACCGTCCCTAAGCTACCAGTCCCTCCGGTG
ACCGTCCCTAAGCTACCCGTTCCCTCCTGTGACCATCCCTAAGCTACCCGTTCCACCAGTGACTGTACCTAA
GCTACCCGTTCCCTCCTGTGACCGTCCCCAAGCTACCCGTTCCCTCCAGTGACCGTCCCCAAGCTACCCGTTCC
CTCCAGTGACAGTCCCTAAGCTACCCGTTCCCCCGGTAAGTGTACCTAAGCTACCCGTTCCCTCCAGTGACC
GTCCCTAAGCTACCCCTTCCCTCCGATTTTCAGGGCTACCCATACCTCCAGTGGTAGGTCCCAATCTGCCATT
GCCACCTTTGCCAATTGTAGGTCTTATTCTTCCACCGGGAACAACCCACCAGCCACAGGAGGAAGGACT
GTCTCCACCGCCAGGGAGCGTAAGCCACCATCAGGGGGCGGGAAGGCGACATGTCCAATAGACACGCTG
AAGTTAGGTGCTTGCGTCGACTTGTTGGGAGGTTTAGTAAAGATAGGGCTTGGGGATCCAGCAGTTAACAA
ATGTTGTCCGTTACTTAAAGGCCTCGTTGAAATCGAAGCCGCGGCTTGCTCTGCACTACCCCTCAAGCTCA
AAGCTCTTGACCTCAATCTTTATGTCCCTGTTGCTCTTCAGCTTCTCCTTACCTGTGGCAAAAATCCACCT
CCGGGTACACTTGTTCCATAGCCAGCCATGGTGAGCAAGGGCGAGGAGCTGTTACCGGGGTGGTGCCCA
TCTTGGTTCGAGCTGGACGGCGACGTAAACGGCCACAAGTTCAGCGTGTCCGGCGAGGGCGAGGGCGATGCC
ACCTACGGCAAGCTGACCCCTGAAGTTCATCTGCACCACCGCAAGCTGCCCCTGCCCTGGCCACCCCTCGT
GACCACCTTACCTACGGCGTSCAGTGCTTCAGCCGCTACCCCGACCACATGAAGCAGCAGCACTTCTTCA
AGTCCCGCATGCCCCGAAGGCTACGTCCAGGAGCGCACCATCTTCTTCAAGGACGACGGCAACTACAAGACC
CGCGCCGAGGTGAAGTTTCGAGGGCGACACCCTGGTGAACCGCATCGAGCTGAAGGGCATCGACTTCAAGGA
GGACGGCAACATCTGGGGCACAAGCTGGAGTACAACATAACAGCCACAACGTCTATATCATGGCCGACA
AGCAGAAGAACGGCATCAAGGTGAAGTTCAAGATCCGCCACAACATCGAGGACGGCAGCGTGCAGCTCGCC
GACCACTACCAGCAGAACACCCCCATCGGCGACGGCCCCGTGCTGCTGCCCCACAACCACTACCTGAGCAC
CCAGTCCGCCCCTGAGCAAAGACCCCAACGAGAAGCGCGATCACATGGTCCTGCTGGAGTTCGTGACCGCCG
CCGGCATCACTCTCGGCATGGACGAGCTGTACAAGTAA

Appendix 4-2. The sequence of At2g10940-*GFP* fusion ORF. The At2g10940 ORF is in black letters and the *GFP* ORF is in green letters. The start codons and stop codon are in red and bold letters. The three nucleotides connecting At2g10940 ORF without stop codon and *GFP* ORF are underlined. The putative N-terminal signal sequence of At2g10940 is highlighted with blue color.



 GCGGGCAGCCCCGCTCCAGAGCCTGCTGGTCCCATCAACCTCACTGCGATCCTCGAAAAAGGTG

 GTCAATTCACTACTTTTCATCCATCTTCTAAACATCACTCAAGTCGGTAGTCAAGTGAACATTCAAGTCAAT

 AGTTCATCCGAAGGTATGACGGTGTTTCGCACCAACAGACAATGCTTTTCAAAACCTTAAACCCGGAACCCT

 AAACCAGTTAAGCCCTGACGATCAAGTTAAACTCATTCTCTACCACGTTAGCCCCAAATATTACAGTATGG

 ATGATCTCCTCTCCGTGAGTAACCCGGTTAGGACTCAAGCTTCTGGCCGAGACAACGGTGTTTACGGGCTT

 AACTTCACCGGCCAAACAAACCAAATCAATGTCTCTACTGGTTATGTGGAGACACGTATTAGCAATTCGTT

 GAGGCAACAACGTCCTCTCGCAGTTTATGTTGTGCGACATGGTTTTGTTGCCCGGTGAGATGTTTCGGAGAGC

 ACAAGCTTTCGCCGATTGCTCCTGCCCCCTAAATCTAAATCCGGTGGGGTTACCGATGACTCCGGCTCCACT

 AAGAAGGCAGCGTCACCGTCGGATAAGTCAGGCTCCGGTGAGAAGAAAGTCGGACTAGGGTTTGGTCTTGG

 ACTTATTGTCTTATGTTTGAAATTTCTCTTTCCATGGATGGTGAGCAAGGGCGAGGAGCTGTTACCGGGG

 TGGTGCCCATCCTGGTCGAGCTGGACGGCGACGTAAACGGCCACAAGTTCAGCGTGTCCGGCGAGGGCGAG

 GGCGATGCCACCTACGGCAAGCTGACCCTGAAGTTCATCTGCACCACCGGCAAGCTGCCCGTGCCCTGGCC

 CACCCTCGTGACCACCTTCACCTACGGCGTGCACTGCTTCAGCCGCTACCCCGACCACATGAAGCAGCAGC

 ACTTCTTCAAGTCCGCCATGCCGAAGGCTACGTCCAGGAGCGCACCATCTTCTTCAAGGACGACGGCAAC

 TACAAGACCCGCGCCGAGGTGAAGTTCGAGGGCGACACCCTGGTGAACCGCATCGAGCTGAAGGGCATCGA

 CTTCAGGAGGACGGCAACATCCTGGGGCACAAGCTGGAGTACAACACTACAACAGCCACAACGTCTATATCA

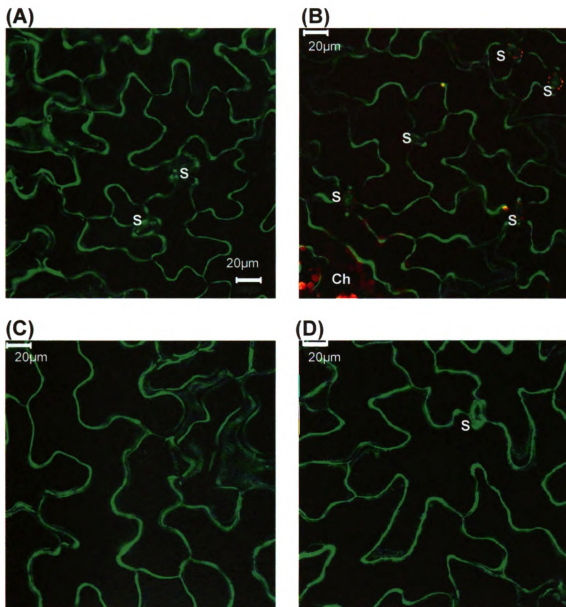
 TGGCCGACAAGCAGAAGAACGGCATCAAGGTGAACCTCAAGATCCGCCACAACATCGAGGACGGCAGCGTG

 CAGCTCGCCGACCACTACCAGCAGAACACCCCATCGGCGACGGCCCCGTGCTGCTGCCCGACAACCACTA

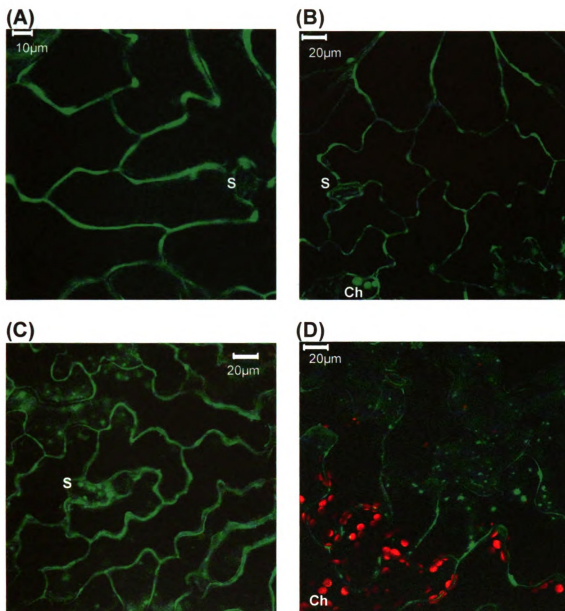
 CCTGAGCACCCAGTCCGCCCTGAGCAAAGACCCCAACGAGAAGCGCGATCATATGGTCTGCTGGAGTTCTG

 TGACCGCCGCGGGGATCACTCTCGGCATGGACGAGCTGTACAAGTAA

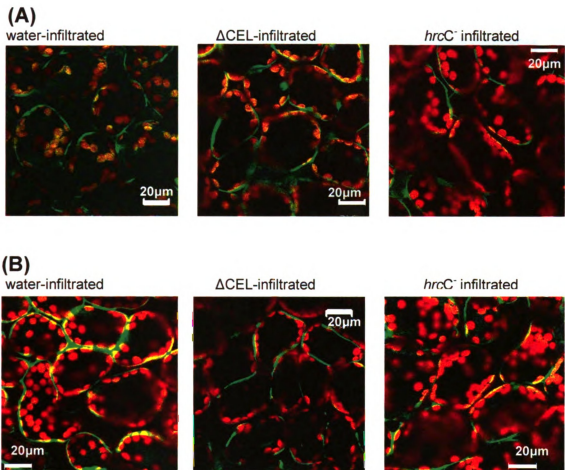
Appendix 4-3. The sequence of *FLA9-GFP* fusion ORF. The *FLA1* ORF is in black letters and the *GFP* ORF is in green letters. The start codons and stop codon are in red and bold letters. The six nucleotides connecting *FLA9* ORF without stop codon and *GFP* ORF are underlined. The putative N-terminal signal sequence of *FLA9* is highlighted with blue color.



Appendix 4-4. PR1-GFP in *Arabidopsis*. (A) PR1-GFP in Col-0 (line#1). (B) PR1-GFP in Col-0 (line #3). (C) PR1-GFP in the *atmin7* plant (line#1). (D) PR1-GFP in the *atmin7* plant (line#5). All images are from single focal planes. Ch: chloroplast. S: stomata.



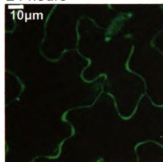
Appendix 4-5. *At2g10940-GFP* in *Arabidopsis*. (A) *At2g10940-GFP* in Col-0 (line#9). (B) *At2g10940-GFP* in Col-0 (line #16). (C) *At2g10940-GFP* in the *atmin7* plant (line#41). (D) *At2g10940-GFP* in the *atmin7* plant (line#71). All images are from single focal planes except D, which was from Z-stack. Ch: chloroplast. S: stomata.



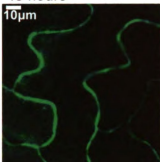
Appendix 4-6. Comparison of the localization of PR1-GFP in *Arabidopsis* after infiltrating *hrcC*⁻ or Δ CEL mutant, in Col-0 (A) or in *atmin7* background (B).

Sprayed with water

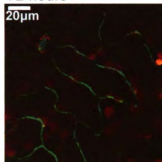
24 hours



48 hours

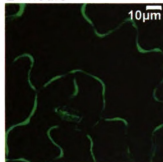


72 hours

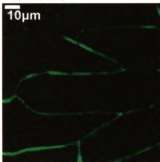


Sprayed with BTH

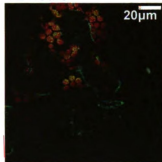
24 hours



48 hours



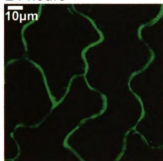
72 hours



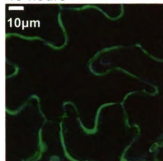
Appendix 4-7. Comparison of the localization of PR1-GFP in Col-0 background, after spraying water or 300 μ M BTH.

Sprayed with water

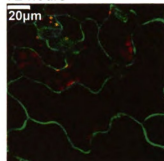
24 hours



48 hours

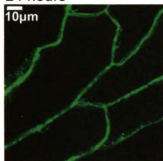


72 hours

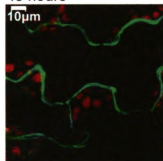


Sprayed with BTH

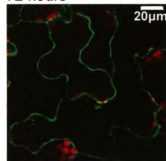
24 hours



48 hours



72 hours



Appendix 4-8. Comparison of the localization of PR1-GFP in *atmin7* background, after spraying water or 300 μM BTH.

MICHIGAN STATE UNIVERSITY LIBRARY



3 1293 03063 118